PREX-II: Measuring the Neutral Weak Form-Factor of ^{208}Pb

INT Seminar
January 21, 2021

Caryn Palatchi

UNIVERSITY of VIRGINIA

Center for Frontiers in Nuclear Science

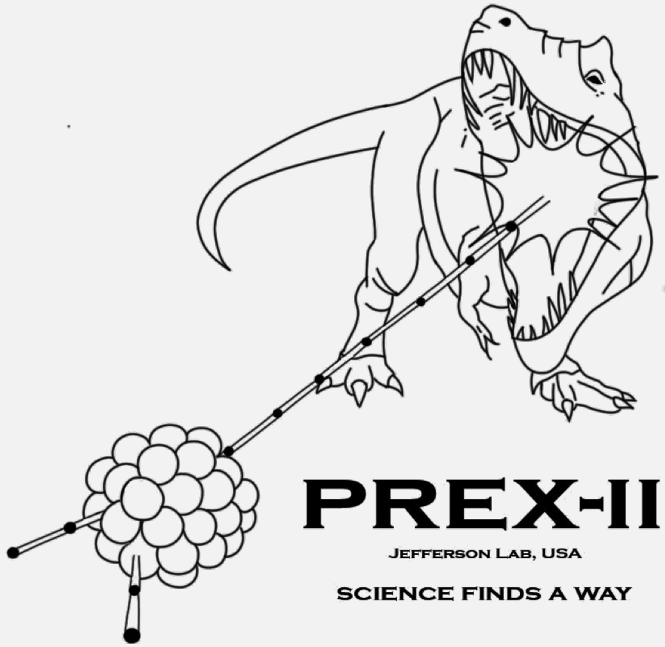

*Artwork by Marisa Petrusky

Thanks for many borrowed slides from Kent Paschke and Ciprian Gal

ELASTIC ELECTRON-NUCLEAR SCATTERING

Heavy, spin-0 nucleus

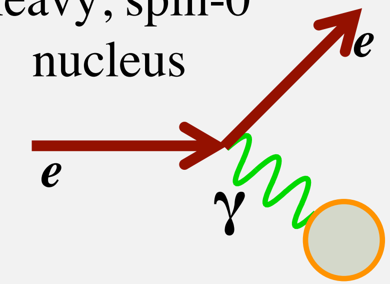

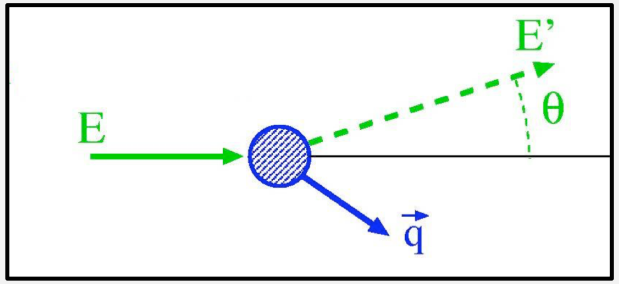

Differential cross-section

$$\frac{d\sigma}{d\Omega} = \left(\frac{d\sigma}{d\Omega}\right)_{\text{Mott}} \left| F(q) \right|^2$$

$$\left(\frac{d\sigma}{d\Omega}\right)_{\text{Mott}} = \frac{4Z^2\alpha^2E^2}{Q^4}$$

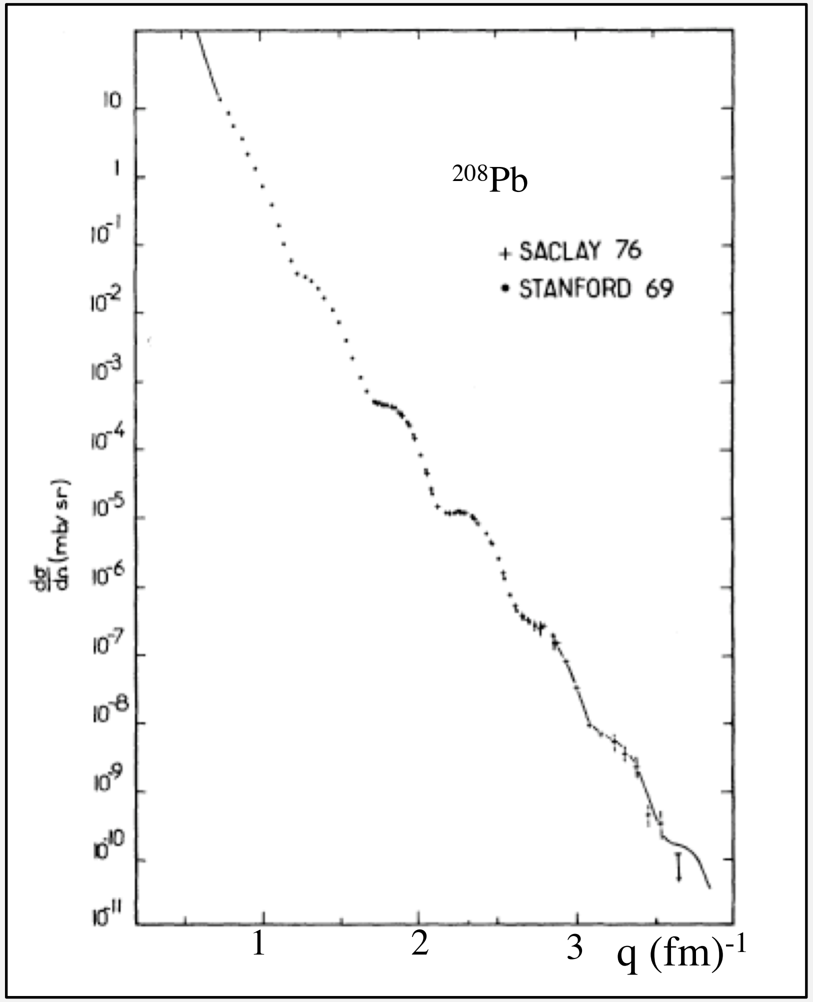

Neglecting relativistic recoil, the form-factor ***F(q)*** is the Fourier Transform of charge density

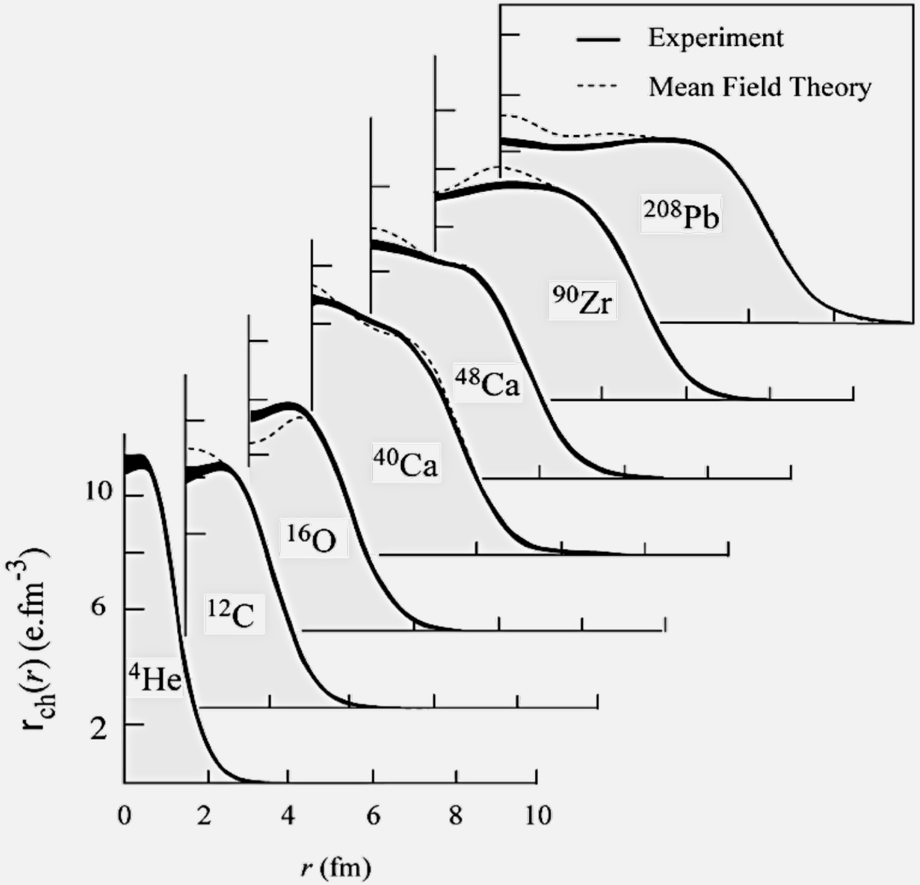

Weak Charge Distribution of Heavy Nuclei

Thiel et al J.Phys.G 46 (2019) 9, 093003

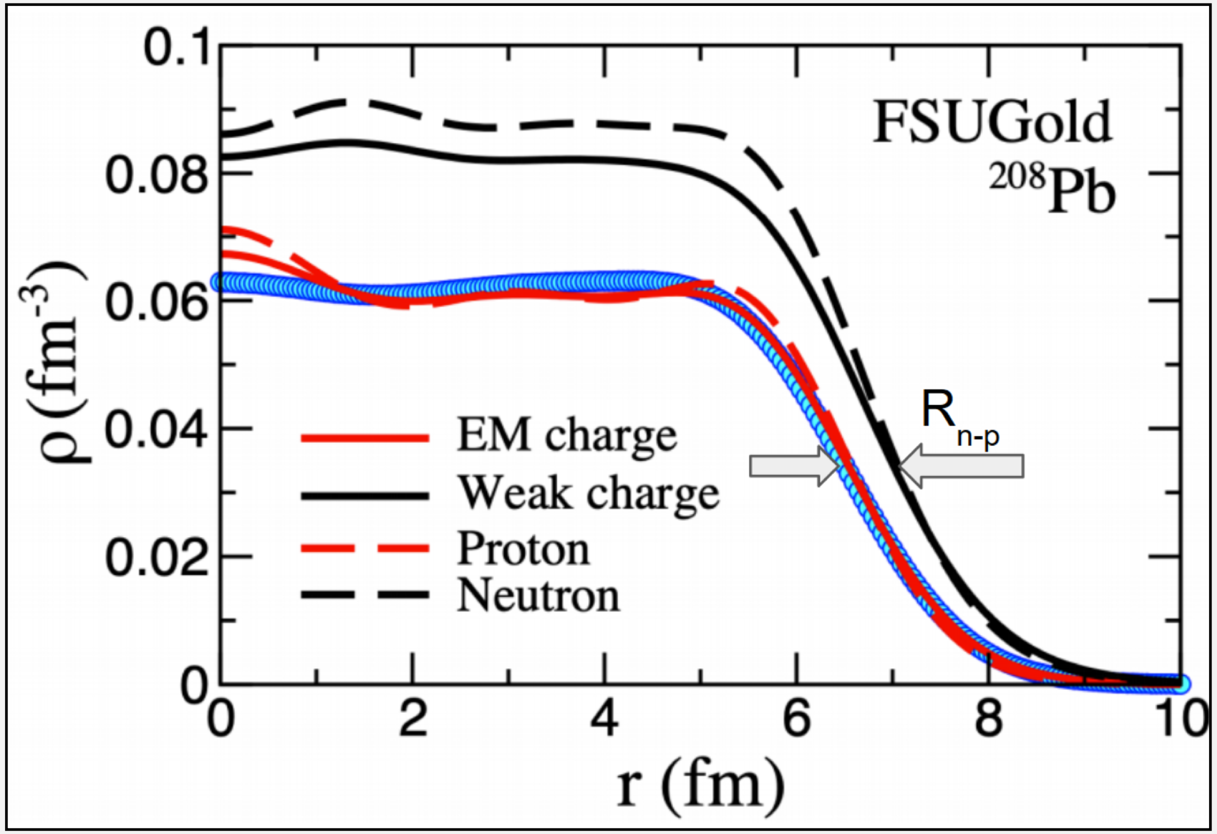

Nuclear theory predicts a neutron "skin" on heavy nuclei

- Neutron skin thickness is highly sensitive to the pressure in neutron-rich matter.
- The greater the pressure, the thicker the skin as neutrons are pushed out against surface tension.
- Knowledge of R_n is highly model dependent, and is not well constrained by robust measurements. Neutrons are hard to measure!

Weak charge of the proton is heavily suppressed compared to the neutron

$(1\text{-}4\sin^2\theta_W$ so $Q_W^p \sim 0.07$, while $Q_W^n \sim 1)$

Neutron distribution matches the weak charge distribution

Measuring the weak charge distribution

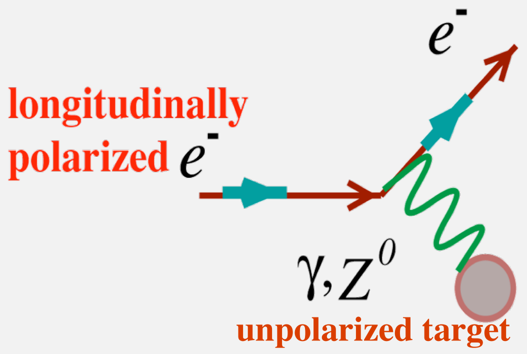

$$A_{PV} = \frac{\sigma_R - \sigma_L}{\sigma_R + \sigma_L}$$

$$\sigma \propto |M_\gamma + M_{\mathrm{weak}}|^2$$

$$\sim |M_\gamma|^2 + 2M_\gamma(M_{\mathrm{weak}})^* + \ldots$$

$$A_{PV} \approx \frac{G_F Q^2}{4\pi\alpha\sqrt{2}} \frac{Q_W\, F_W(Q^2)}{Z\, F_{ch}(Q^2)}$$

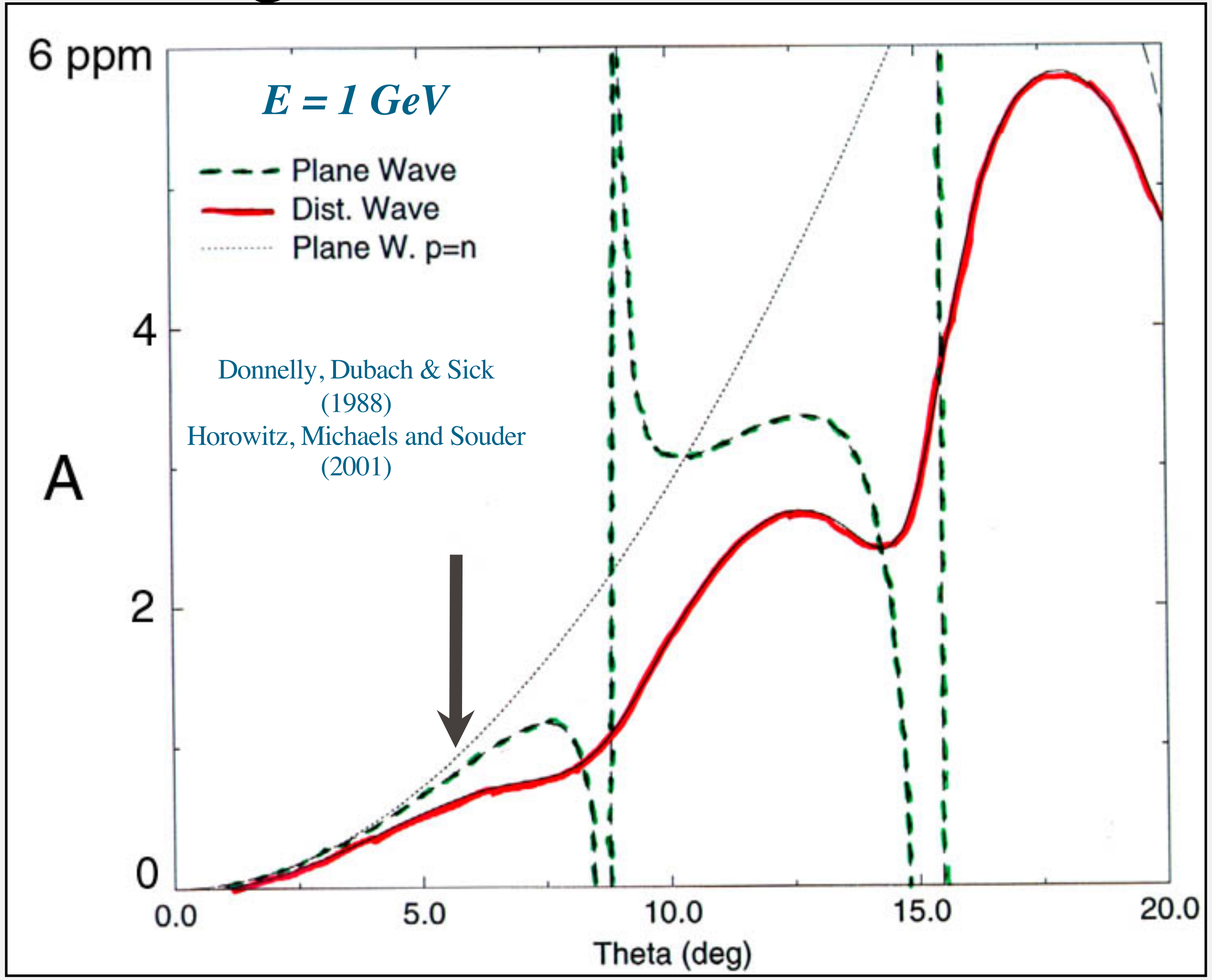

Parity violation in electron scattering accesses the weak form factor

At specific kinematics, this is highly sensitive to the neutron skin thickness R_{n-p}

Neutron skin measured by APV

Robust correlation between ^{208}Pb APV and neutron skin over existing nuclear structure models

Models → Weak charge density → (Solve Dirac Eq.) → Predicted Asymmetry

Models → Predicted Neutron Skin

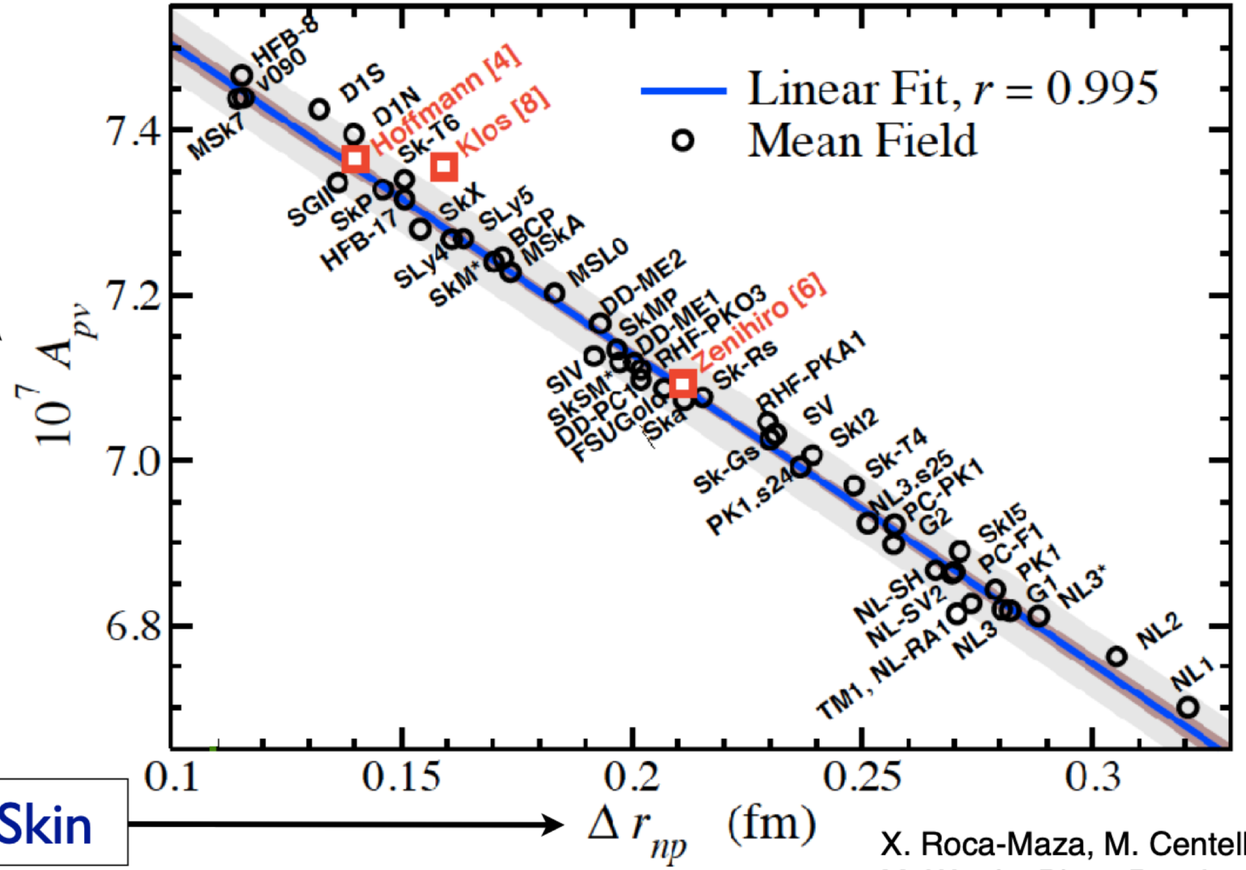

X. Roca-Maza, M. Centelles, X. Vĩnas, and M. Warda, Phys. Rev. Lett. 106 252501 (2011)

L vs. R_{n-p}

Energy penalty for breaking N=Z symmetry $S = \frac{E}{N}$

Slope of symmetry energy at saturation density $L \propto \frac{\partial S(\rho)}{\partial \rho}\Big|_{\rho_0}$

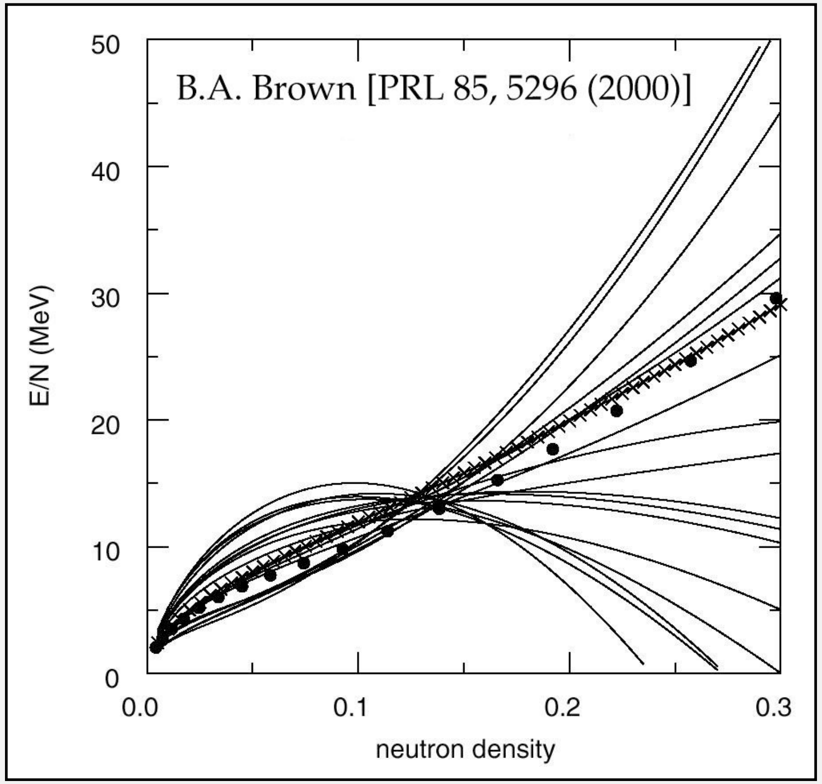

Mean-Field predictions show a clear correlation between neutron skin of a heavy nucleus and the density slope of the symmetry energy.

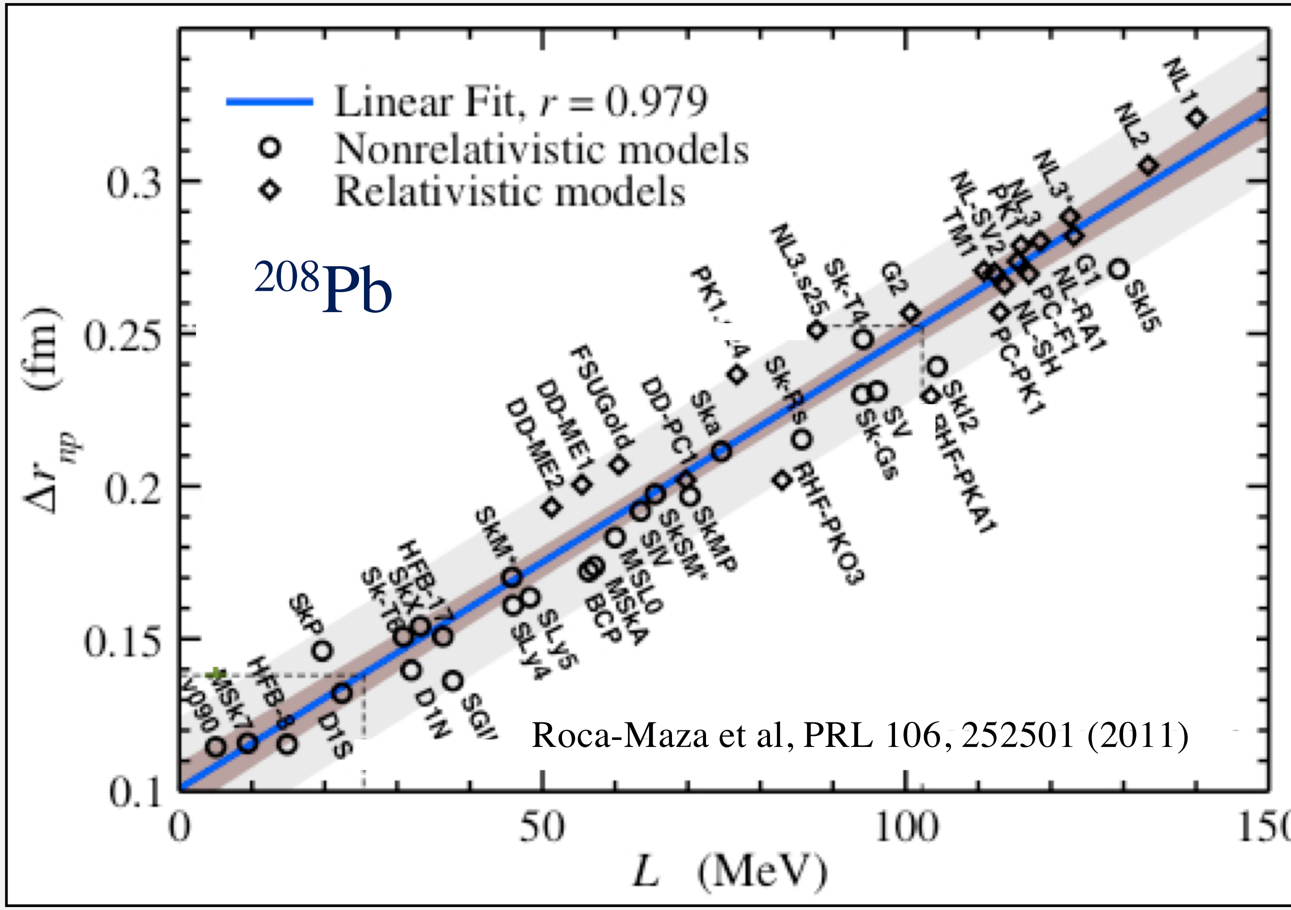

r_n calibrates the **Equation of State** of neutron rich matter

New information in a poorly measured sector

Isovector properties are not well measured. Models informed mostly by measurements of properties sensitive to p+n.

Neutron properties in stable medium and heavy nuclei have been mainly measured by using strongly interacting probes.

Good Isovector Indicators

Poor Isovector Indicators (collective excitations, binding energies, etc.) Relatively well measured

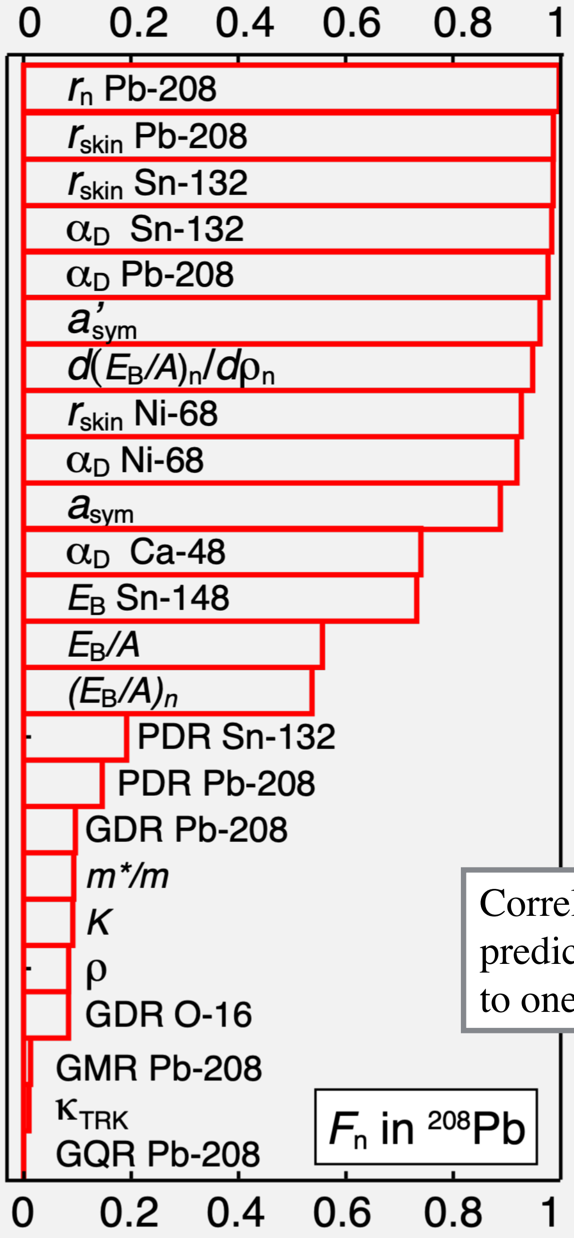

Correlation of prediction vs. changes to one empirical input

Jorge Piekarewicz

Different Systems, same EOS

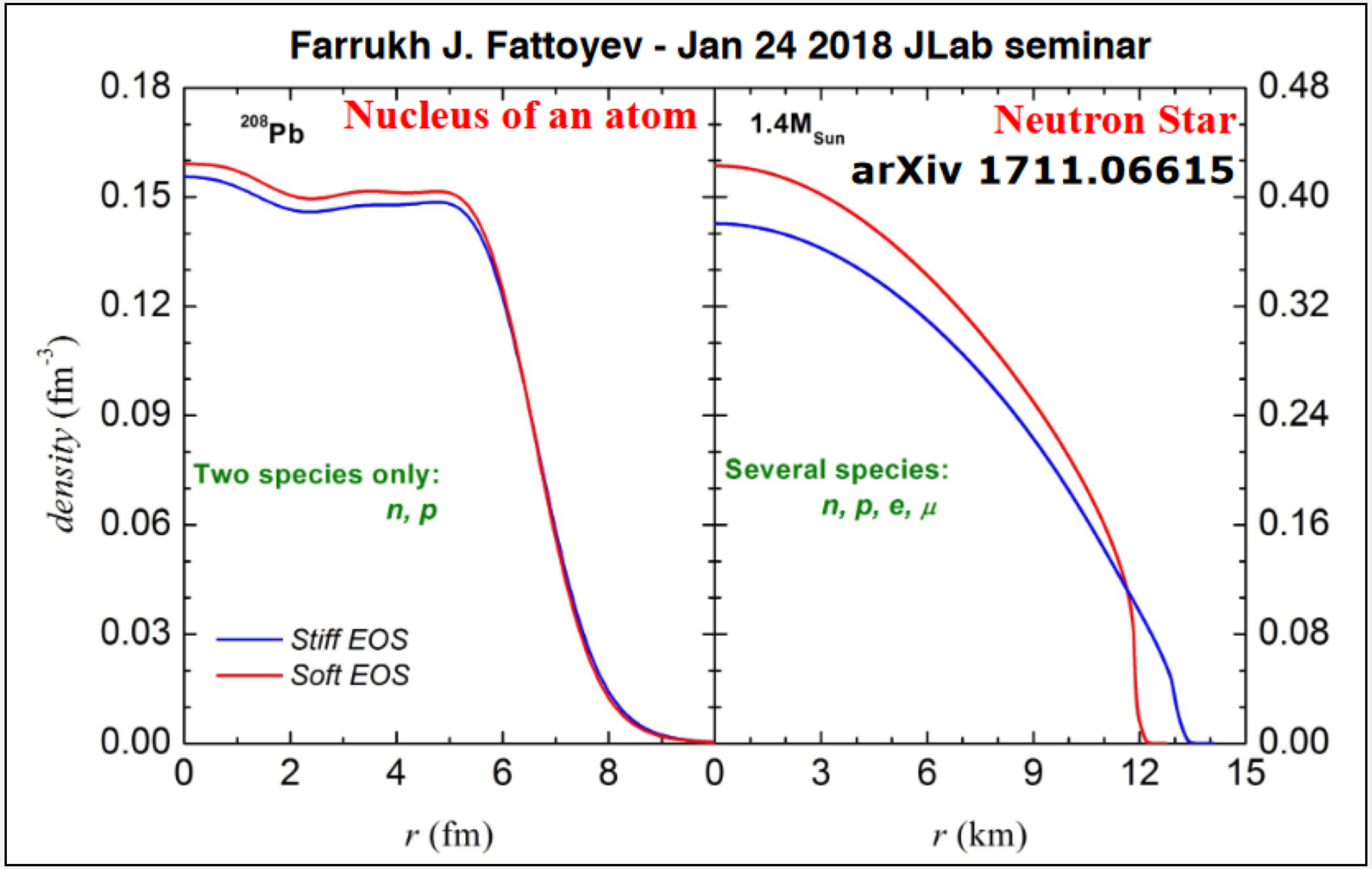

While the ^{208}Pb nucleus and a neutron star are separated by 18 orders of magnitude in size they are thought to be made out of the same stuff and obey one equation of state (EOS)

Studies of 208Pb inform the EOS of neutron-rich nuclear matter

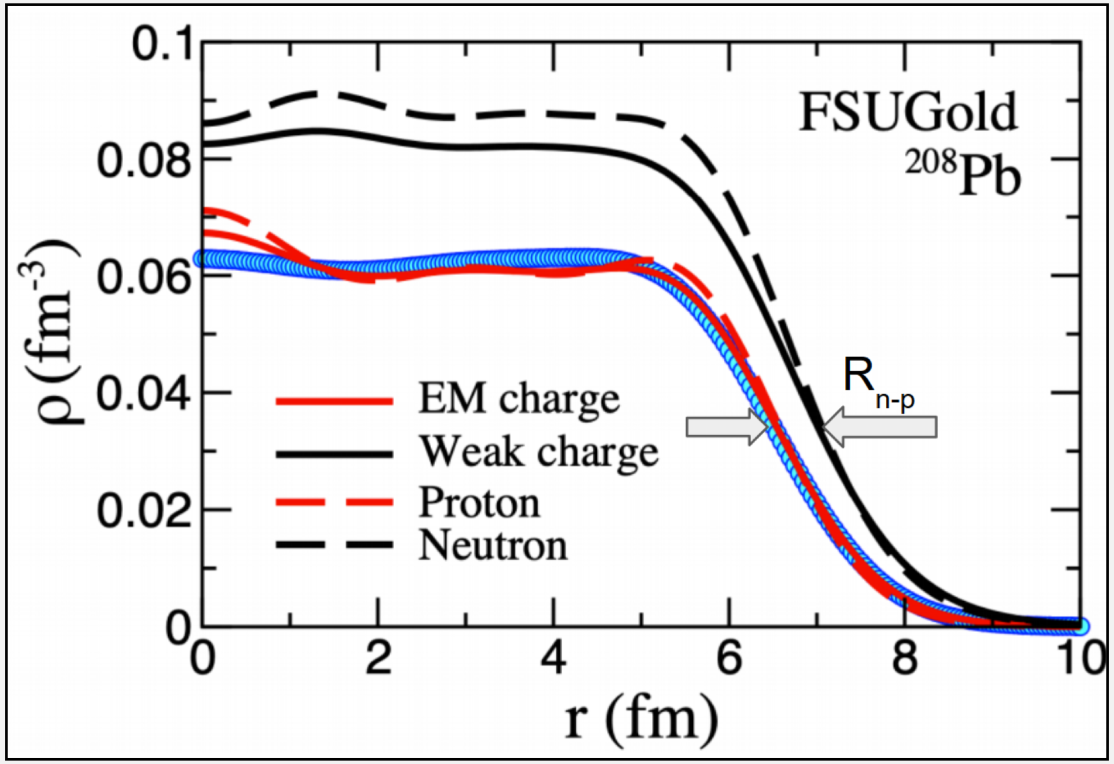

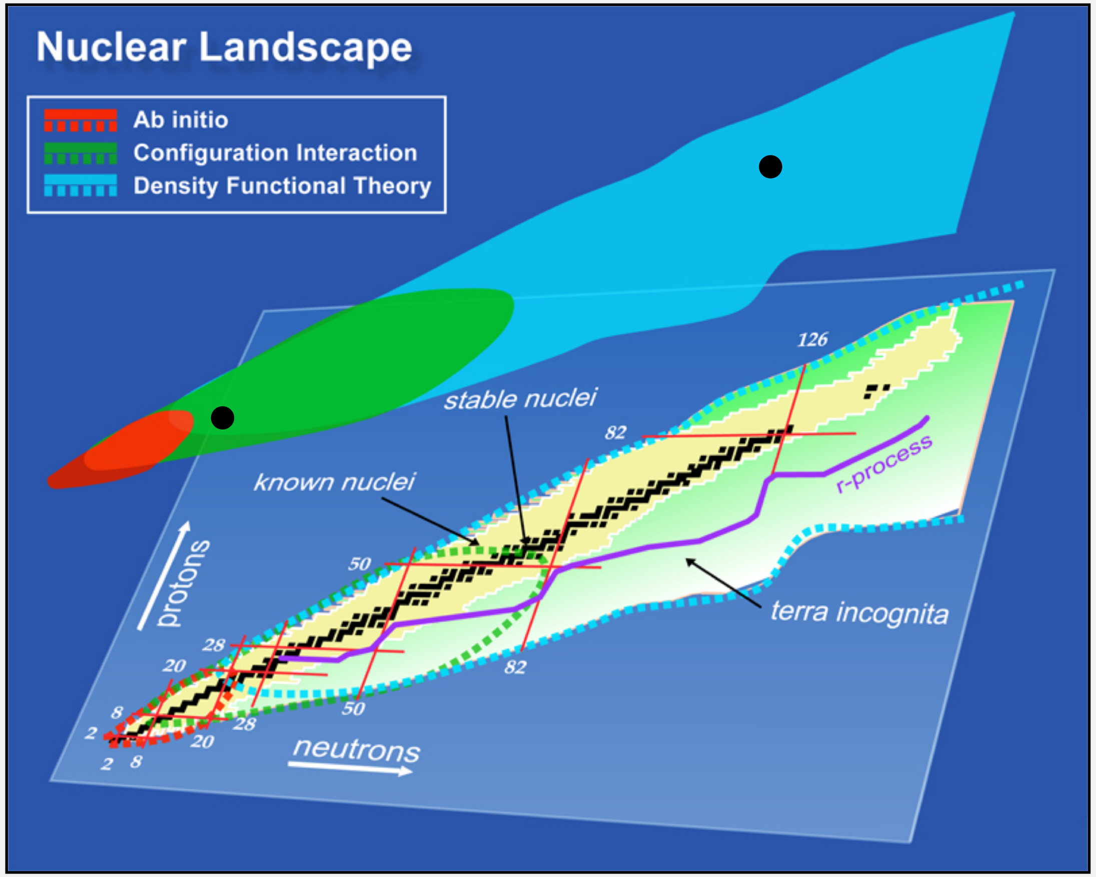

^{208}Pb is well suited to this study: large, uniform, doubly magic

Experimental Overview

Polarized Source

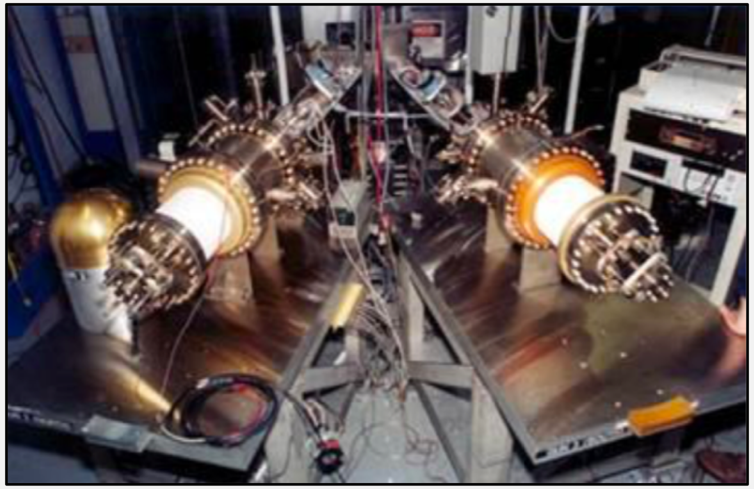

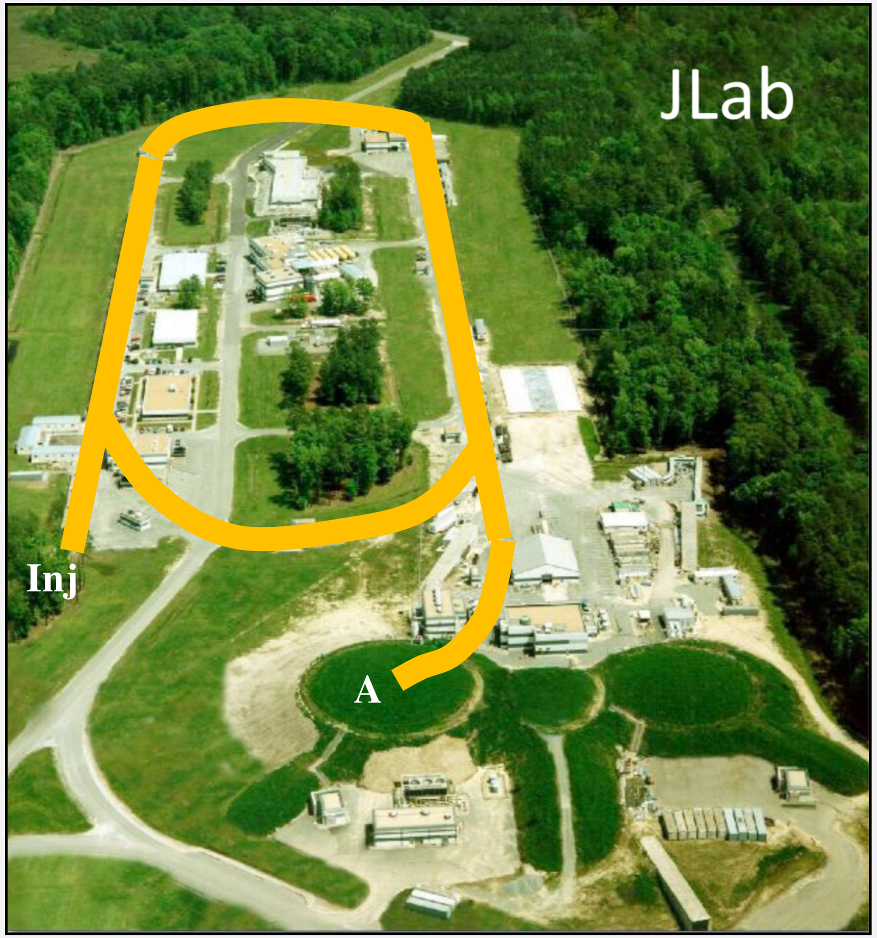

Hall A

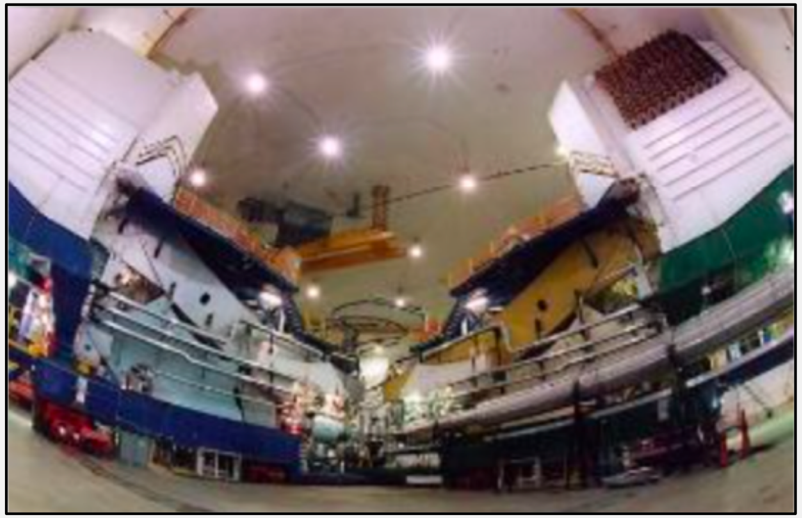

CEBAF is the ONLY operating facility in the world where such an experiment could be attempted

Experimental Challenge

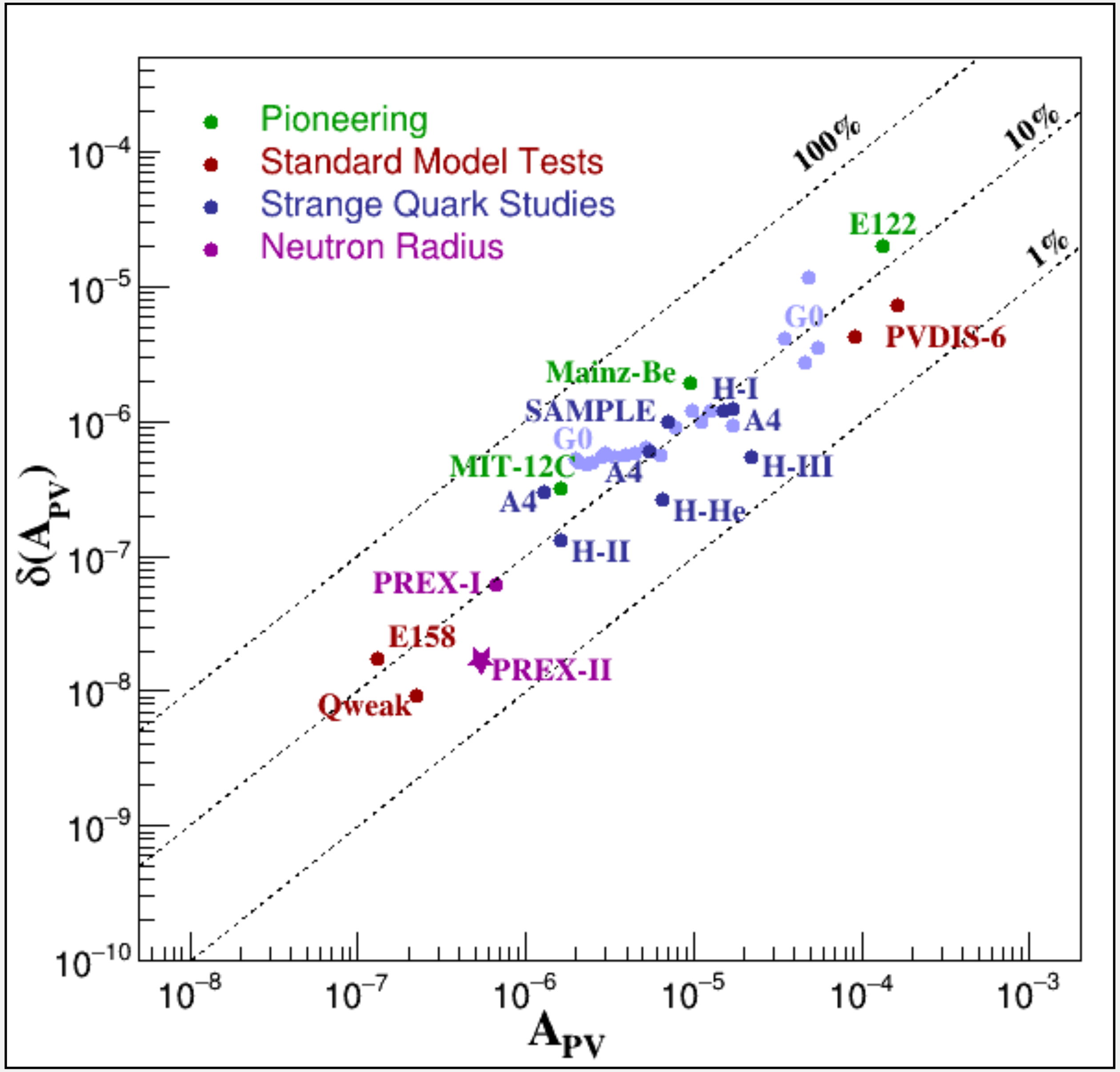

Heavy nucleus at low energy

- radiation
- steep form-factor
- Inelastic states (2.6 MeV)

Measuring small asymmetry

Goal: measure beam-helicity-correlated elastic scattering asymmetry to high precision

$$A_{PV} = \frac{\sigma_R - \sigma_L}{\sigma_R + \sigma_L}$$

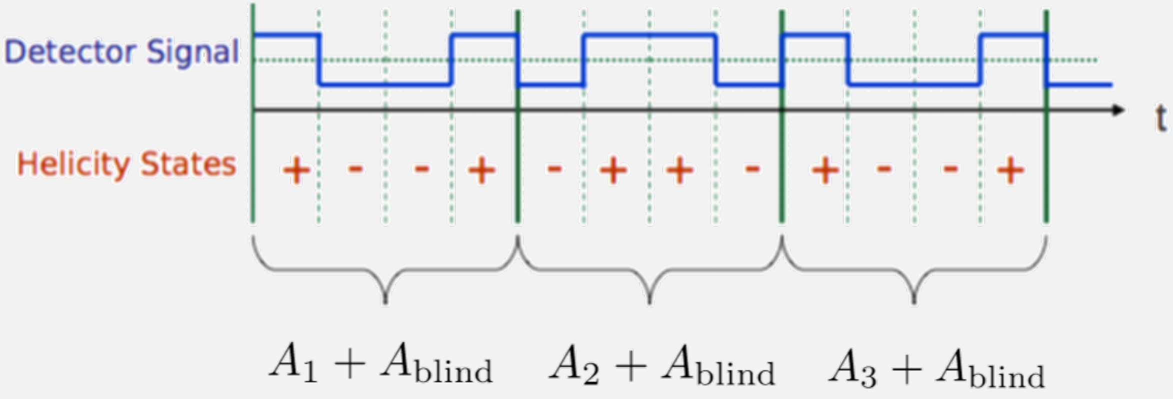

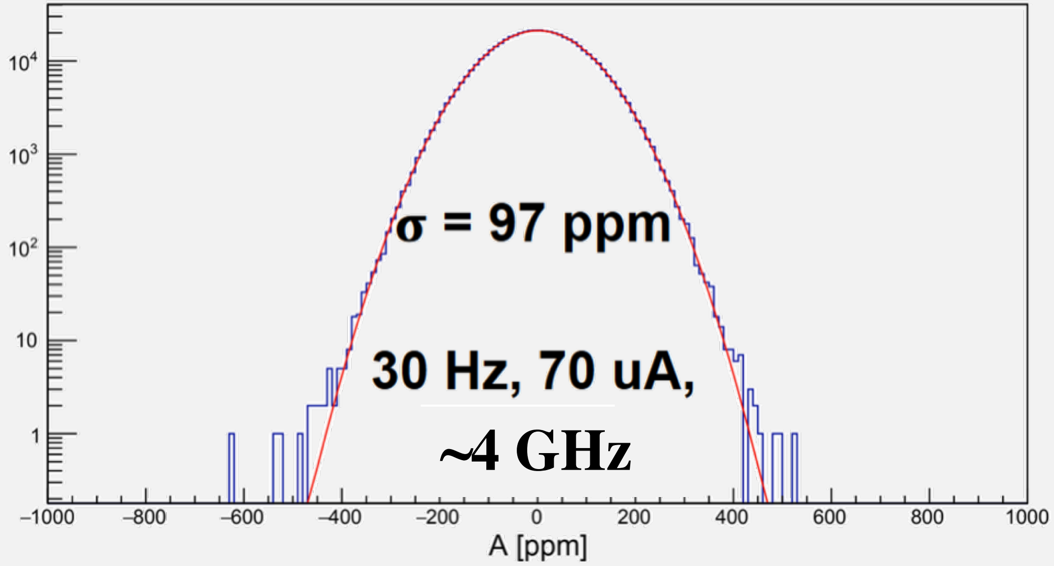

Integrating, not counting (total number of detected electrons was ~6x10^{15}, ~9 mC)

Online analysis showed us were dominated by counting statistics fairly early in the experiment

Number of flips ~ 300 million, octets ~ 40 million

Preparing the beam

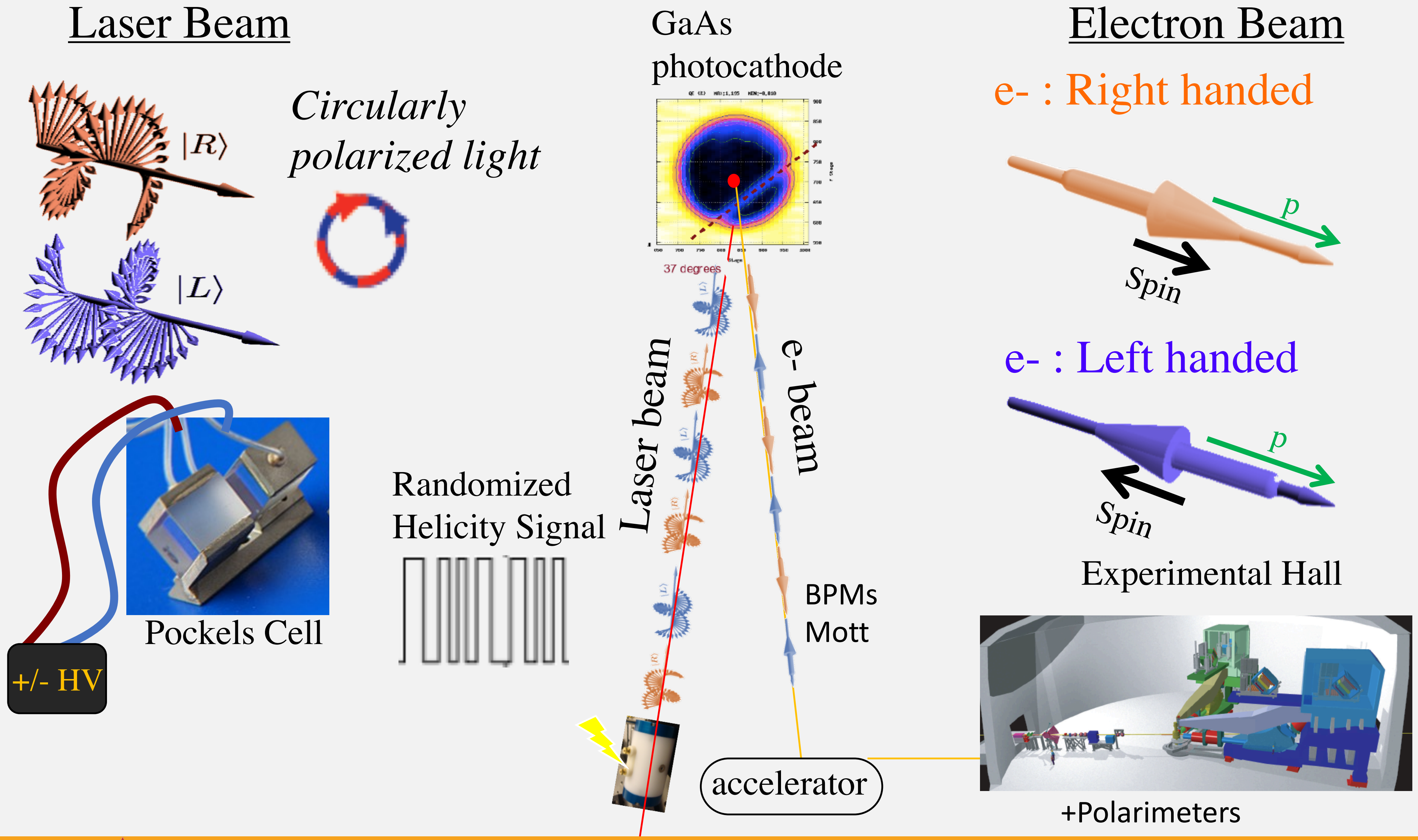

Preparing the beam

Reversal combinations
Helicity: HV +/-, IHWP out/in

Laser Beam

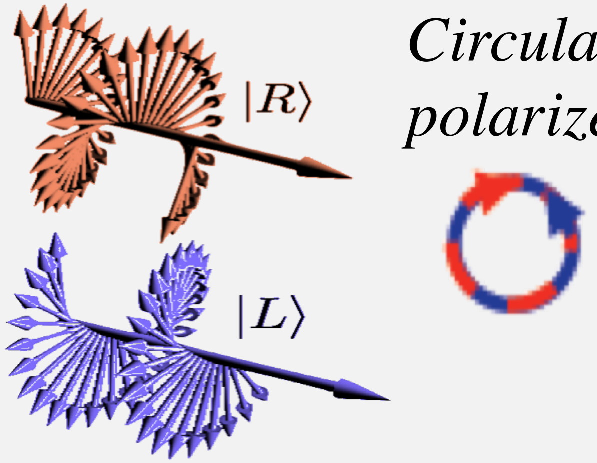

Circularly polarized light

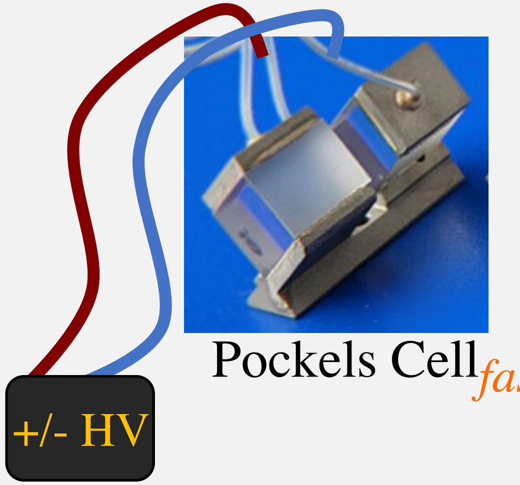

Pockels Cell*fast*

Randomized Helicity Signal

slow

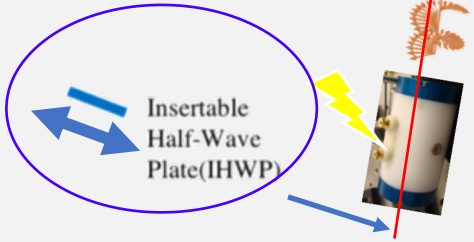

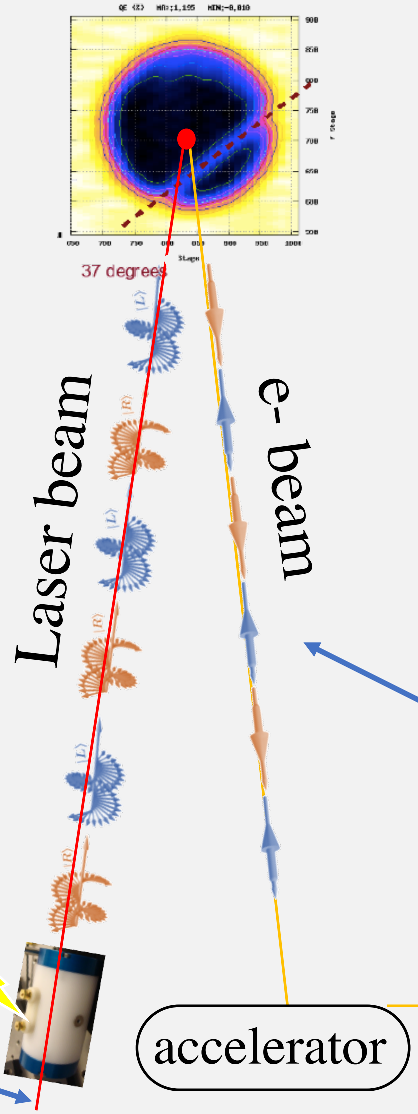

Electron Beam

e- : Vertical ↑

e- : Vertical ↓

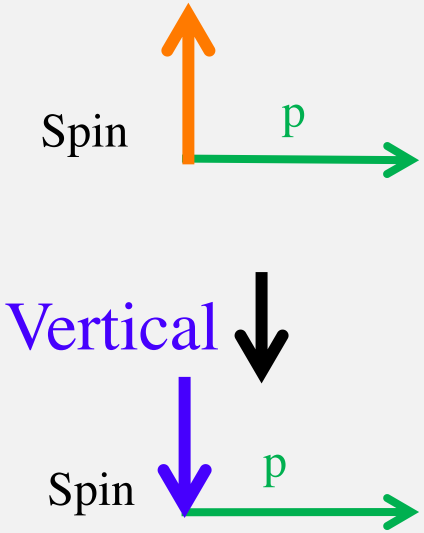

Solenoid off

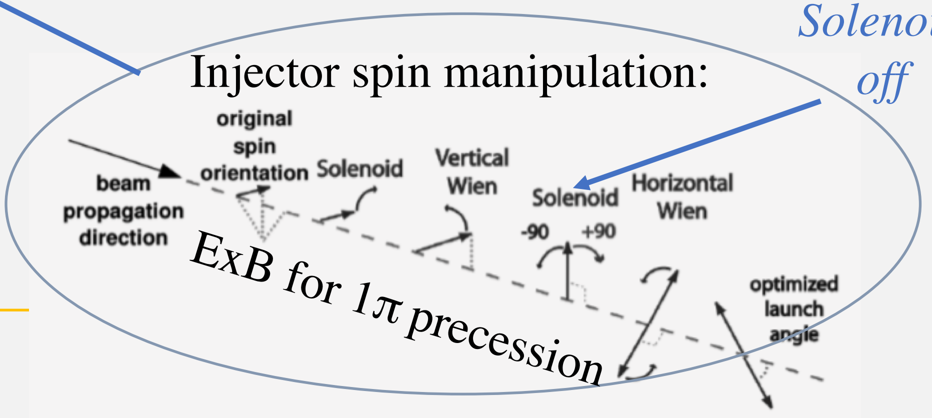

14

Polarized Source: Precision and Systematic Uncertainty

Any change in the polarized beam, correlated to helicity reversal, can be a potential source for a false asymmetry

$$A_{raw} = A_{det} - A_Q + \alpha\Delta_E + \Sigma\beta_i\Delta x_i$$

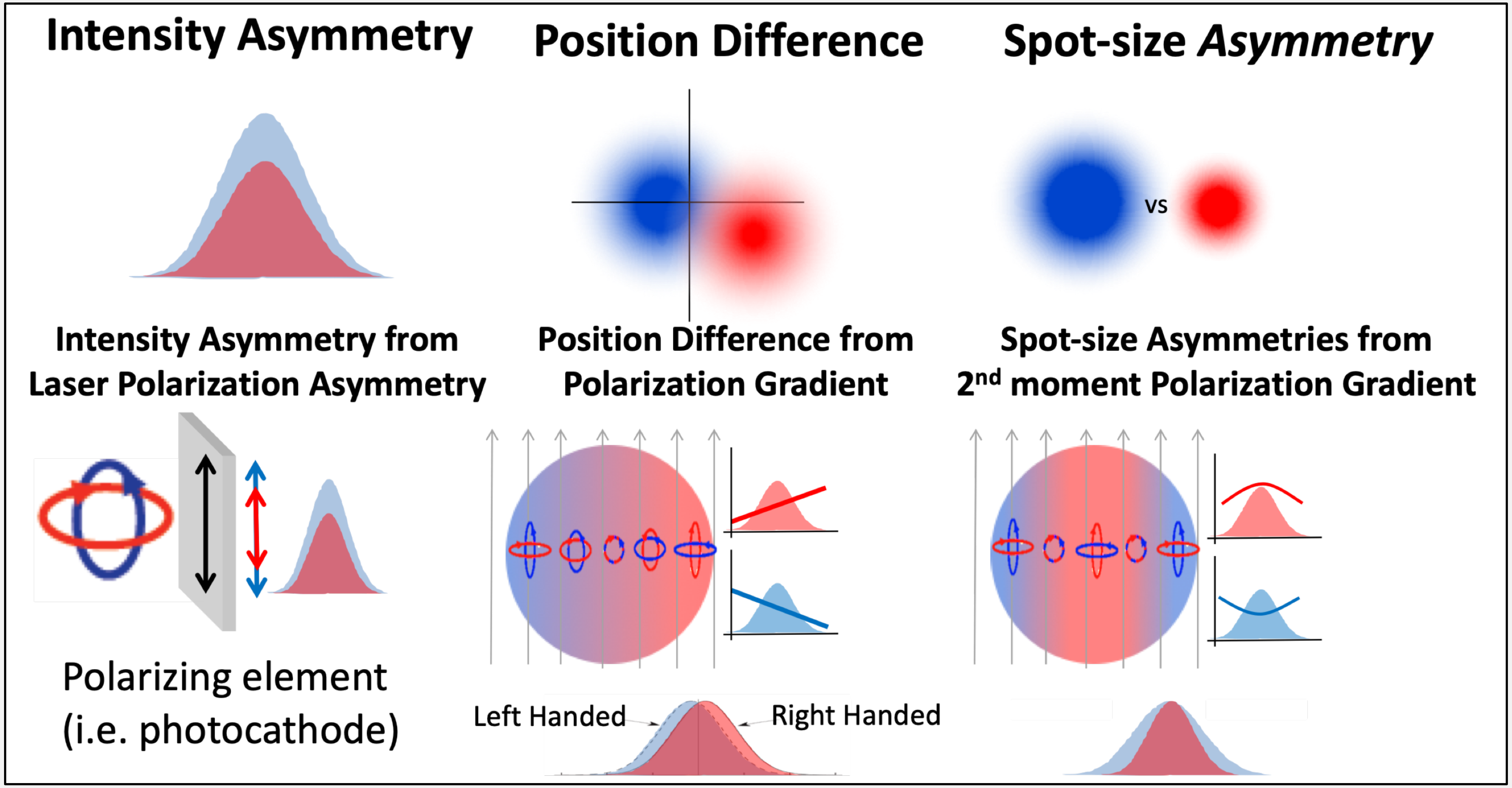

new UVa RTP cell (MOLLER R&D)

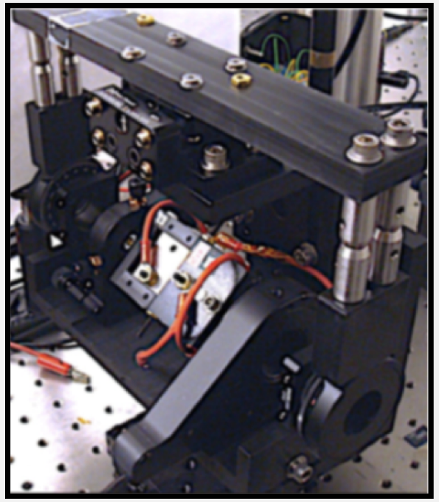

Moller Polarimetry

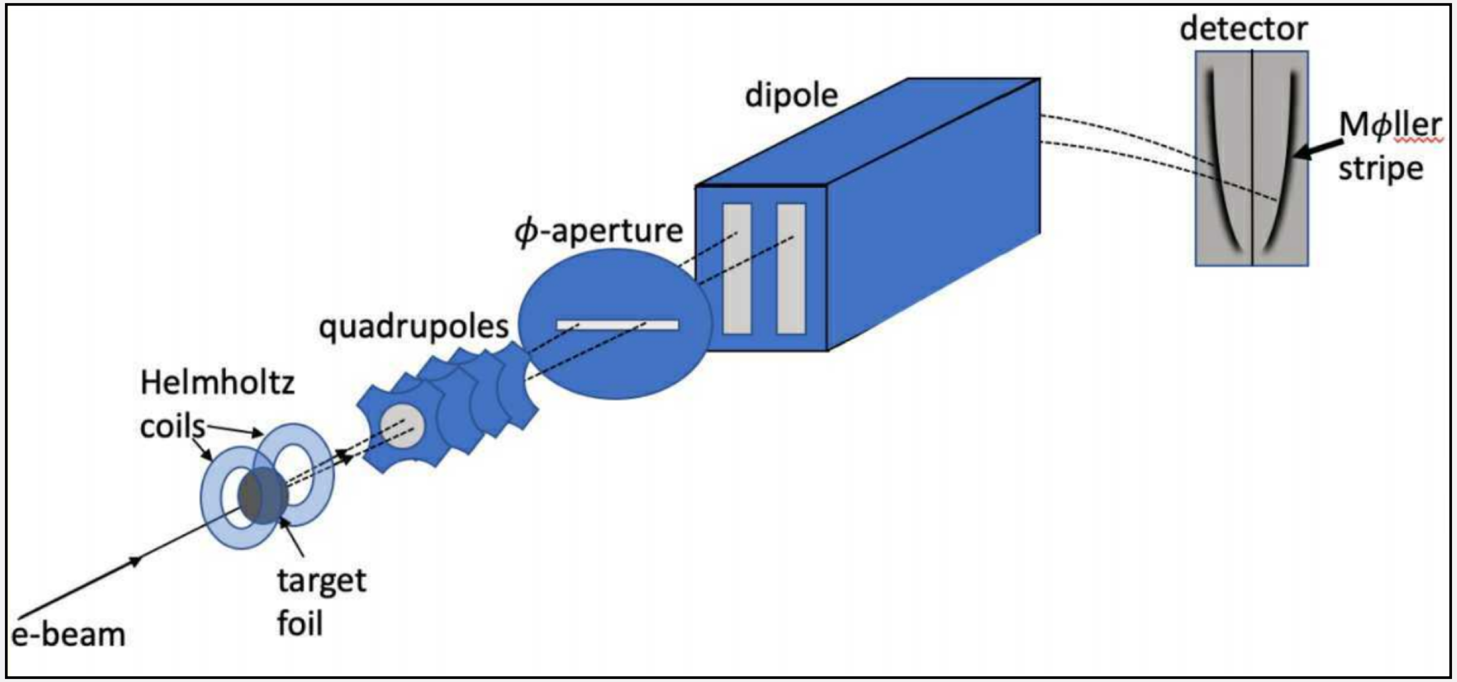

- Low-current, invasive measurement
- 3-4T field provides saturated magnetization perpendicular to the foil
- Spectrometer redesigned for 11 GeV

Average polarization:
(89.7 ± 0.8)%

- PREX-II reoptimized the spectrometer tune (and detector configuration), to provide high precision and sensitivity to systematic effects
- Polarimeter runs were taken approximately every week and established no significant fluctuations in beam polarization over the course of the run

Moller polarimeter results, over the run

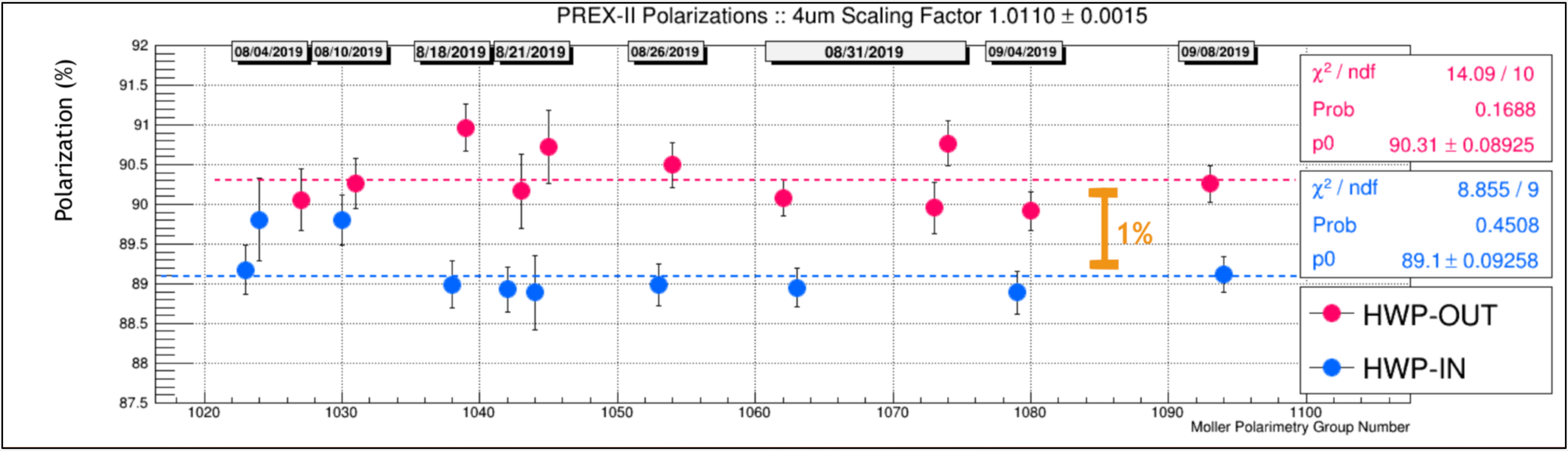

Average polarization:
(89.7 ± 0.8)%

Compton Polarimetry

- Utilized integrating technique with photon detector (as in PREX-1)
- Very challenging as low energy (low signal, small asymmetry)
- Chi-squared is a little poor, but a few far-tail jumps
- Evaluated systematic uncertainty
- No indication of real changes in time, and comparison with MOLLER agrees well

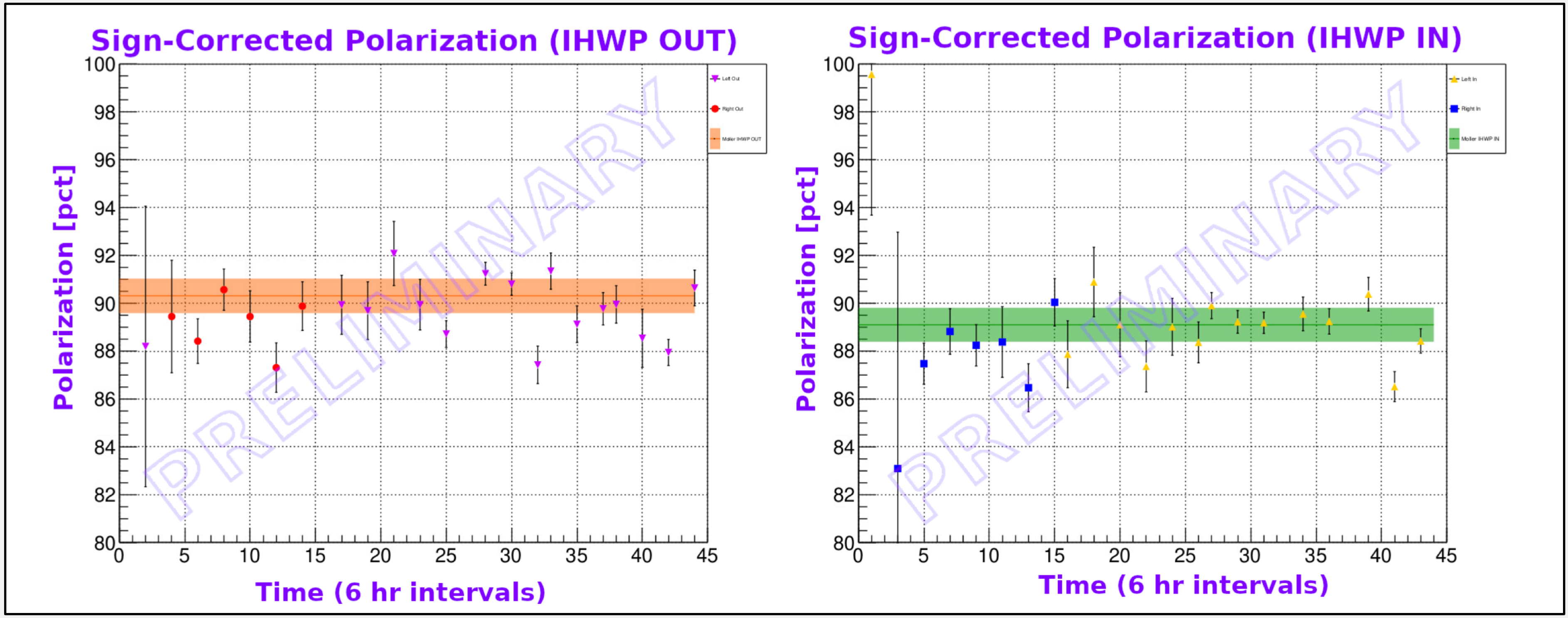

HRS

High-Res Spectrometers

- Spectrometer separates elastic peak, directs it onto integrating detector
- Integrate detector in each of the spectrometer pair independently

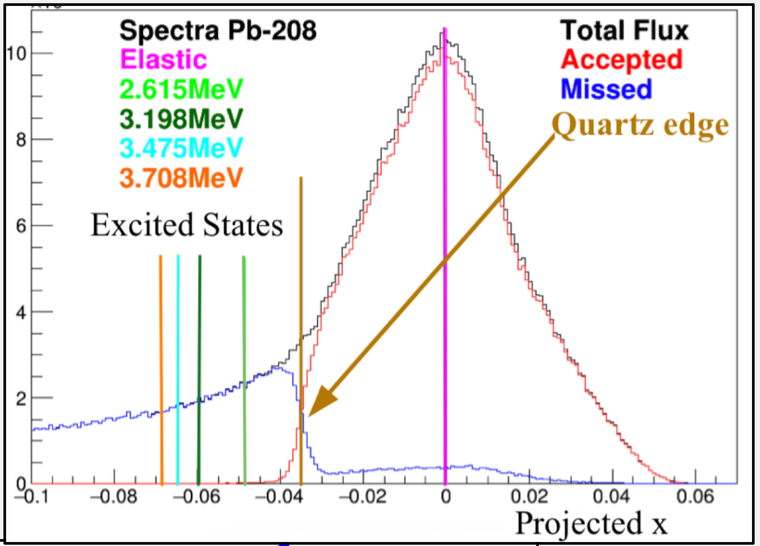

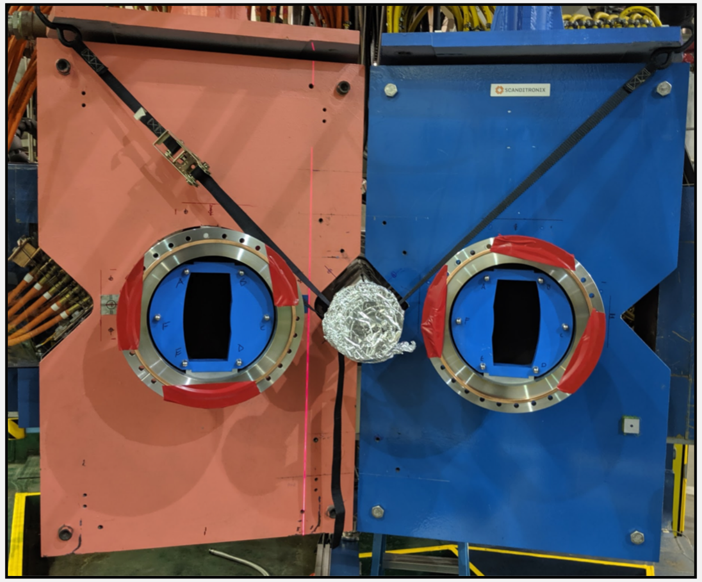

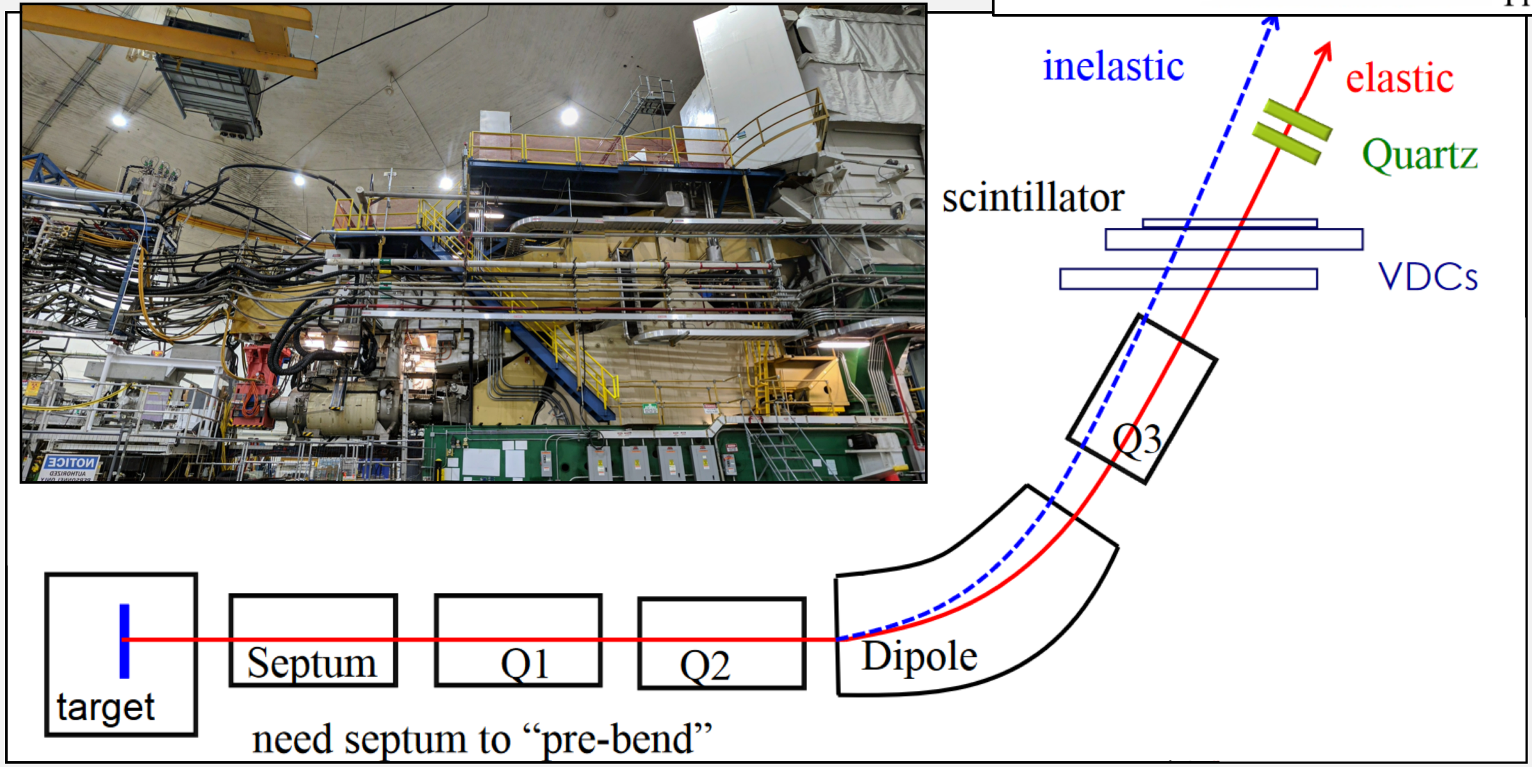

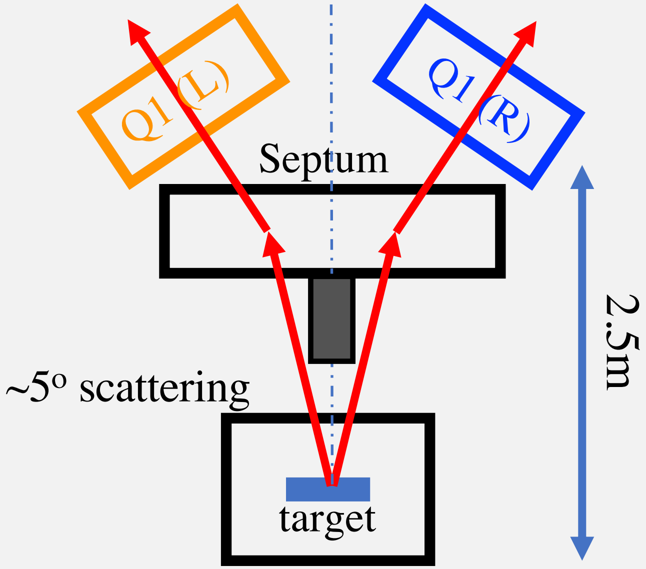

Integrating Detectors

- The challenge: all electrons need to count the same - high photon statistics but low shower fluctuations
- Fused silica Cerenkov radiator, 5mm thick, 3.5x16 cm^2 area, mated to a single PMT
- ~2 GHz signal rate in a 3x3 cm^2 area at the end of the detector
- Non-linearity of detector response was tested on the bench and with beam during the experiment

Dustin McNulty, Devi Adhikari

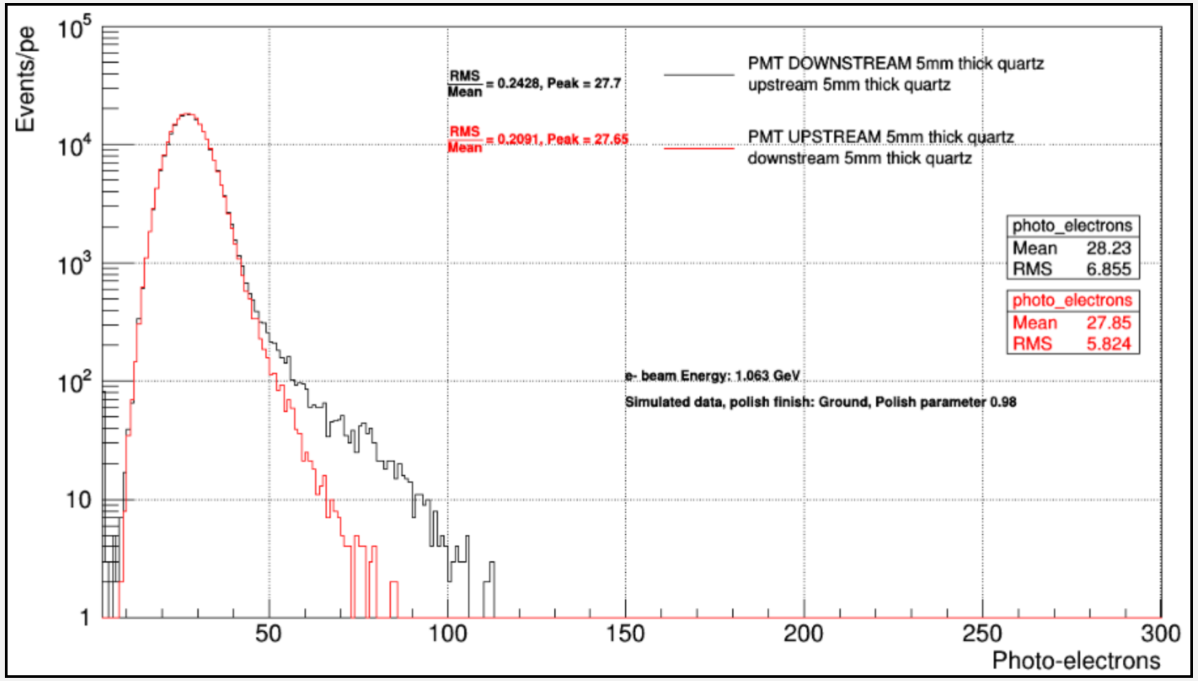

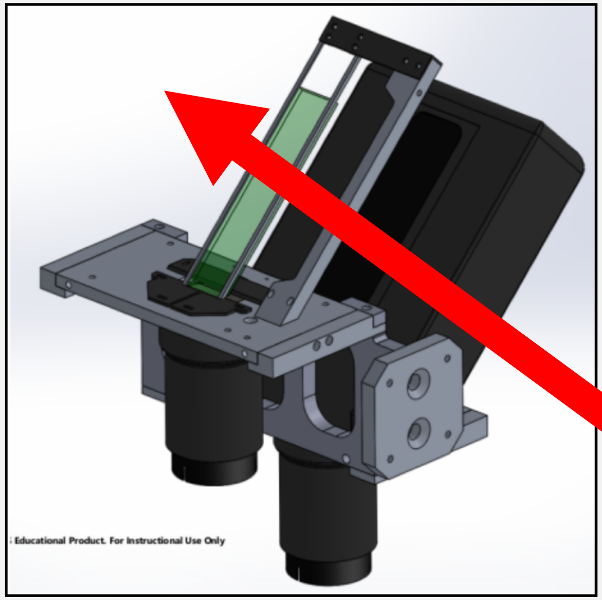

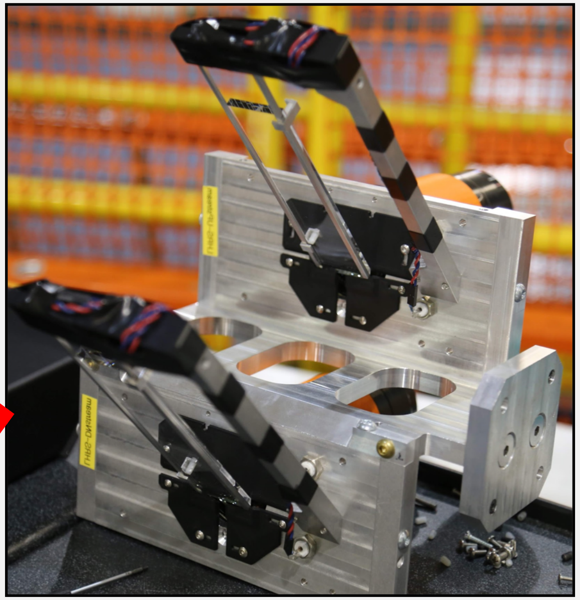

Counting Detectors

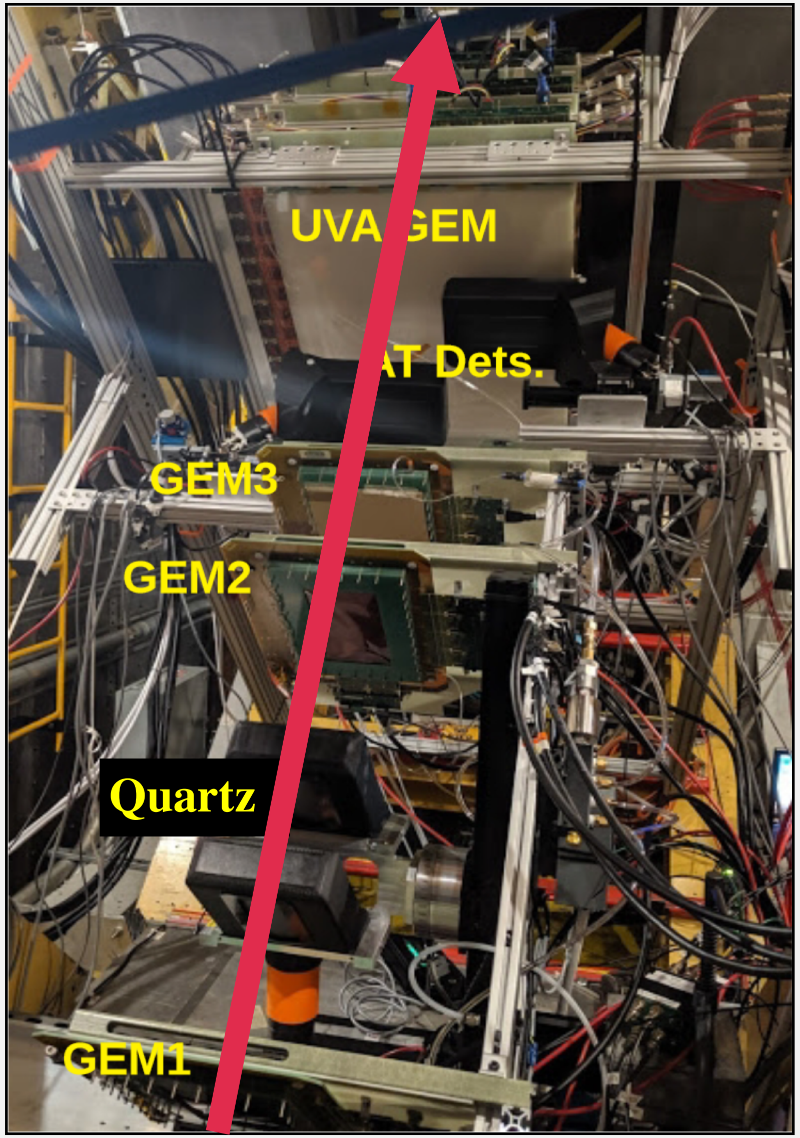

- The HRS Vertical Drift Chambers (VDCs) below the quartz detectors
- GEMs that we installed upstream and downstream of our quartz detectors
- Used to align the elastic peak on the quartz and to measure accepted kinematics
- Used at very low currents (30 nA) "counting experimental mode"

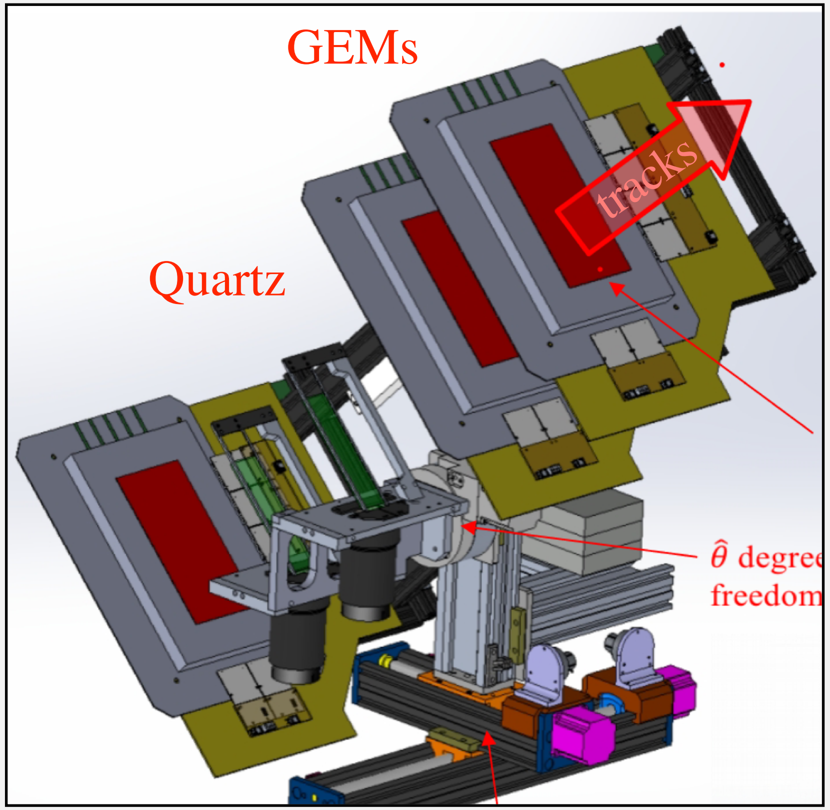

Tight fit in the target area

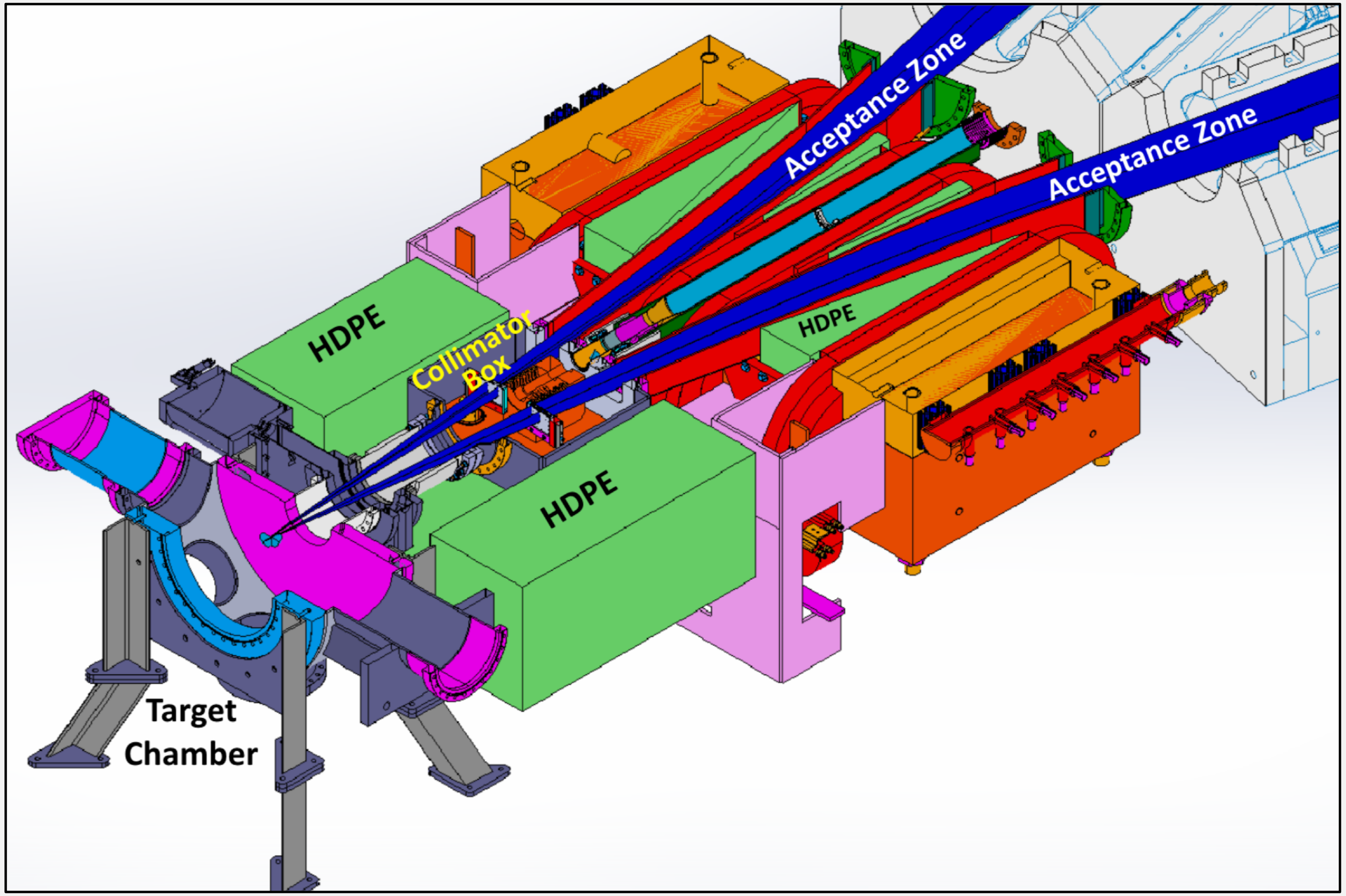

- The experimental hall provides unique challenges for a high luminosity, high Z, low energy experiment
- Large angle scattered electrons need to be stopped close to the target and that region needs to be heavily shielded
- Electronics inside the hall need to be protected from both the electromagnetic and neutron radiation damage that will stop it from functioning properly

- Tight acceptance, space requirements, collimator power, shielding made for tricky installation

(kudos to Hall A designers, Jesse Beams and the Hall A technical staff)

Radiation shielding

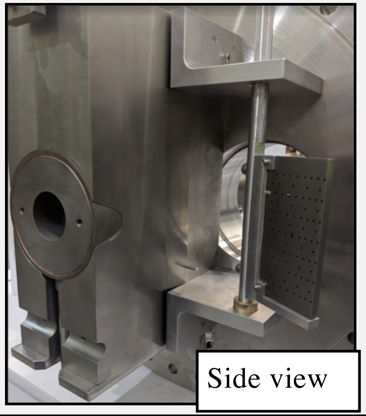

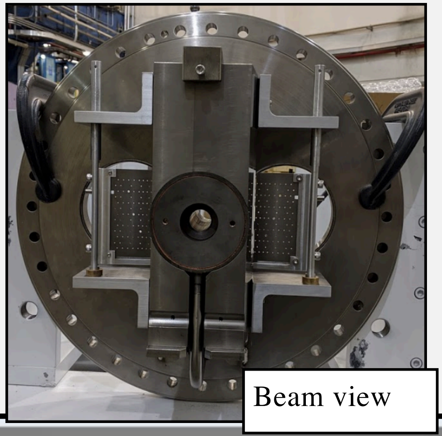

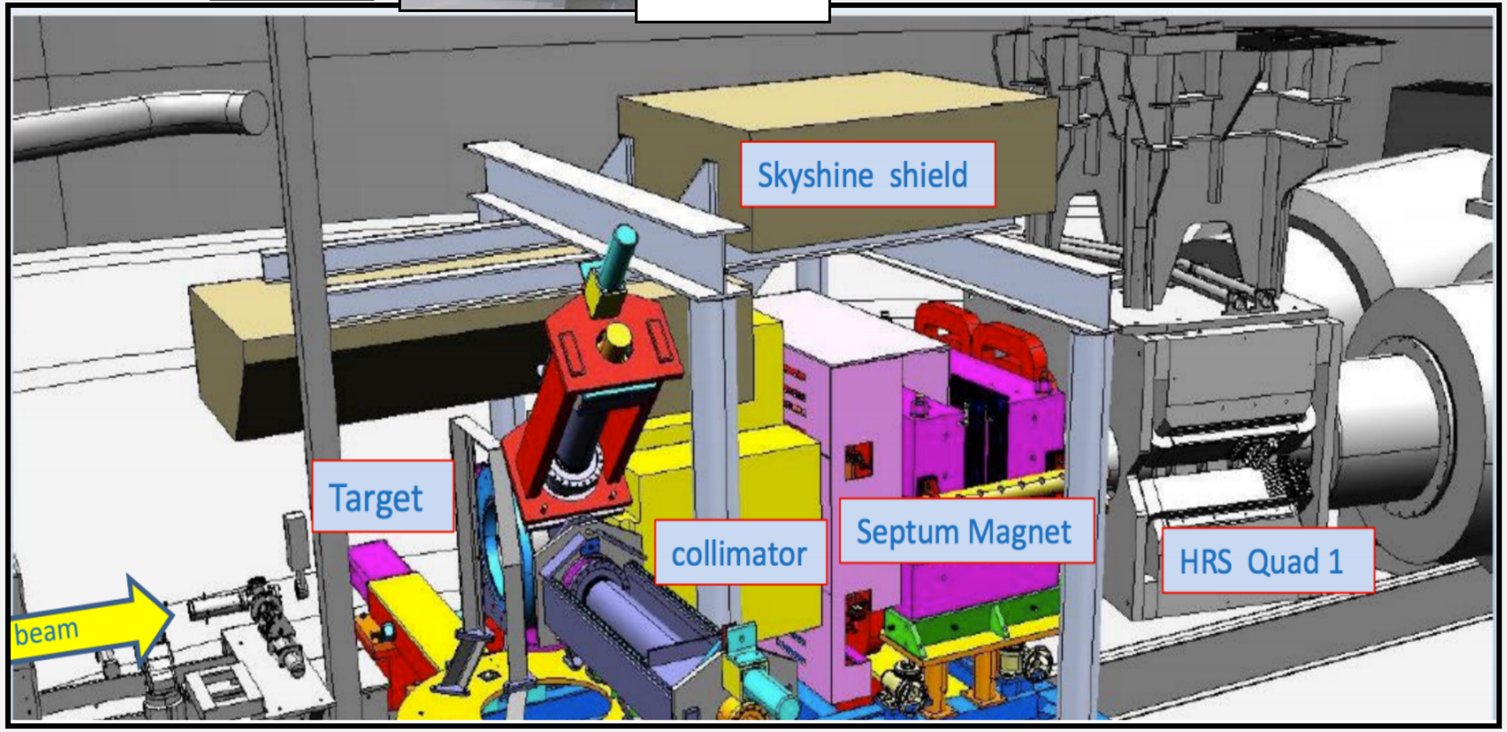

- 2.5 kW power in collimator
- Concrete and plastic around collimator region
- Concrete above to stop up-going neutrons creating “skyshine” boundary dose rates

^{208}Pb Target

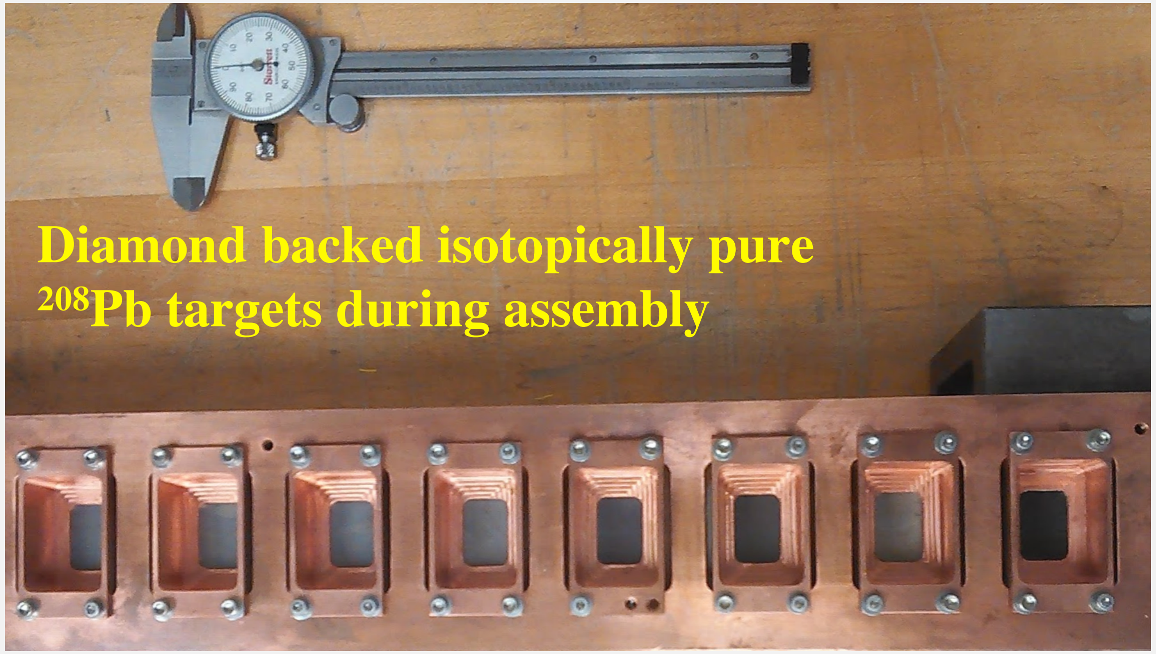

- Diamond-lead-diamond sandwich targets were used to get heat out of the target to cryocooling
- Diamond eventually breaks down, and lead is damaged
- PREX-1 proved concept and demonstrated target lifetime
- For PREX-2 we prepared a complement of 10 isotopically pure targets (used 6, as expected)
- Simulations predicted approximately 72 W of power deposition from the 70 μA rastered beam

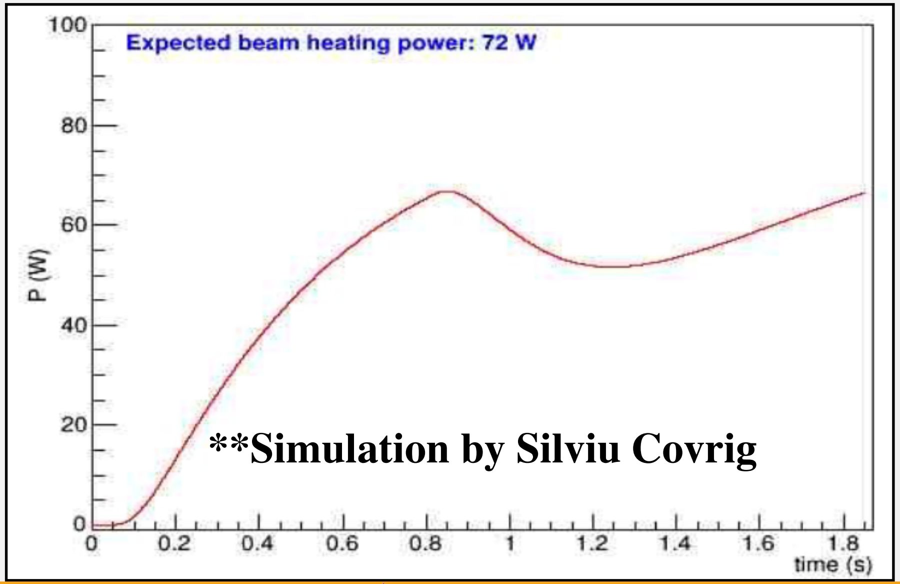

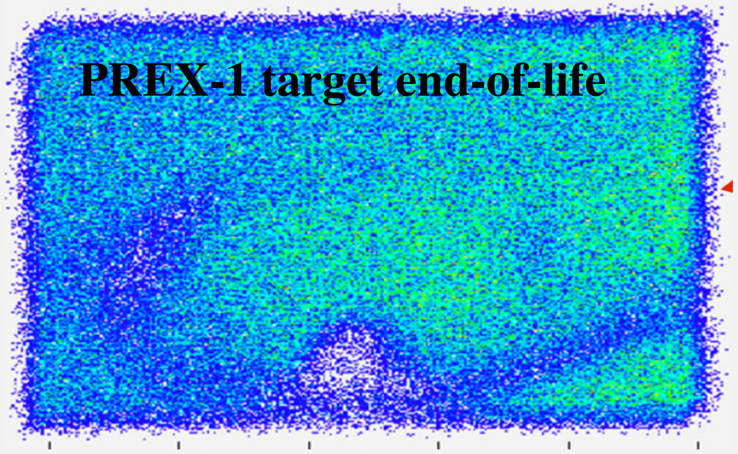

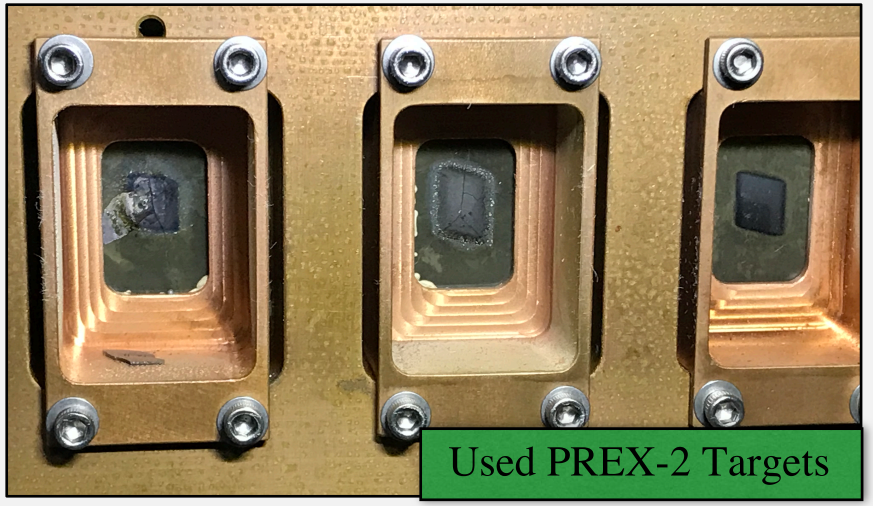

Target Design

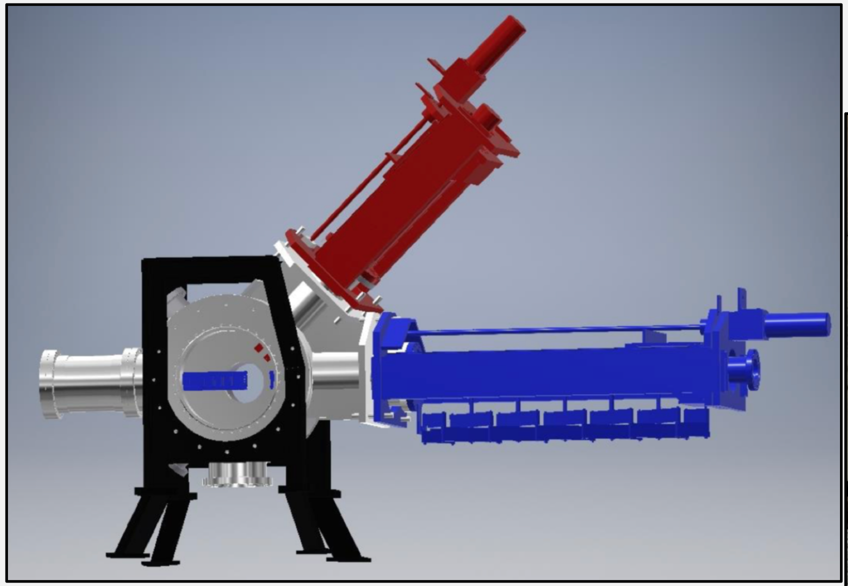

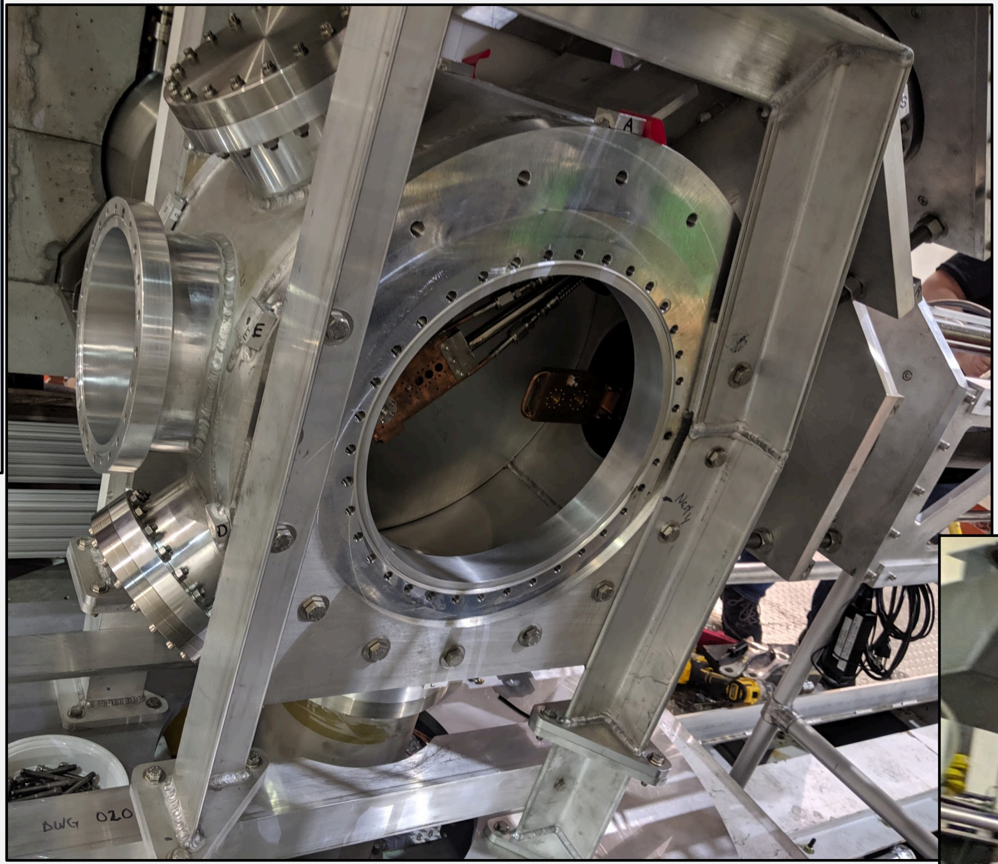

Watercell target

- Long horizontal target ladder
- 45^0 optics ladder

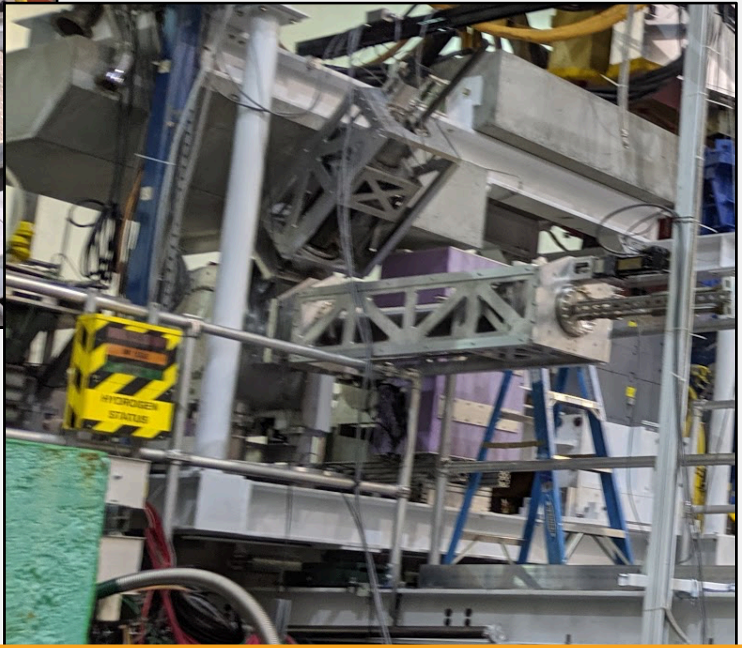

Challenging system, successfully implemented by the target group (esp. Dave Meekins)

Absolute Angle Calibration - Watercell

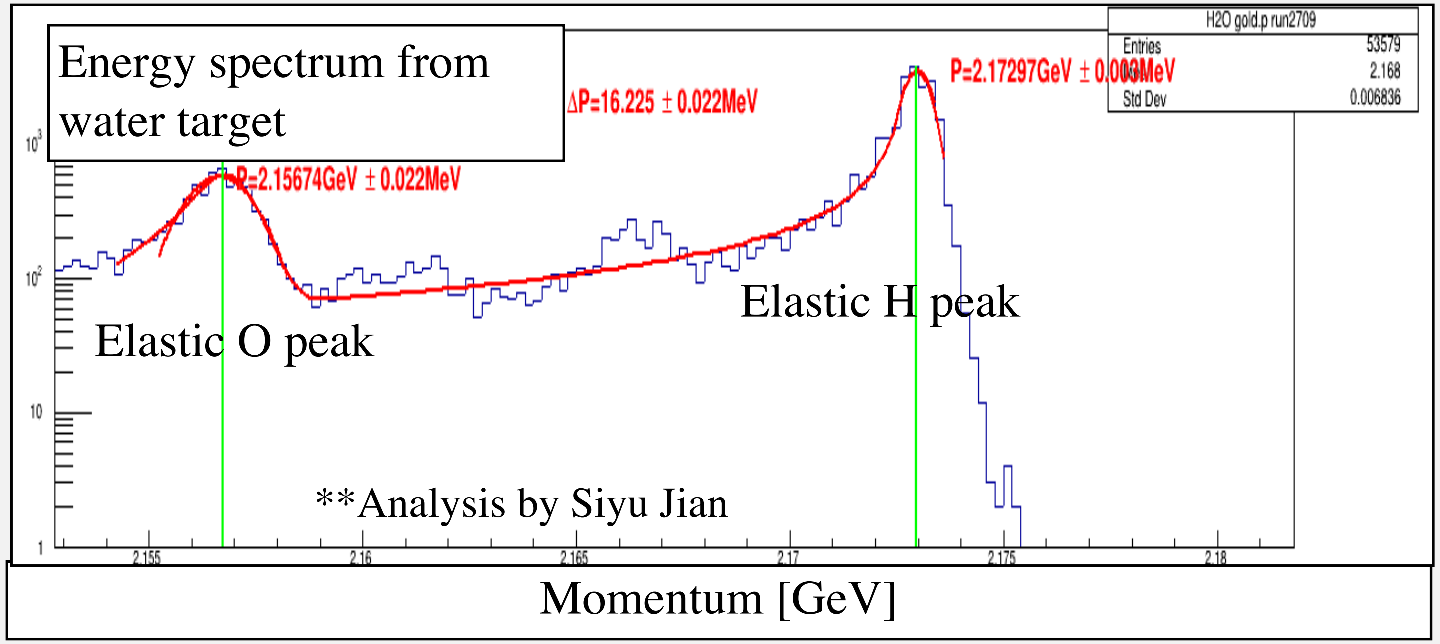

- Critical to measure the absolute scattering angle to high precision
- Nuclear recoil method
- ^{1}H and ^{16}O in one target (same E-loss) provides straightforward measurement of angle, insensitive to other calibrations

$$A_{PV} \approx \frac{G_F \boxed{Q^2}}{4\pi\alpha\sqrt{2}} \frac{Q_W\, F_W(Q^2)}{Z\, F_{\rm ch}(Q^2)}$$

recoil momentum difference ⟶ scattering angle

$$\Delta E' = E'_O - E'_H = E \left(\frac{1}{1 + \frac{2E\sin^2(\frac{\theta}{2})}{M_O}} - \frac{1}{1 + \frac{2E\sin^2(\frac{\theta}{2})}{M_H}} \right)$$

- Determined central angle (4.76^0) to $\delta\theta = 0.02^0$
- $\langle Q^2 \rangle = 0.00616 \pm 0.00004$ GeV^2 ($\delta Q^2/Q^2 = 0.65\%$)

Beam Corrections

- Steep form-factor and very forward angle: very sensitive to beam corrections.
- Beam jitter noise several times greater than counting statistics

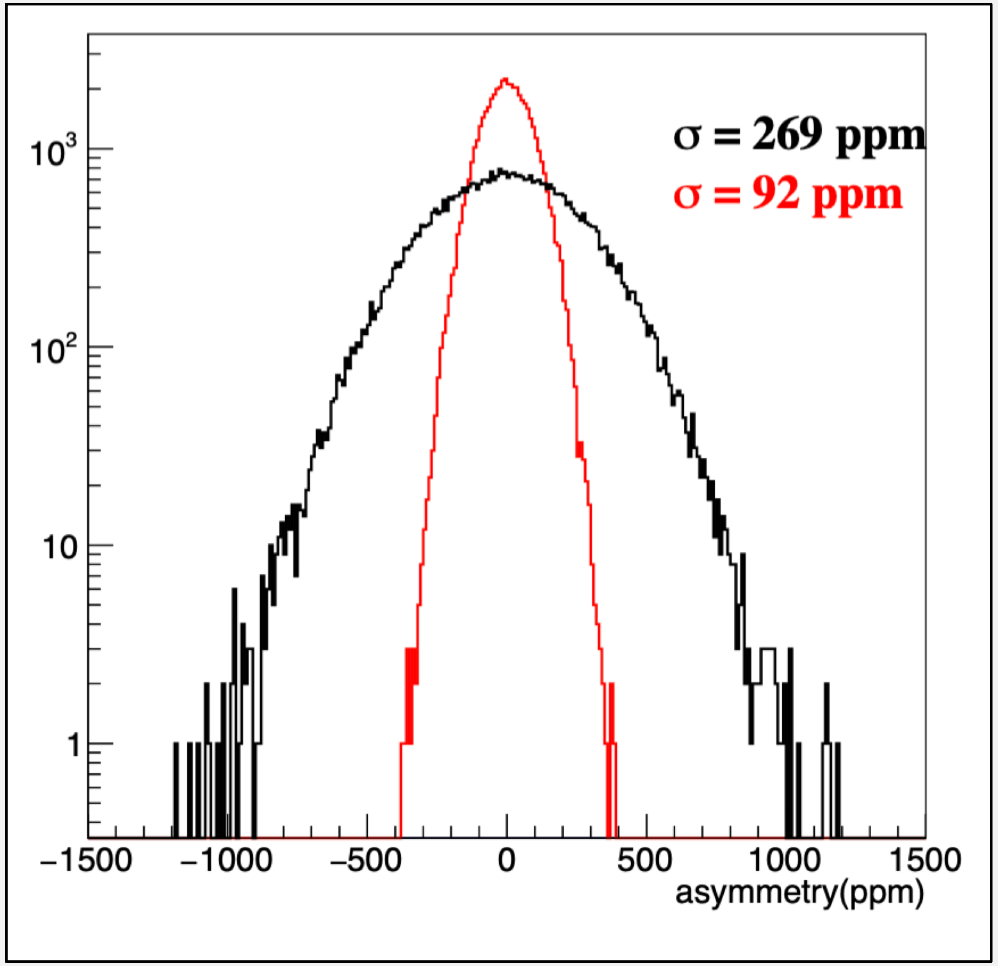

$$A = A_{raw} - A_Q - \sum_i \beta_i \Delta x_i - \beta_E A_E$$

- Potential for systematic error if average beam asymmetries are not well corrected
- Multiple techniques used to calibrate correction factors (β_i)

Beam Modulation system

- To span the 5 dimension phase space of beam motion at the target (position, angle, energy) we made use of a set of 6 coils and an energy vernier
  - The extra set of air-core dipoles (coils) can be used as a cross check to confirm our procedure doesn’t introduce unwanted noise
  - This modulation is automated and was performed throughout the data taking period

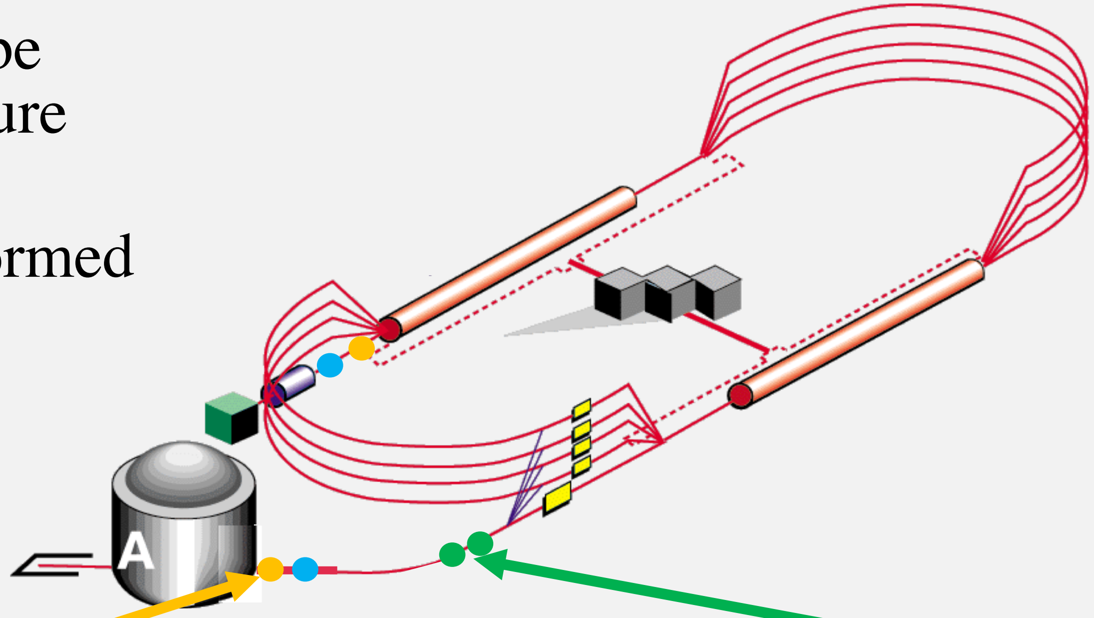

Beam monitors determine trajectory and parameters onto target

Beam modulation system spans the phase space of beam motion

Beam Correction Techniques

Multivariate Regression:

$$\chi^2 = \sum \left(A_{raw} - \sum_i \beta_i \Delta M_i \right)^2, \quad \frac{\partial \chi^2}{\partial \beta_i} = 0$$

- χ^2 **minimization**
- Variation in β_i dominated by **'strength sharing'**
- Bias by **(anti-)correlated electronic noise**
- Slope 'diluted' by **monitor resolution**

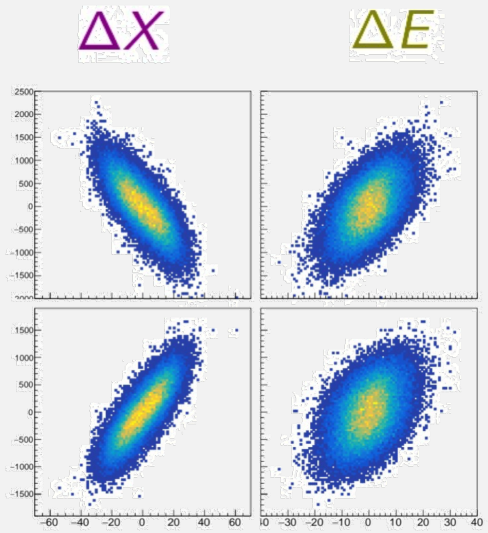

Beam Modulation:

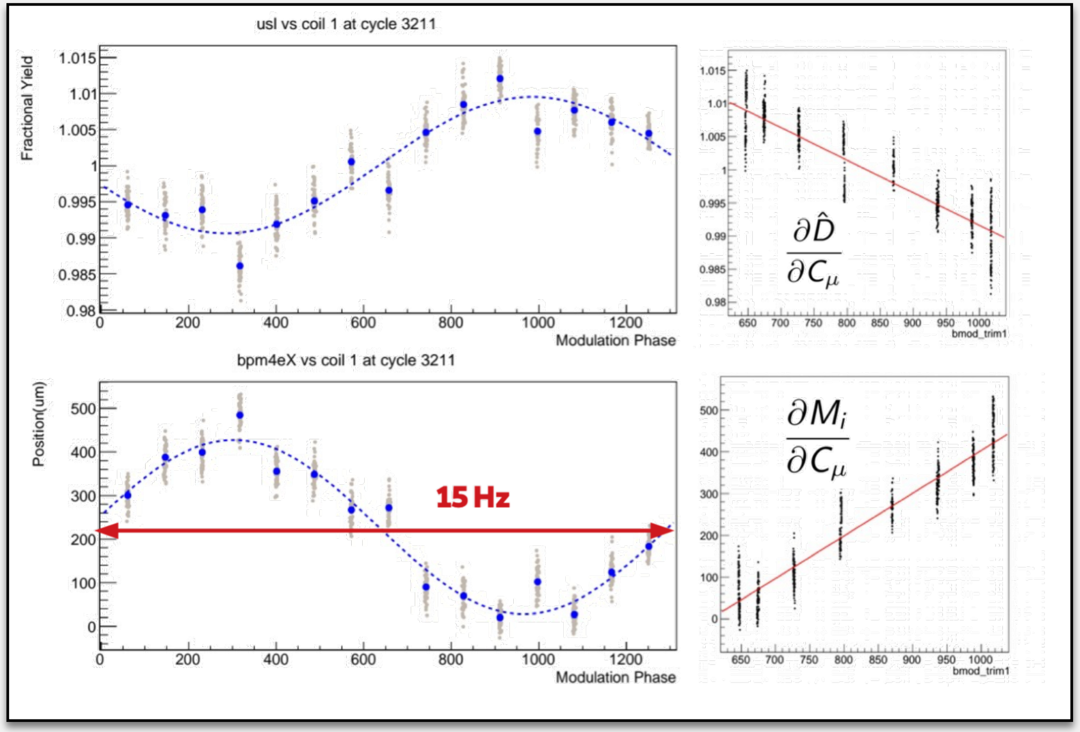

- **Modulation amplitude** $\sim$ 100 um
  - beam random jitter $<$ 10 um
  - monitor resolution 0.4 um
- **15 Hz Frequency** with **repeating measurements** suppresses, e.g.
  - instrumental electronic noise (60 Hz line)
  - random fluctuation in beam motion

Eigenvector analysis and ranking of beam fluctuations

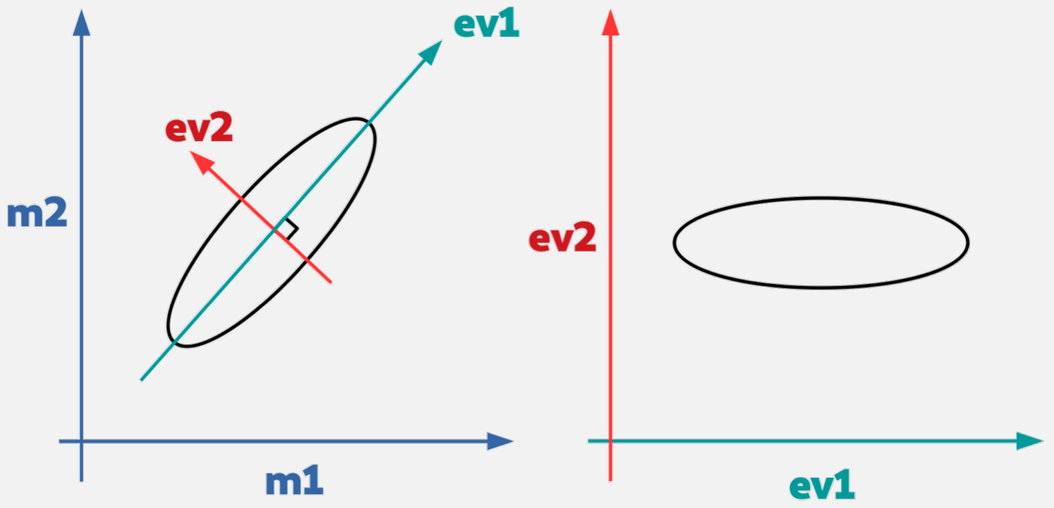

- **Diagonalize** BPMs covariance matrix $\mathcal{S}$ with eigenvalues decomposition: $\mathcal{Q}^T \mathcal{S} \mathcal{Q} = \Lambda$
- **Normalization:** $\mathcal{Q}^T \mathcal{Q} = \mathbb{I}$
- **Ranking** eigenvectors by eigenvalue $\lambda_1 > \lambda_2 > \lambda_3 \ldots$
- $\sqrt{\lambda}$ = RMS: **the ranking of beam fluctuations**

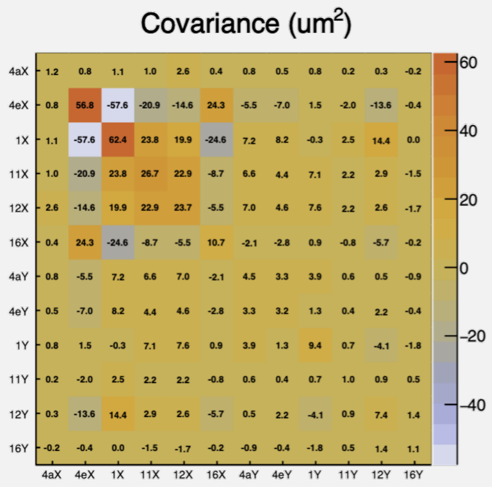

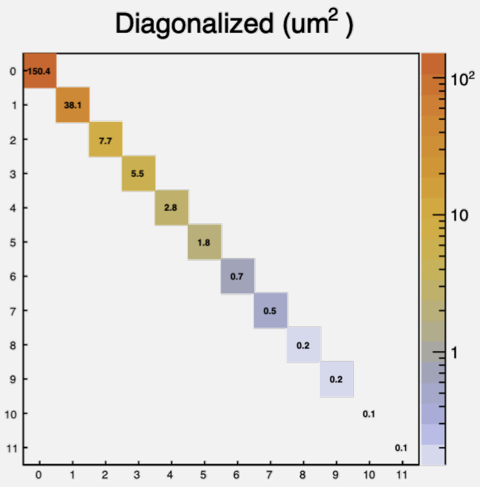

	RMS(um)
X1	14.9
Y1	9.6
E	7.0
Y2	3.3
X2	2.6
	1.3
	0.9
	0.7
	0.4
	0.3
	0.3
	0.3

Mostly BPM Electronic Noise

Over the course of the run, these dynamic eigenvectors retained their identification with dominance of specific beam monitors

- Helps understand the removal of noise/bias from regression with extra bpms
- Assists direct comparison of beam modulation and regression techniques

Work (and figures) by Tao Ye

Method of Lagrange Multipliers

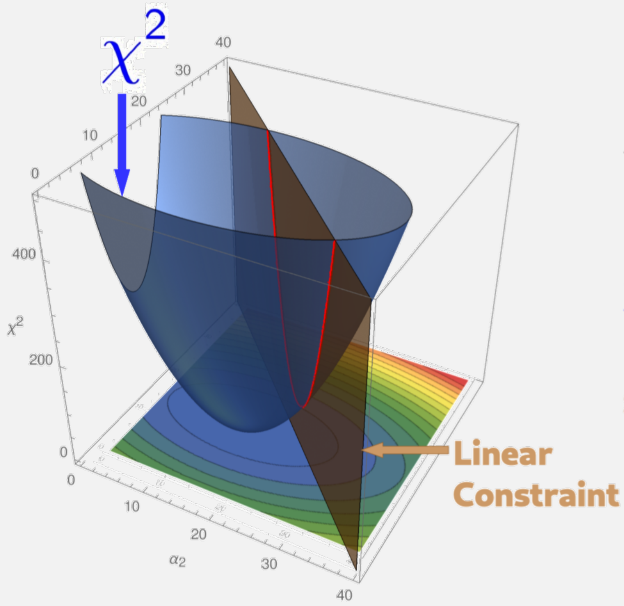

$$\mathcal{L} = \chi^2 + \sum_{\mu} \lambda_\mu \left(\frac{\partial D}{\partial C_\mu} - \sum_i \beta_i \frac{\partial M_i}{\partial C_\mu} \right)$$

χ^2 minimization with **beam modulation sensitivities constraints**:

$$\frac{\partial \mathcal{L}}{\partial \beta_i} = 0, \quad \frac{\partial \mathcal{L}}{\partial \lambda_\mu} = 0$$

"Hybrid" of regression and beam modulation techniques

- regression precision but beam modulation accuracy
- Assists direct comparison of beam modulation and regression techniques

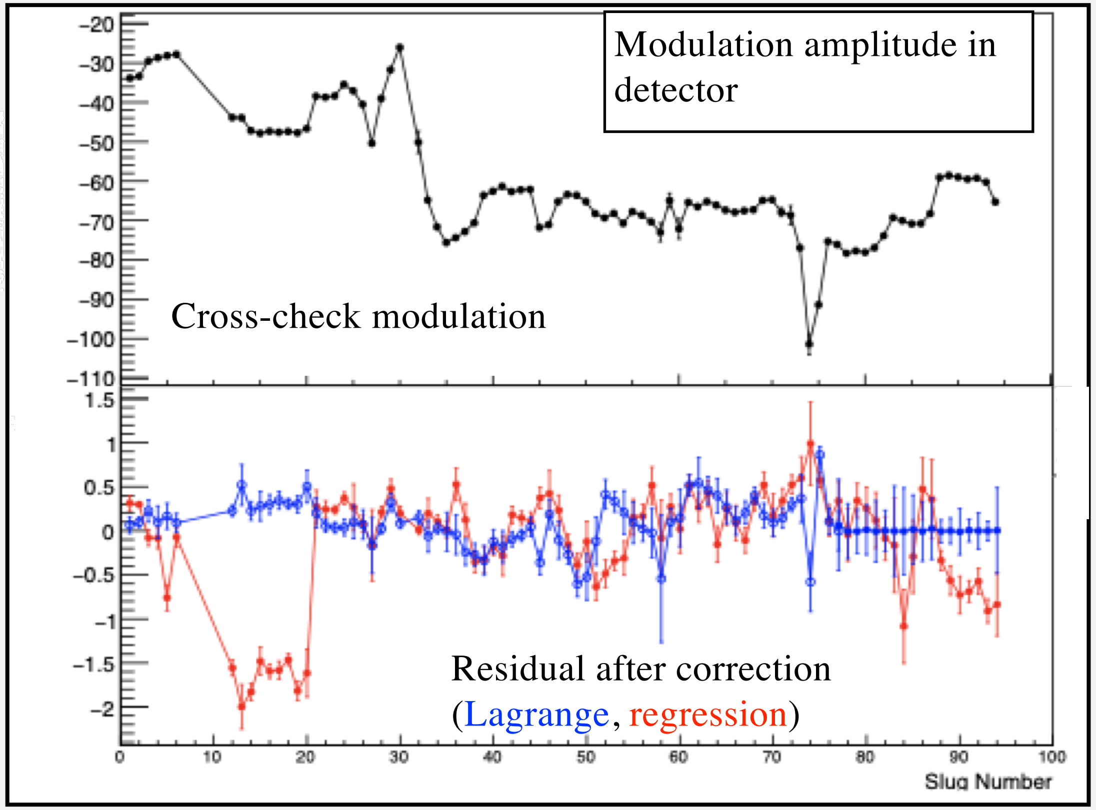

Analysis chain

- **Constraint** 12 BPMs with chosen 5 coils
- **Residual Sensitivity** is checked by other 2 coils
- **Statistics** test
- **Regression** cross-check

Beam corrections cross-checks

Three independent techniques are used and compared

- Lagrange multiplier regression
- regression
- beam modulation

Corrections are compared over the run and seen to be statistically compatible

Slopes are compared:
very small (<3%) differences

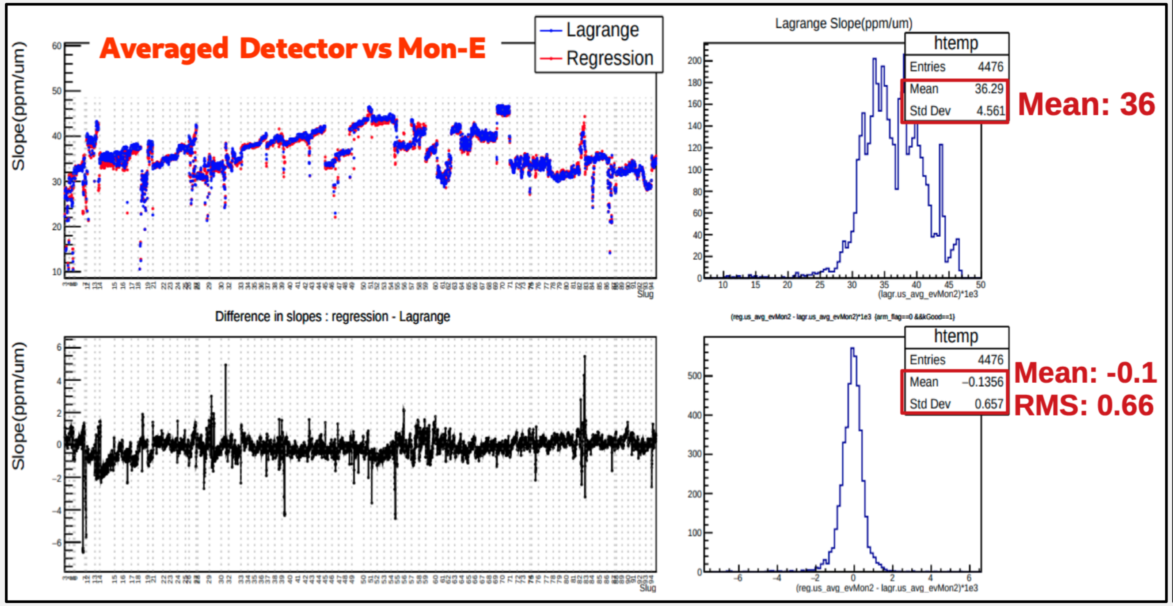

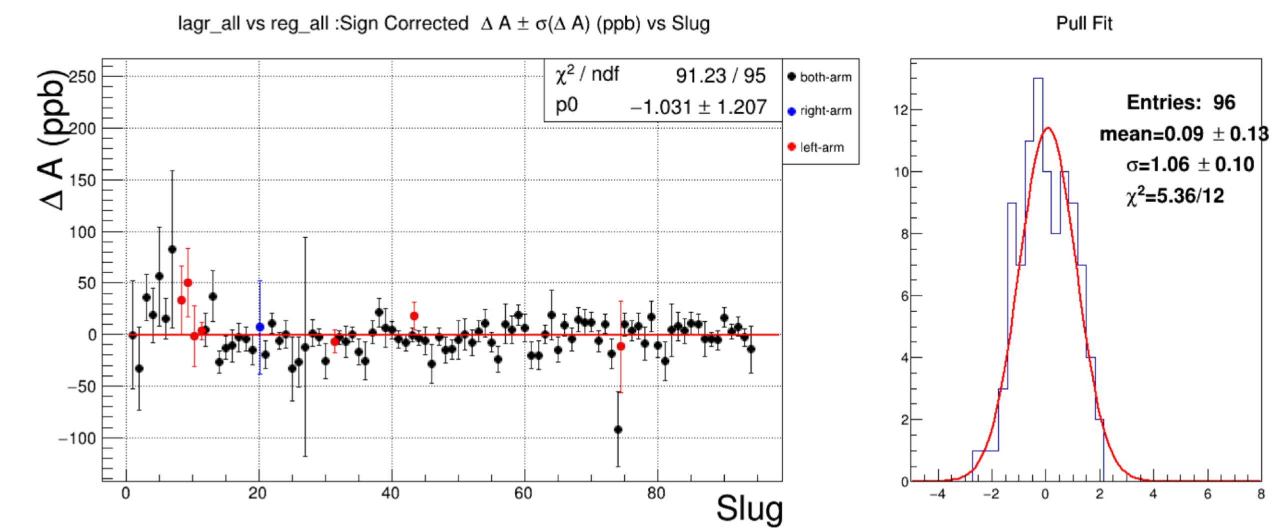

Figure: ΔA between Regression and Lagrange Multiplier by slug

	ΔA (ppb)	$\sigma(\Delta A)$(ppb)	χ^2/ndf
dit vs Lagrange	2.2	3.5	86.4 / 95
Lagrange vs Reg	-1.0	1.2	91.2 / 95

Beam correction summary

- Use Lagrange Multiplier Regression, 3% slope uncertainty
- Three independent techniques agree

Careful configuration of the polarized source kept beam difference averages very small

Δx_i	Mean (nm)	Convergence (nm)
Target x	-1.1 nm	2.0 nm
Target y	1.1 nm	0.5 nm
Angle x	-0.28 nrad	0.32 nrad
Angle y	0.14 nrad	0.09 nrad
Energy BPM	2.3 nm	1.1 nm

- Left/right symmetric detectors, so correction dominated by energy

type	Mean(ppb)
X1	-22.33
Y1	22.5
E	-70.44
Y2	-2.84
X2	9.7
	1.27
	-0.01
	1.06
	0.26
	0.24
	0.18
	0.06
Total	-60.38

Total beam corrections:
(60.4 ± 2.5) ppb

PREX-II Data Set

- Very close watch on-line data stream - beam conditions, detector response, etc.
- Frequent contact with MCC operators to maintain running conditions
- “prompt" analysis process flagged more subtle problems
- Daily grooming and review in “WAC" process
- (analysis development leader Paul King)

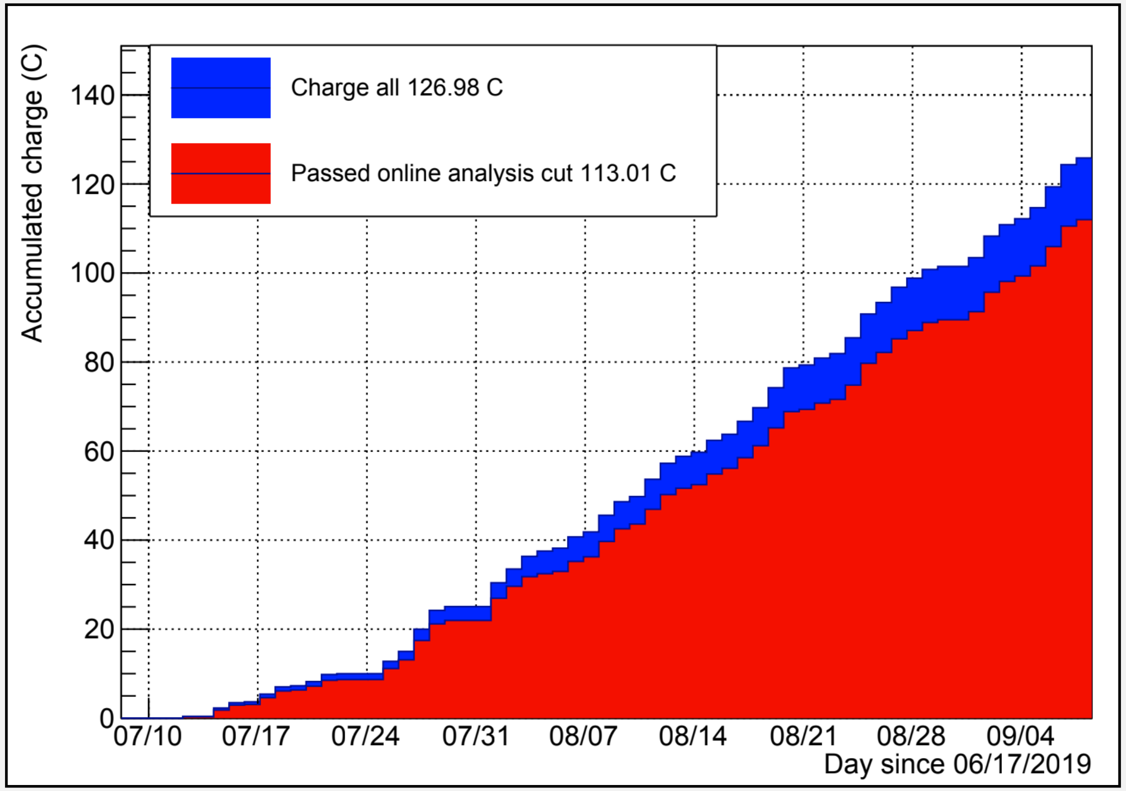

- At the end of the experiment after our realtime analysis we collected about 113 C of charge on target with only about 14 C being excluded in calibrations or due to poor beam conditions (mostly, trip recovery, beam excursions, or beam monitor issues)
- For our final analysis we managed to recover a bit more data ~ 114 C

Data Overview: Corrected Asymmetry

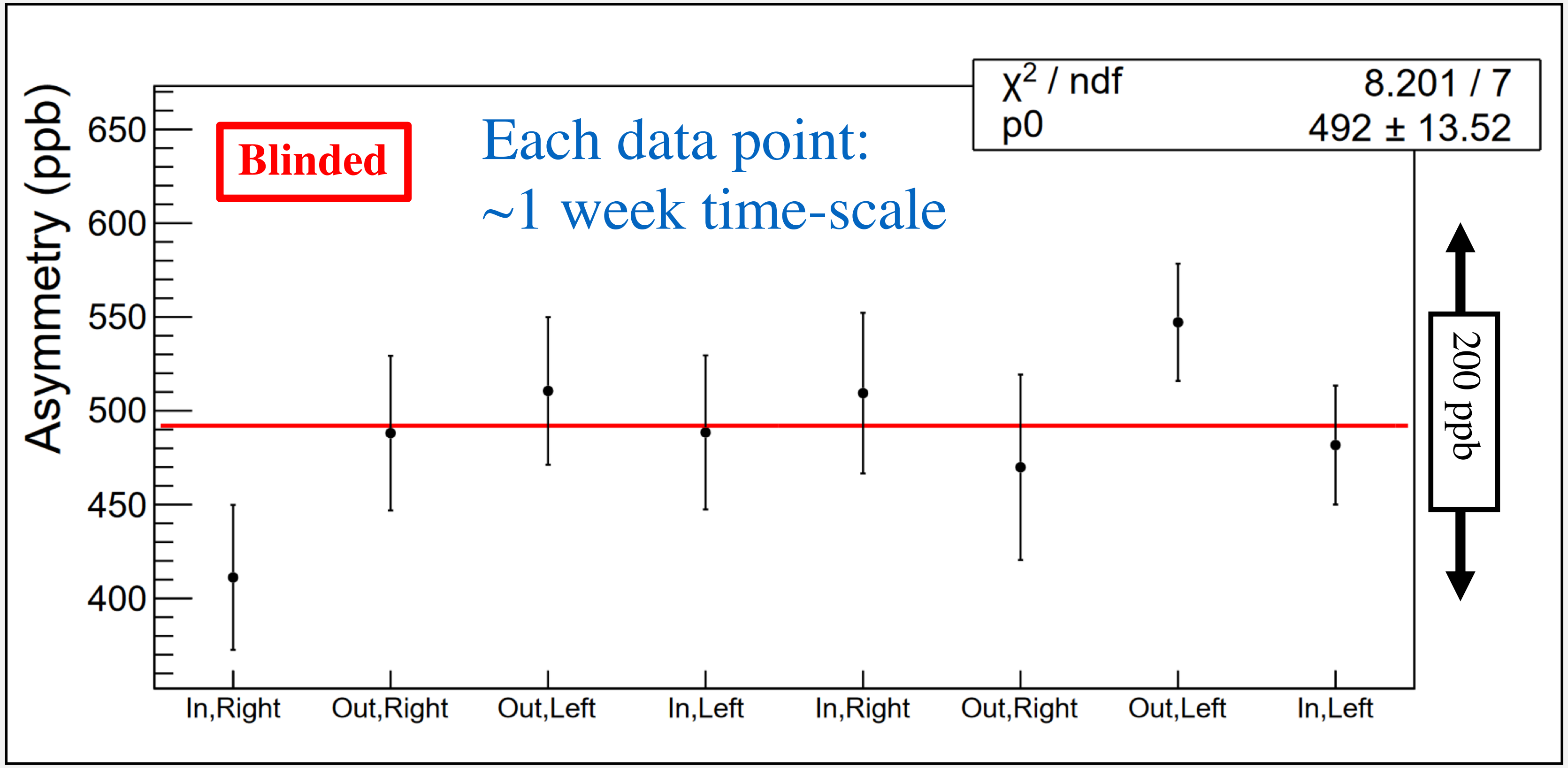

Half Wave Plate: IN/OUT
Wien: Left/Right

Total beam corrections:
(60.4 ± 2.5)ppb

- The corrected asymmetry removed effects from beam asymmetries and noise
- Still to come: polarization and background corrections

Data Overview: Corrected Asymmetry

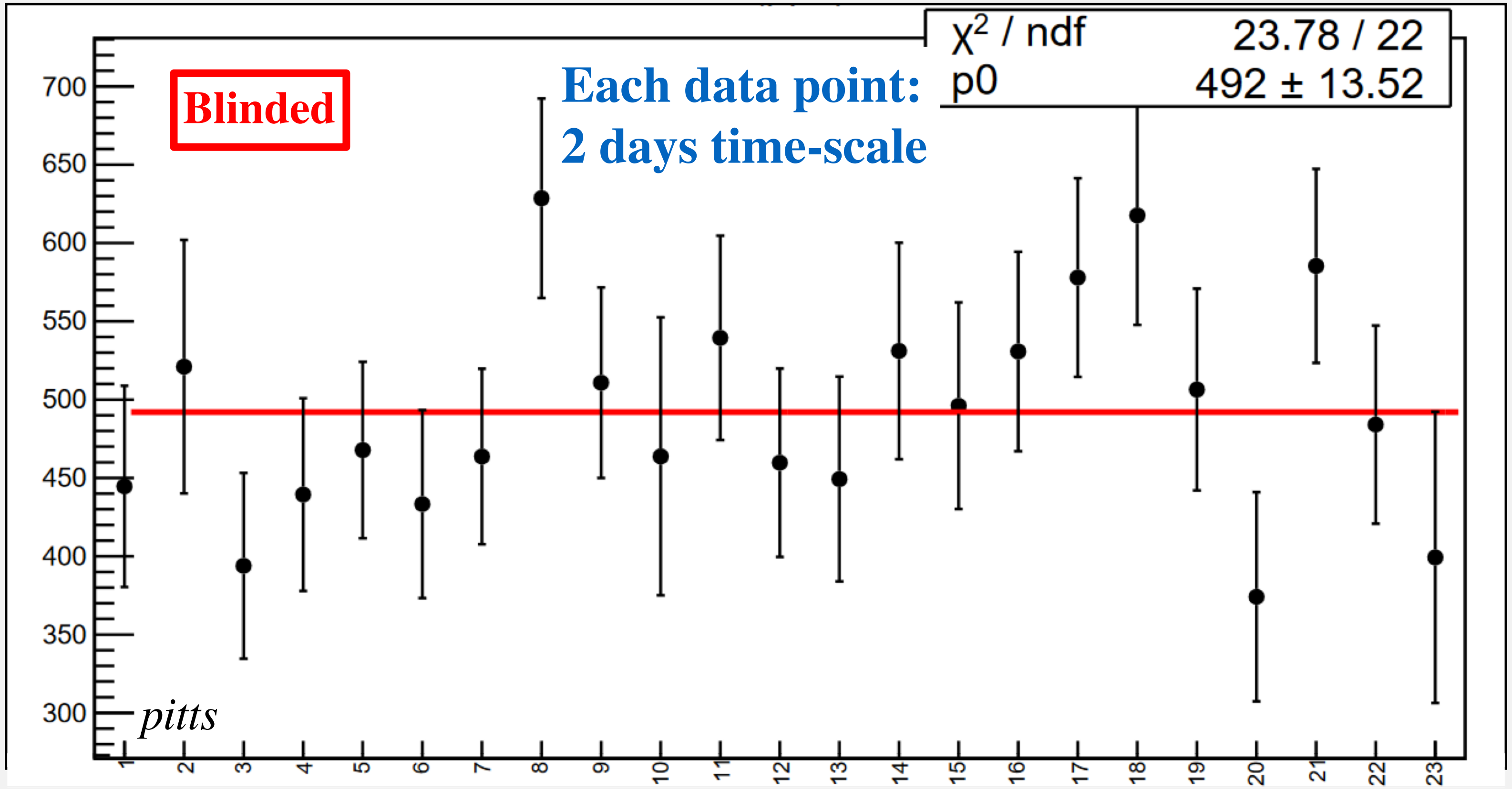

Averaged over IHWP states

- The corrected asymmetry removed effects from beam asymmetries and noise
- Still to come: polarization and background corrections

Null Asymmetry

$$A_{null} = \frac{A_{IN} - A_{OUT}}{2}$$

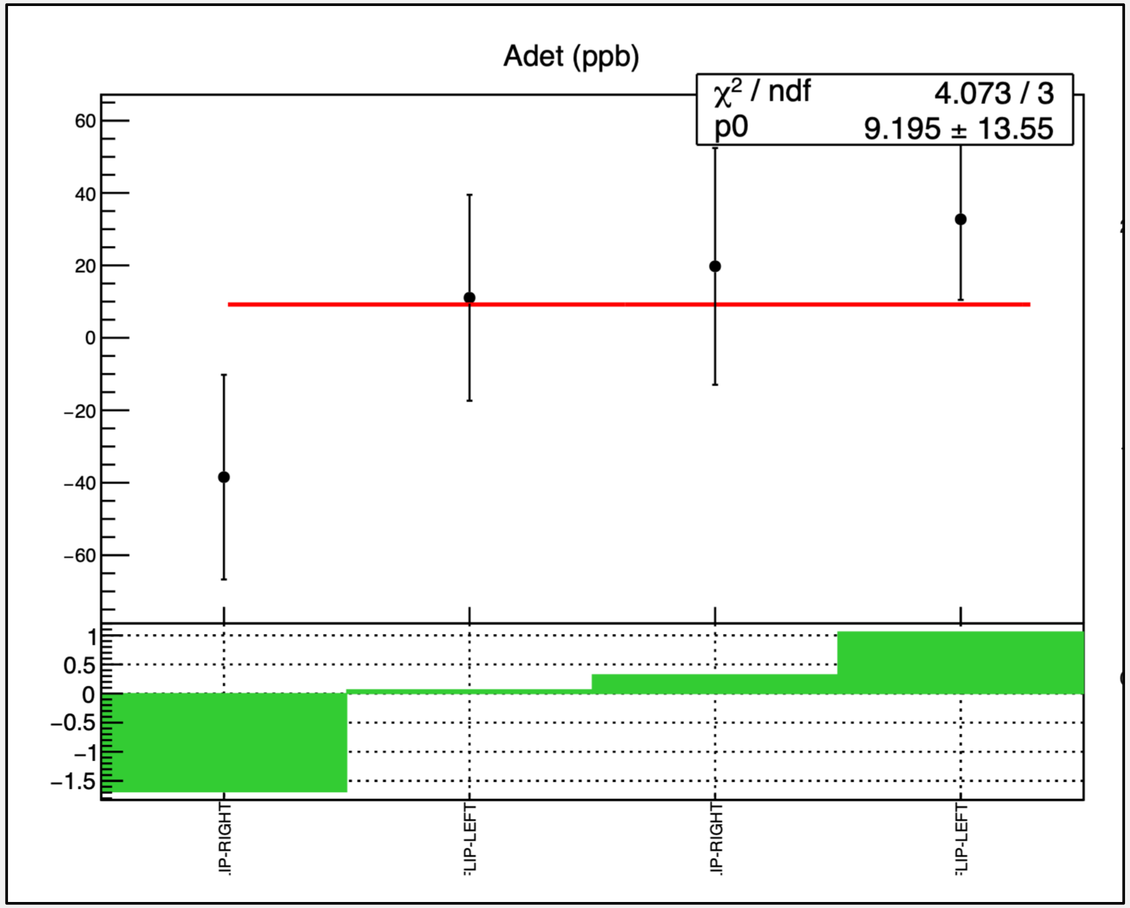

Wien states

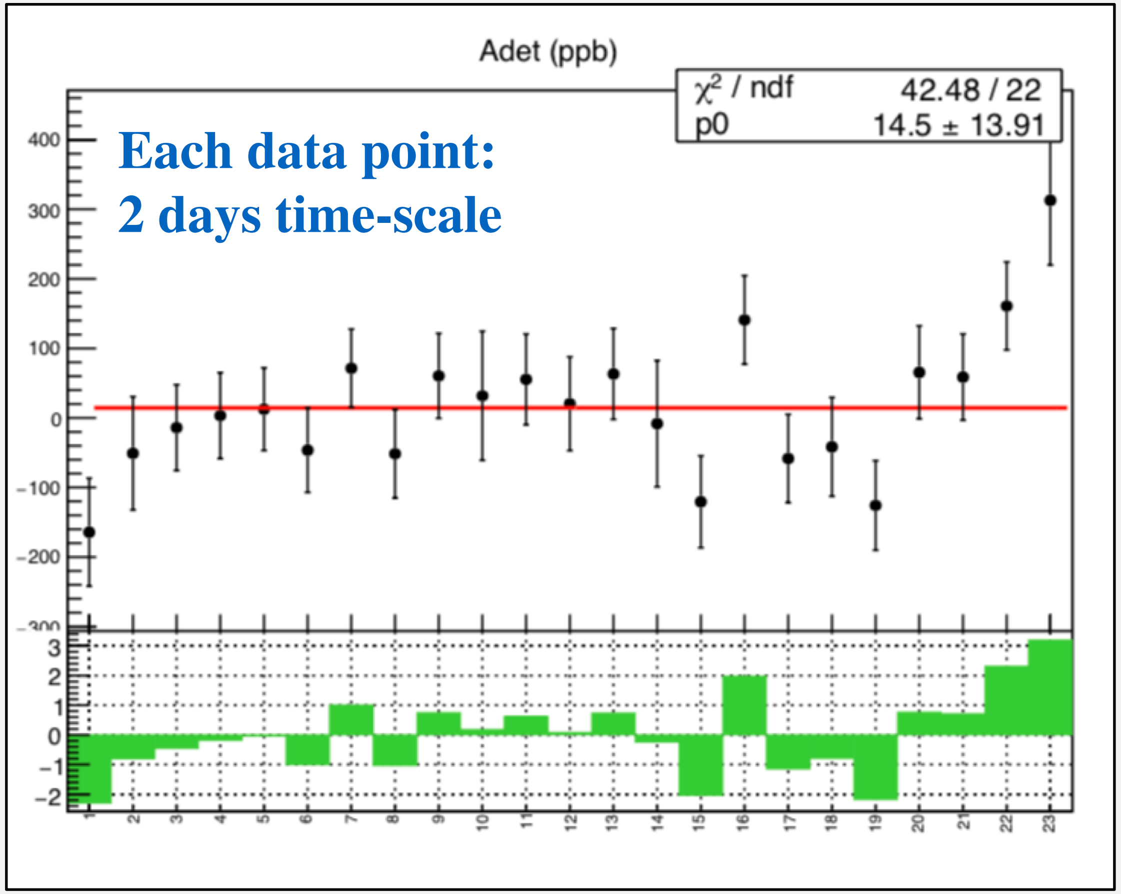

pitt timescale

Data Overview: Corrected Asymmetry

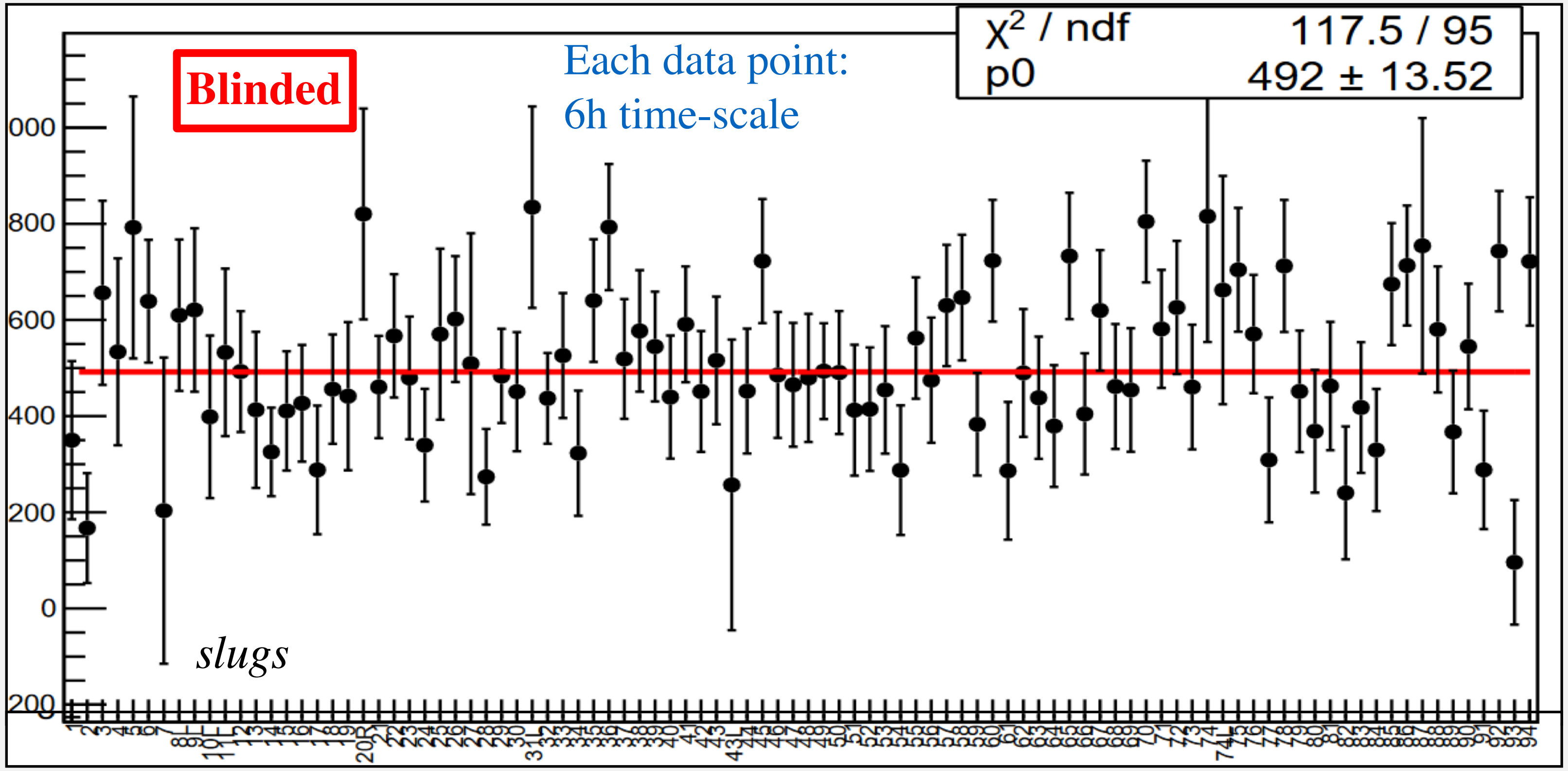

- The corrected asymmetry removed effects from beam asymmetries and noise
- Still to come: polarization and background corrections

Data Overview: Corrected Asymmetry

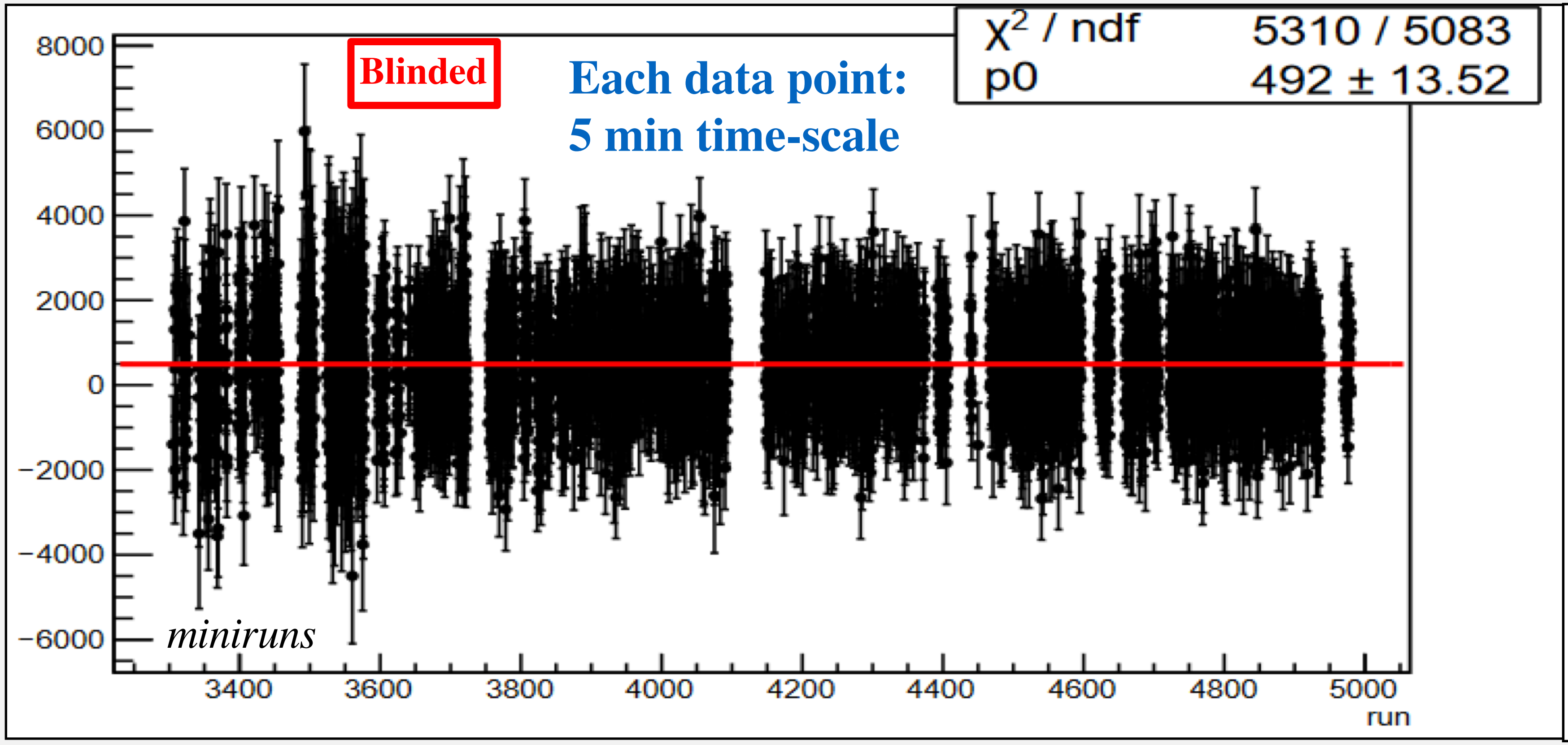

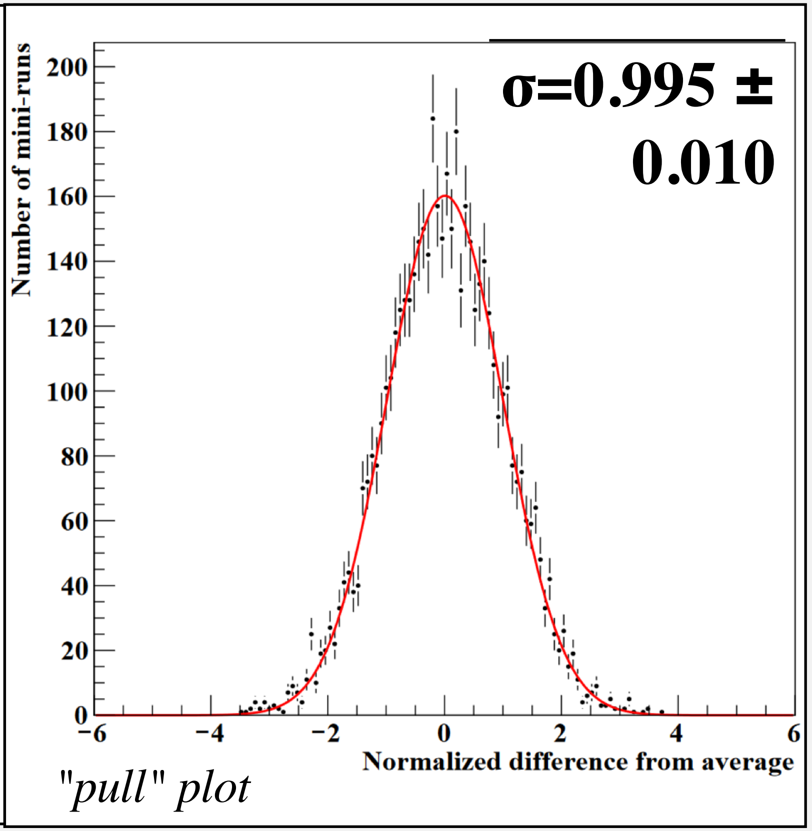

- The corrected asymmetry removed effects from beam asymmetries and noise
- Still to come: polarization and background corrections

Data Overview: Corrected Asymmetry

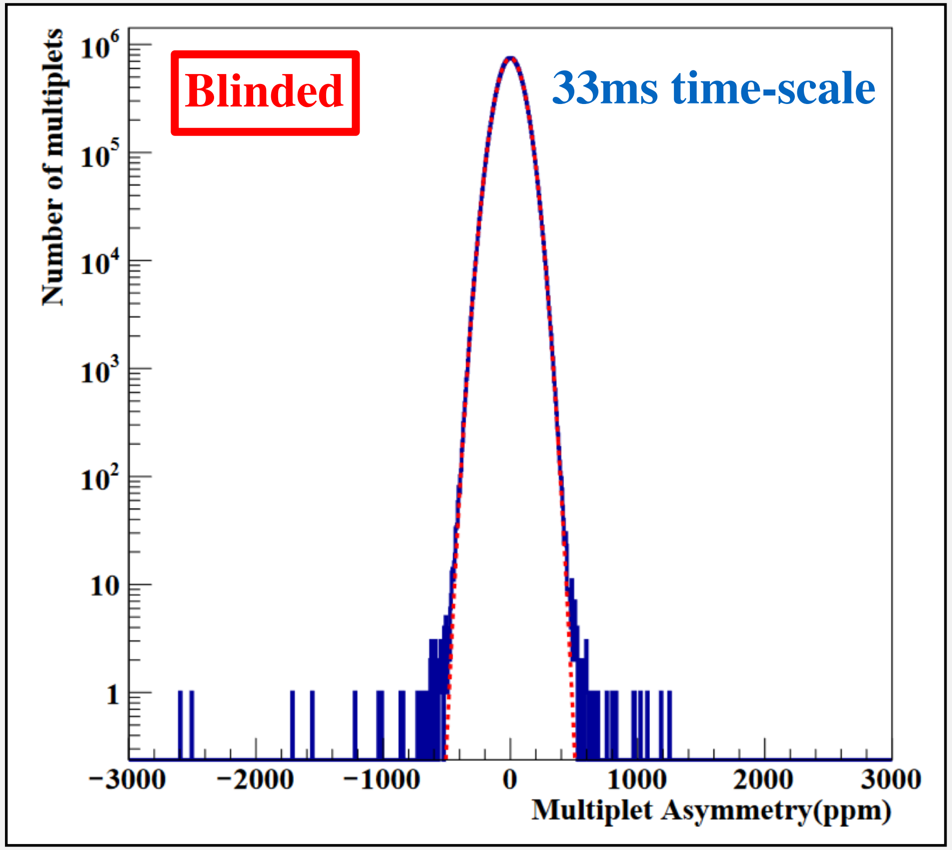

- Individual octets (70μA, 240Hz)
- Extremely consistent widths, negligible tails

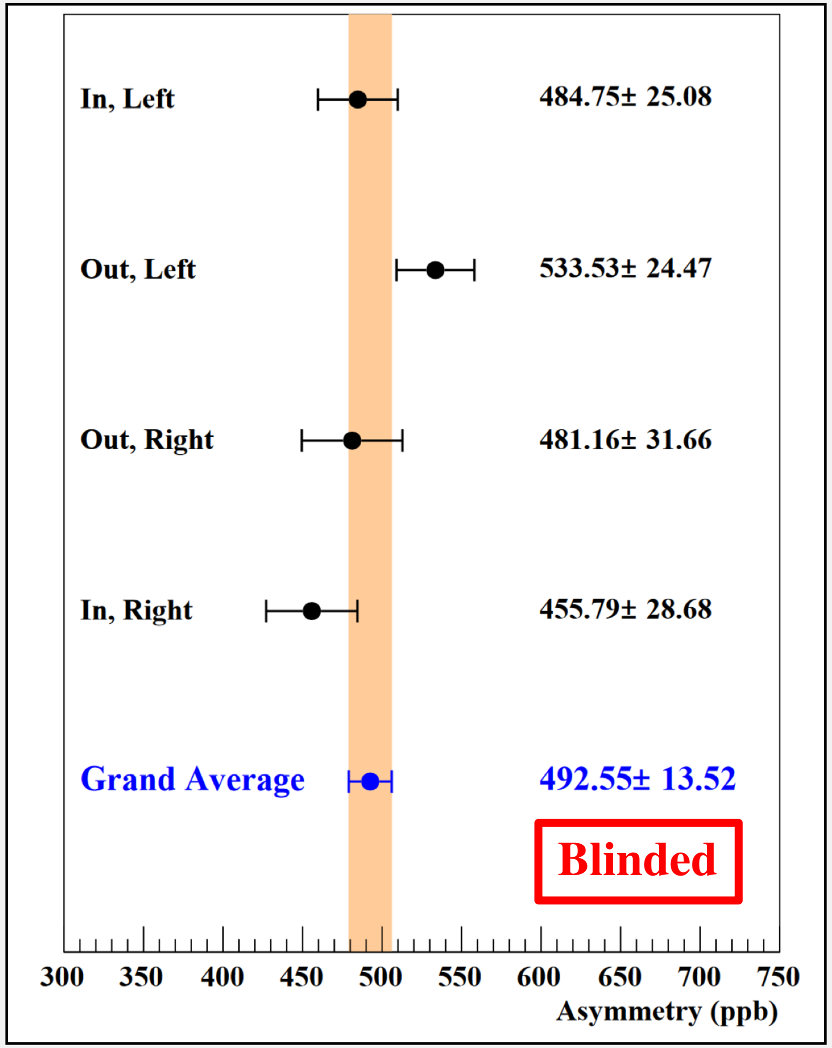

Final result averaging over all IHWP and Wien flip configurations

Extracting APV

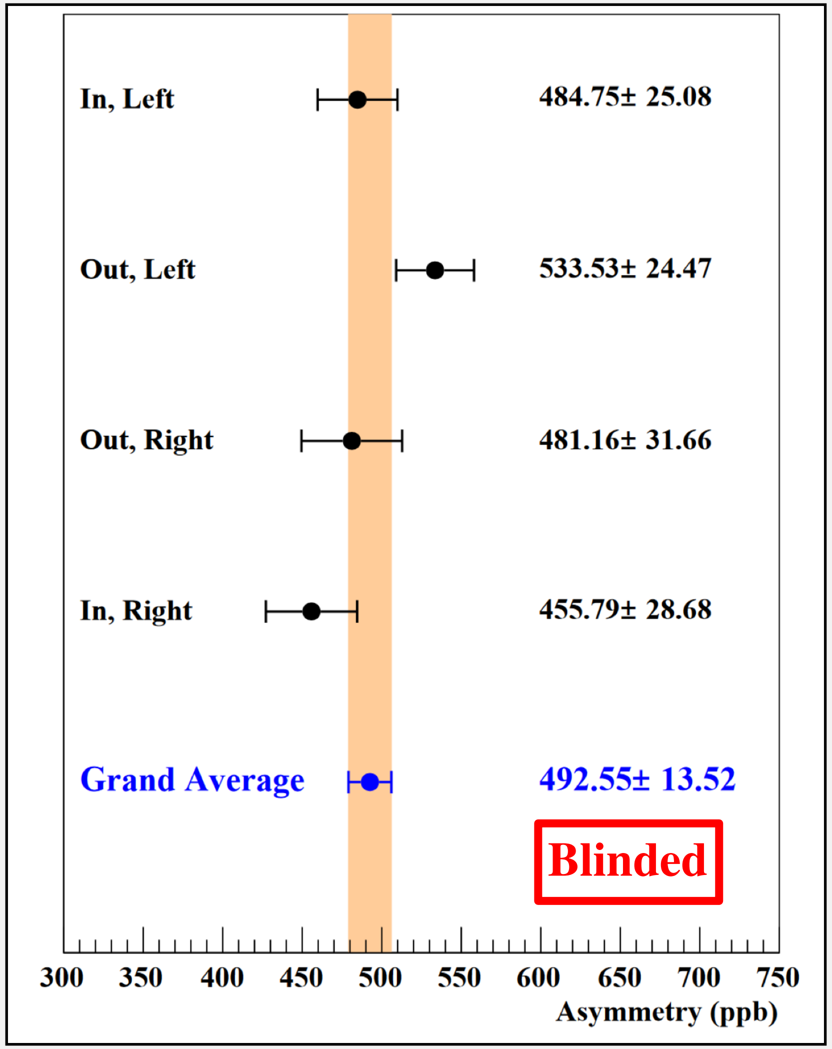

$$A_{PV} = R_{acceptNorm} \frac{A_{corr}/P_e - \sum_i A_i f_i}{1 - \sum_i f_i}$$

$$A_{corr} = A_{raw} + A_{beam} + A_{nonLin} - A_{blind}$$

- $R_{acceptNorm}$: Acceptance normalization
- A_{corr}: Corrected asymmetry
- P_e: Polarization
- A_i: Background asymmetry
- f_i: Background fraction

Extracting A_{PV}

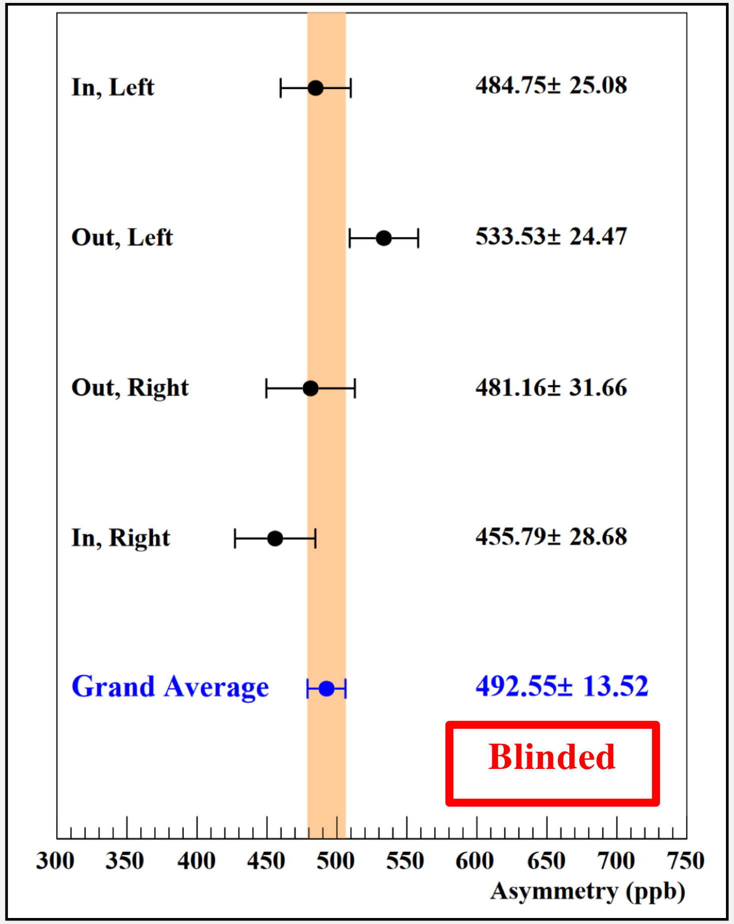

$$A_{PV} = R_{acceptNorm} \frac{A_{corr}/P_e - \sum_i A_i f_i}{1 - \sum_i f_i}$$

$$A_{corr} = A_{raw} + A_{beam} + A_{nonLin} - A_{blind}$$

Blinded A_{PV}:
(549.4 ± 16.1)ppb

	A_{PV} uncertainty contribution [ppb]	A_{PV} uncertainty contribution [%]
Polarization	5.23	0.95%
Acceptance normalization	4.56	0.83%
Beam correction	2.98	0.54%
Non-linear detector response	2.69	0.49%
Carbon dilution	1.45	0.26%
Charge correction	0.25	0.04%
Inelastic contamination	0.12	0.02%
Total	**8.16**	**1.48%**

When taken all into account the experimental systematic uncertainty comes to just shy of 1.5%

Compared to proposal

PREX-2: 3% stat, 0.06 fm
CREX: 4% stat, 0.02fm

PREX-I
E=1.1 GeV, 5°
A=0.6 ppm

Charge Normalization	0.2%
Beam Asymmetries	1.1%
Detector Non-linearity	1.2%
Transverse Asym	0.2%
Polarization	1.3%
Target Backing	0.4%
Inelastic Contribution	<0.1%
Effective Q^2	0.5%
Total Systematic	**2.1%**
Total Statistical	**9%**

Achieved, published
statistics limited result,
systematics well under control

PREX-II
E=1.1 GeV, 5°
A=0.6 ppm
70 μA, 25+10 days

Charge Normalization	0.1%
Beam Asymmetries*	1.1%
Detector Non-linearity*	1.0%
Transverse Asym	0.2%
Polarization*	1.1%
Target Backing	0.4%
Inelastic Contribution	<0.1%
Effective Q^2	0.4%
Total Systematic	**2%**
Total Statistical	**3%**

*Experience suggests that leading systematic errors can be improved beyond proposal

	A_{PV} uncertainty contribution [ppb]	A_{PV} uncertainty contribution [%]
Polarization	5.23	0.95%
Acceptance normalization	4.56	0.83%
Beam correction	2.98	0.54%
Non-linear detector response	2.69	0.49%
Carbon dilution	1.45	0.26%
Charge correction	0.25	0.04%
Inelastic contamination	0.12	0.02%
Total	**8.16**	**1.48%**

Improved on proposed systematic uncertainties (as expected)

Unblinding

Blinded A_{PV}:
(549.4 ± 16.1)ppb

"Blinding box": an additive term on every octet asymmetry, randomly selected (flat) at the start of the run, from ± 160 ppb

Unblinded A_{PV}:
(550.0 ± 16.1)ppb

Blinding term turned out to be 0.5313 ppb

This is entirely just luck-of-the-draw 🙄

	Blindedasym - rawasym (ppb)	
ops	0.5313	Roadkill stew sounds mighty good right NOW. --- Unspecified collaborator
test1	6.0223	Roadlife stew sounds mighty good right NOW. --- Unspecified collaborator
test2	-96.6812	Porkbean stew sounds mighty good right NOW. --- Unspecified collaborator
test3	53.2091	Suspicious stew sounds mighty good right NOW. --- Unspecified collaborator
test4	-121.4924	Road-kill stew sounds mighty good right NOW. --- Unspecified collaborator

Weak Radius and Neutron Skin from PREX-II

Calculations by Chuck Horowitz

Preliminary

$$R_W = 5.795 \pm 0.082 \text{ fm} \rightarrow 1.4\%$$

$$R_W - R_{ch} = 0.292 \pm 0.082 \text{ fm}$$

$$R_n - R_p = 0.278 \pm 0.078 \text{ fm}$$

This includes statistical and systematic uncertainty.
There is model uncertainty (from the surface thickness) of 0.013 fm
and radiative γ-Z box correction* uncertainty of 0.006 fm

Thank you Jens Erler and Mikhail Gorchtein for the updated electroweak gamma-Z box corrections

Compare with PREX-I

Measured at different angles, so different Q^2 (and rather different sensitivities)

PREX-1

$$Q^2 = 0.0088 GeV^2$$

$$A_{PV} = [656 \pm 60(stat) \pm 14(syst)] ppb \rightarrow 9.4\%$$

PREX-2

$$Q^2 = 0.0062 GeV^2$$

$$A_{PV} = [550 \pm 16(stat) \pm 8(syst)] ppb \rightarrow 3.3\%$$

Combined: ~ 0.29 ± 0.07 fm (preliminary)

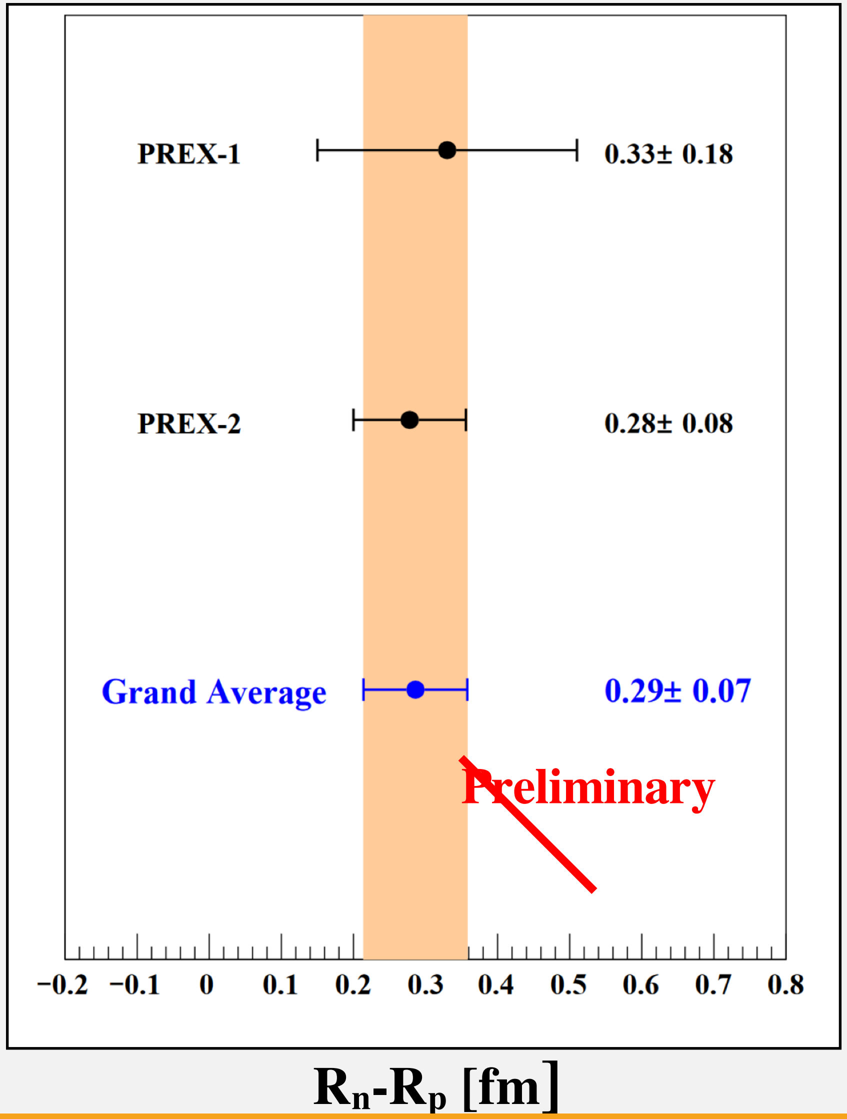

Implications of PREX-II

- We can make use of the existing models to relate the deformability of neutron stars to both neutron skin of Pb and to the neutron star radius

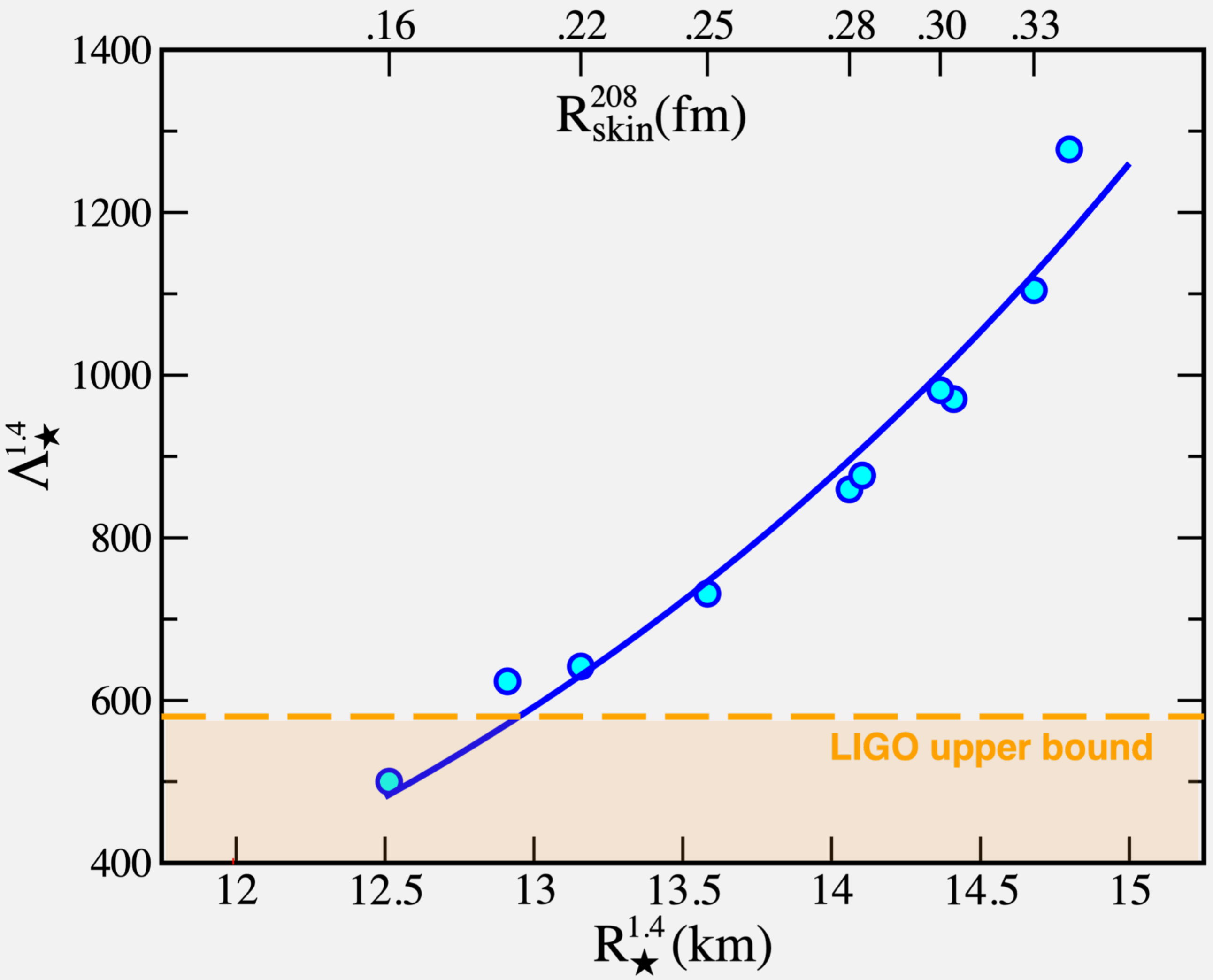

Implications of PREX-II

- We can make use of the existing models to relate the deformability of neutron stars to both neutron skin of Pb and to the neutron star radius
- The NICER result provides a bound on the radius of a neutron star

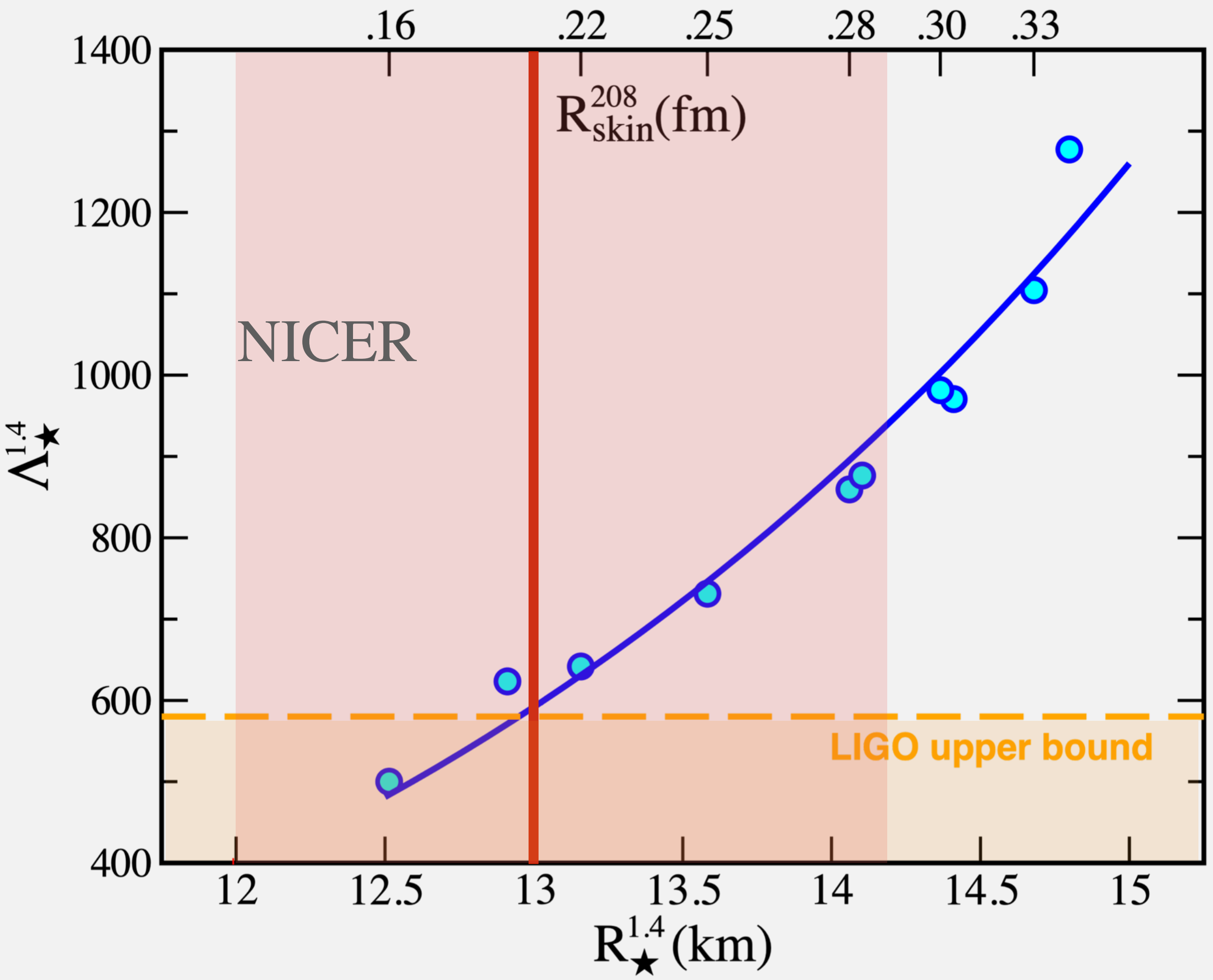

Implications of PREX-II

Preliminary

- We can make use of the existing models to relate the deformability of neutron stars to both neutron skin of Pb and to the neutron star radius
- The NICER result provides a bound on the radius of a neutron star
- The PREX-2 result is in good agreement with the NICER result and in slight tension with the tidal polarizability result obtained from GW170817 neutron star merge event observed by LIGO

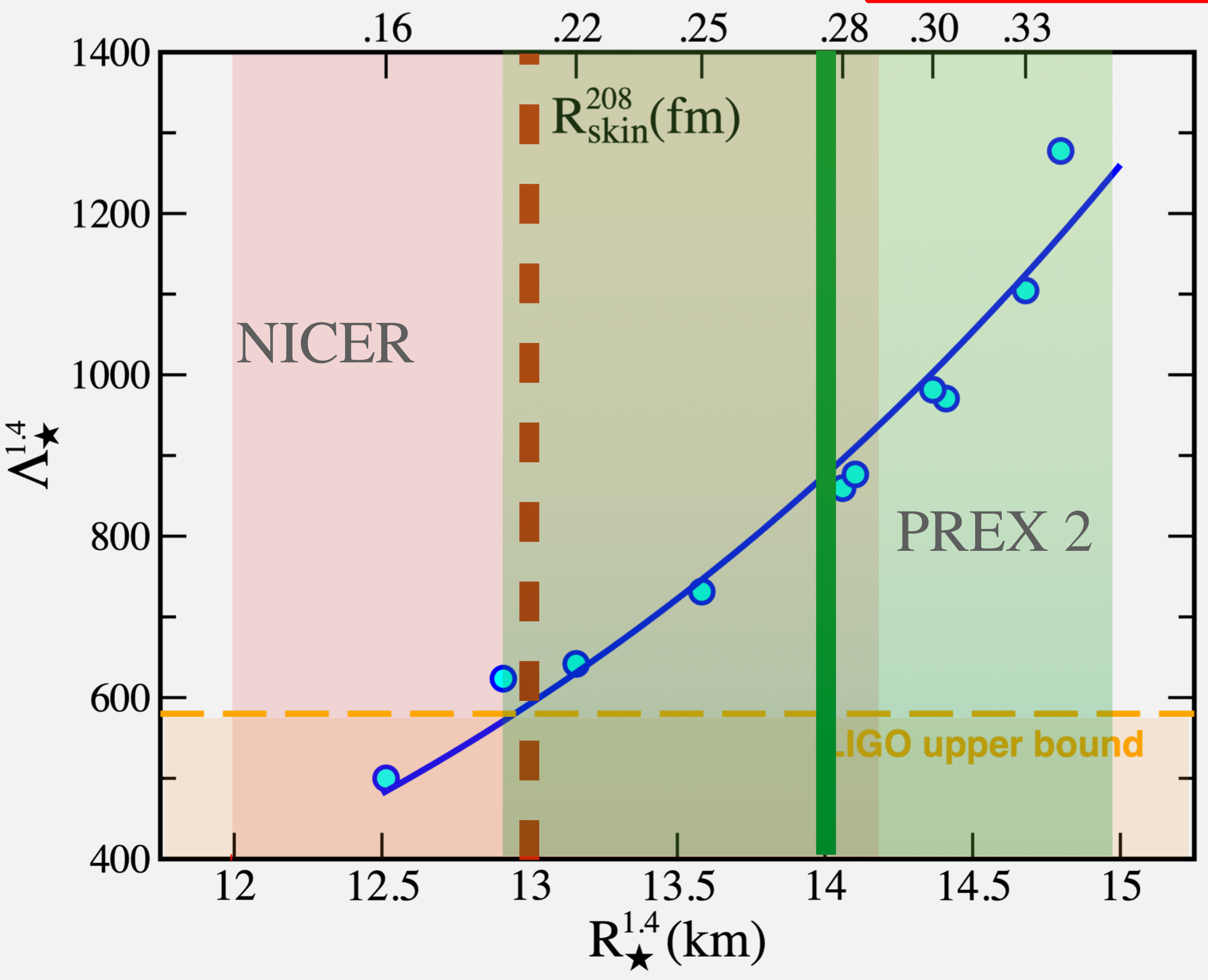

Implications of PREX-II: Central density at saturation

- The weak radius can be combined with the well known charge density to obtain the baryon density of ^{208}Pb
- This is the first clean determination of the central baryon density of a heavy nucleus and is accurate to 2%
- Provides an important benchmark to chiral EFT calculations that is closely related to nuclear saturation density

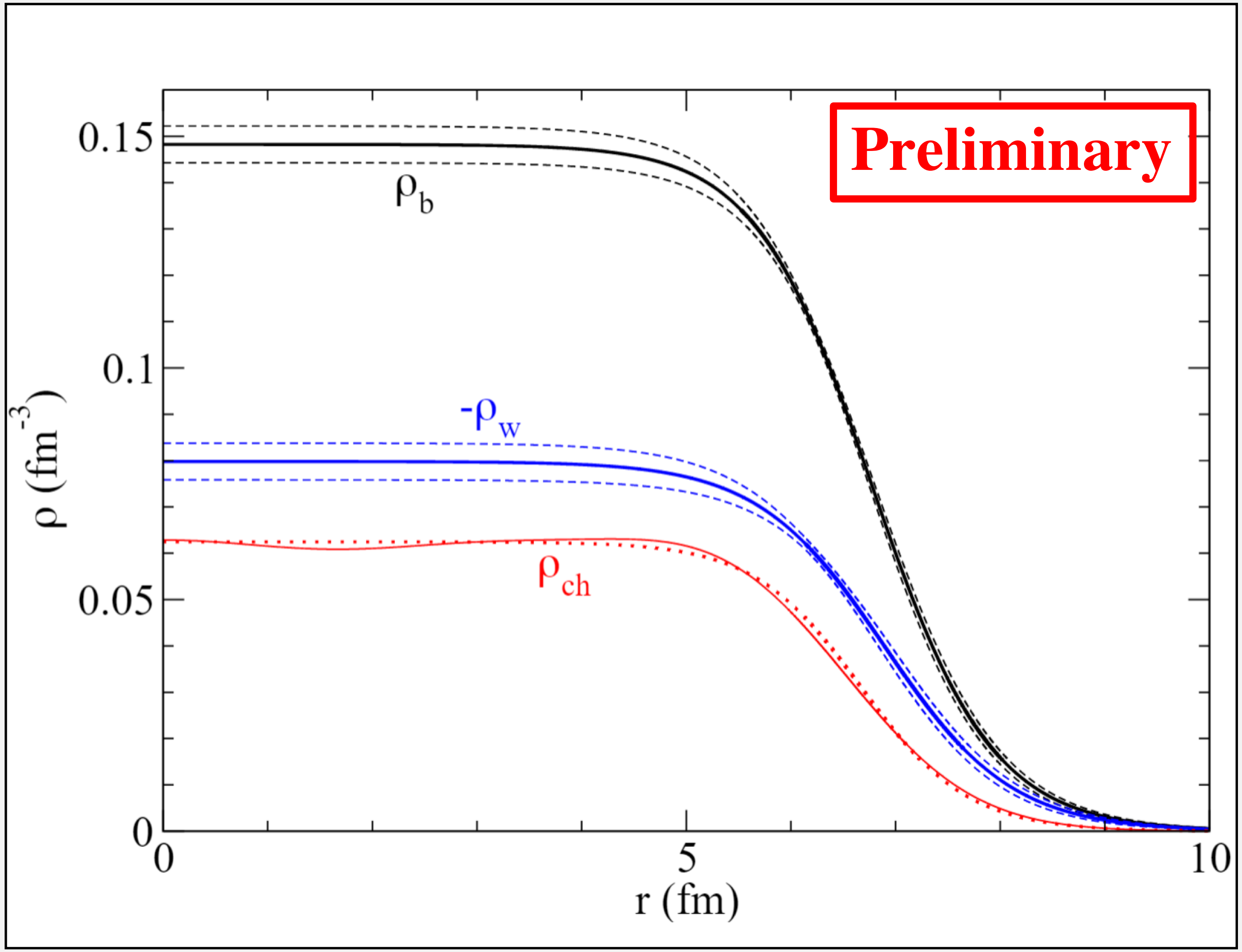

Calculations by Chuck Horowitz following PRC 102(2020) 044321

Density Dependence of Symmetry Energy

$$L \propto \frac{\partial S(\rho)}{\partial \rho}\Big|_{\rho_0}$$

Expectation: 60-70 MeV

Li and Han, PLB 727 (2013)

Tsang et al *Phys.Rev.C* 86 (2012) 015803 (2012)

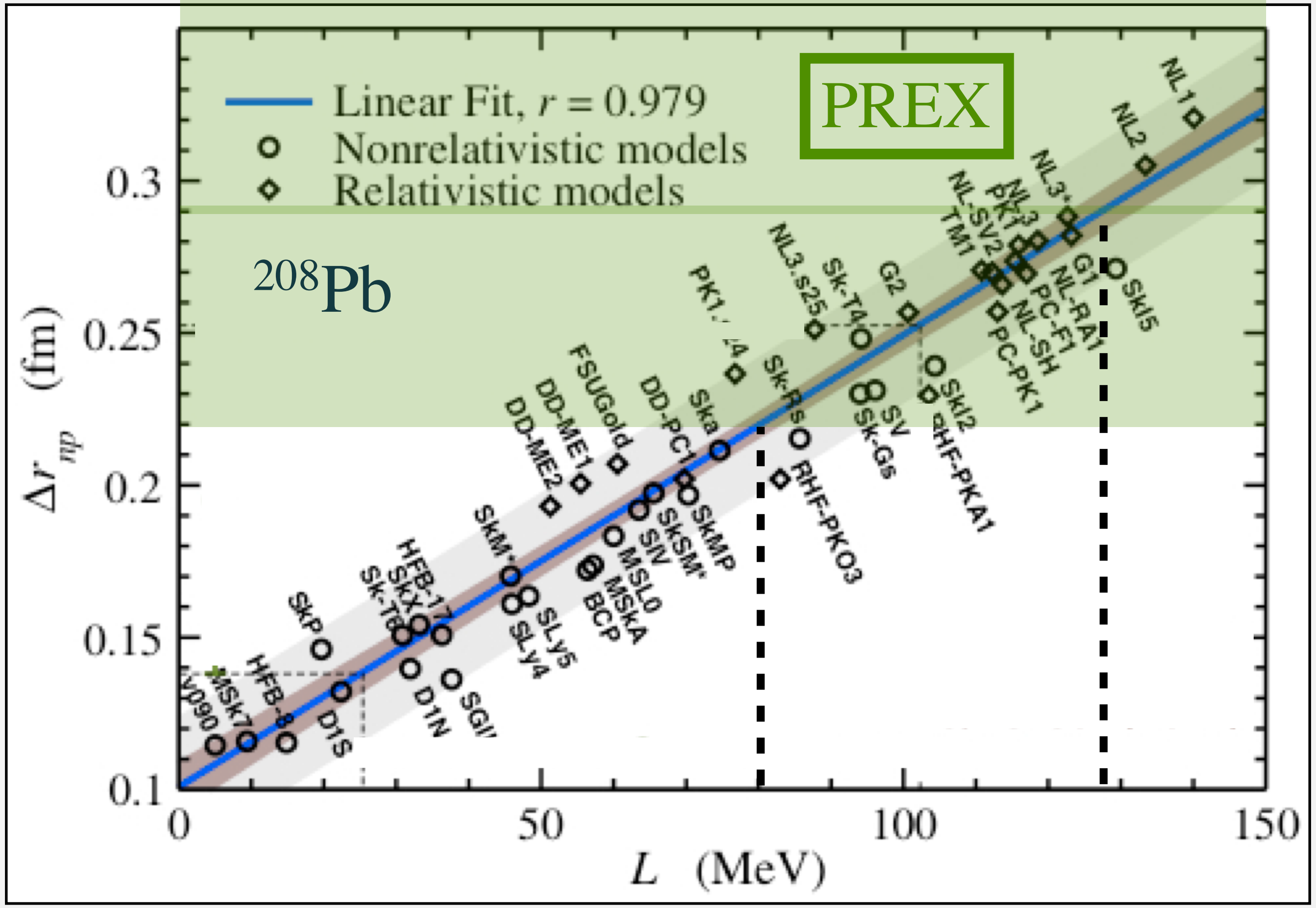

Roca-Maza et al, PRL 106, 252501 (2011)

L vs Symmetry Energy

$$L \propto \frac{\partial S(\rho)}{\partial \rho}|_{\rho_0}$$

Expectation: 60-70 MeV

The PREX-II result is also considerably larger than experimental determinations L wrt S by methods that are highly model dependent

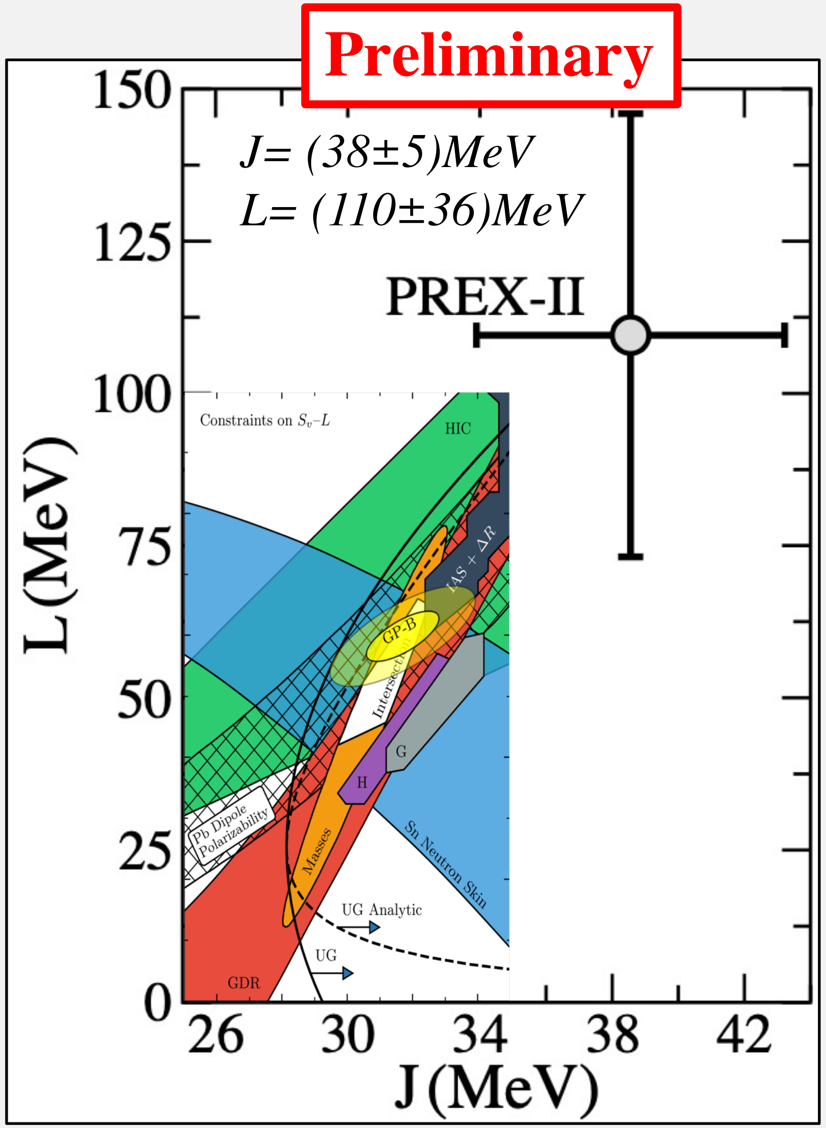

$$S(\tilde{\rho}_0) = J - \frac{L}{9}$$

Adapted by Reed, Fattoyev, Horowitz, Piekarewicz from Drischler et al, PRL(2020)
Original figure: J. M. Lattimer, Ann. Rev. Nucl. Part. Sci. 62, 485 (2012).

Next up

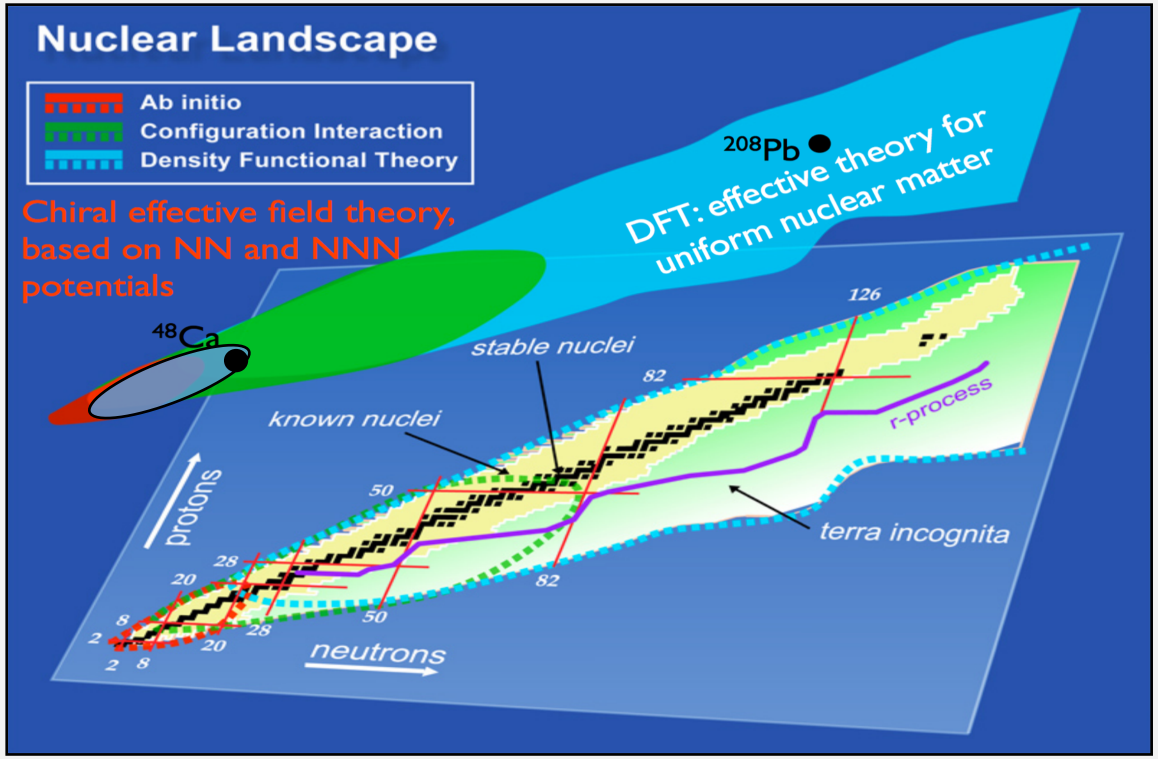

CREX: neutron skin of 48Ca to <0.03 fm

- isovector probe in moderate size system
- finite size effects
- Within reach of microscopic calculations (which suggest the importance of 3-n forces

Coupled cluster calculations predict a neutron skin of: $0.12 \leqq R_{skin} \leqq 0.15$ fm

G. Hagen *et al*, Nature Physics **12**, 186–190 (2016)

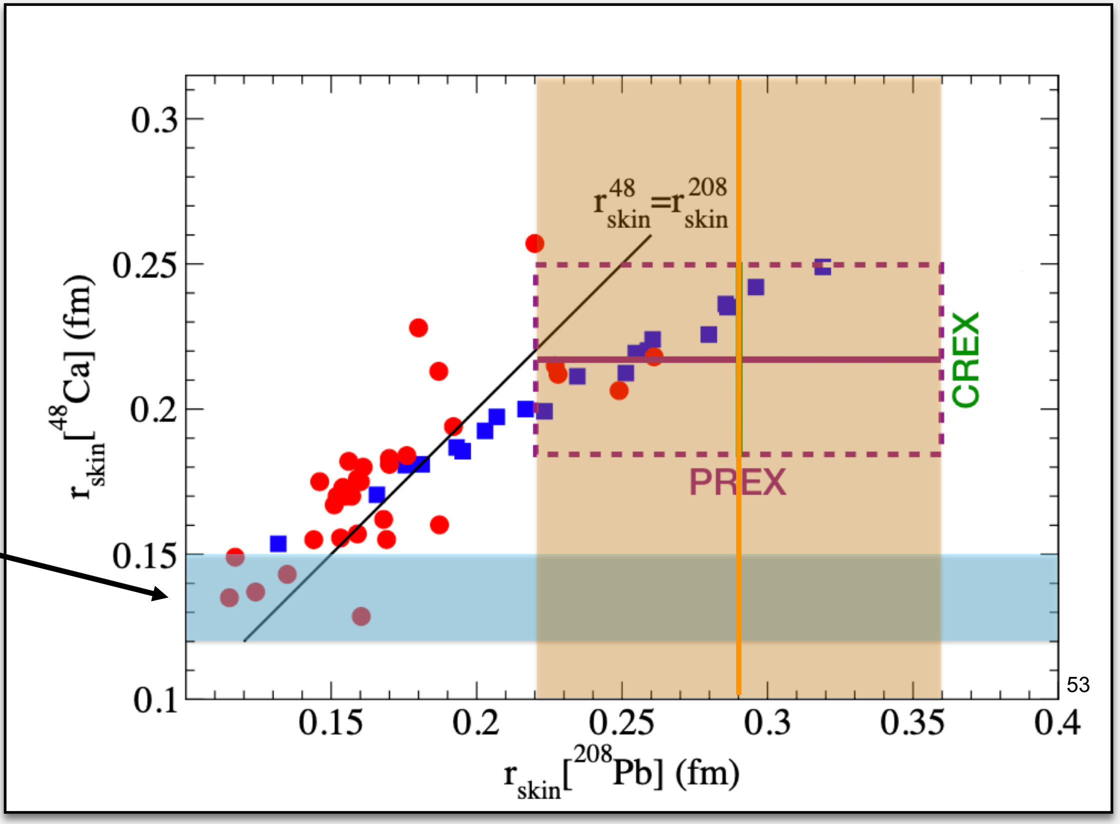

Data in hand, expect result by mid-2021

Future: MREX at MESA (Mainz)

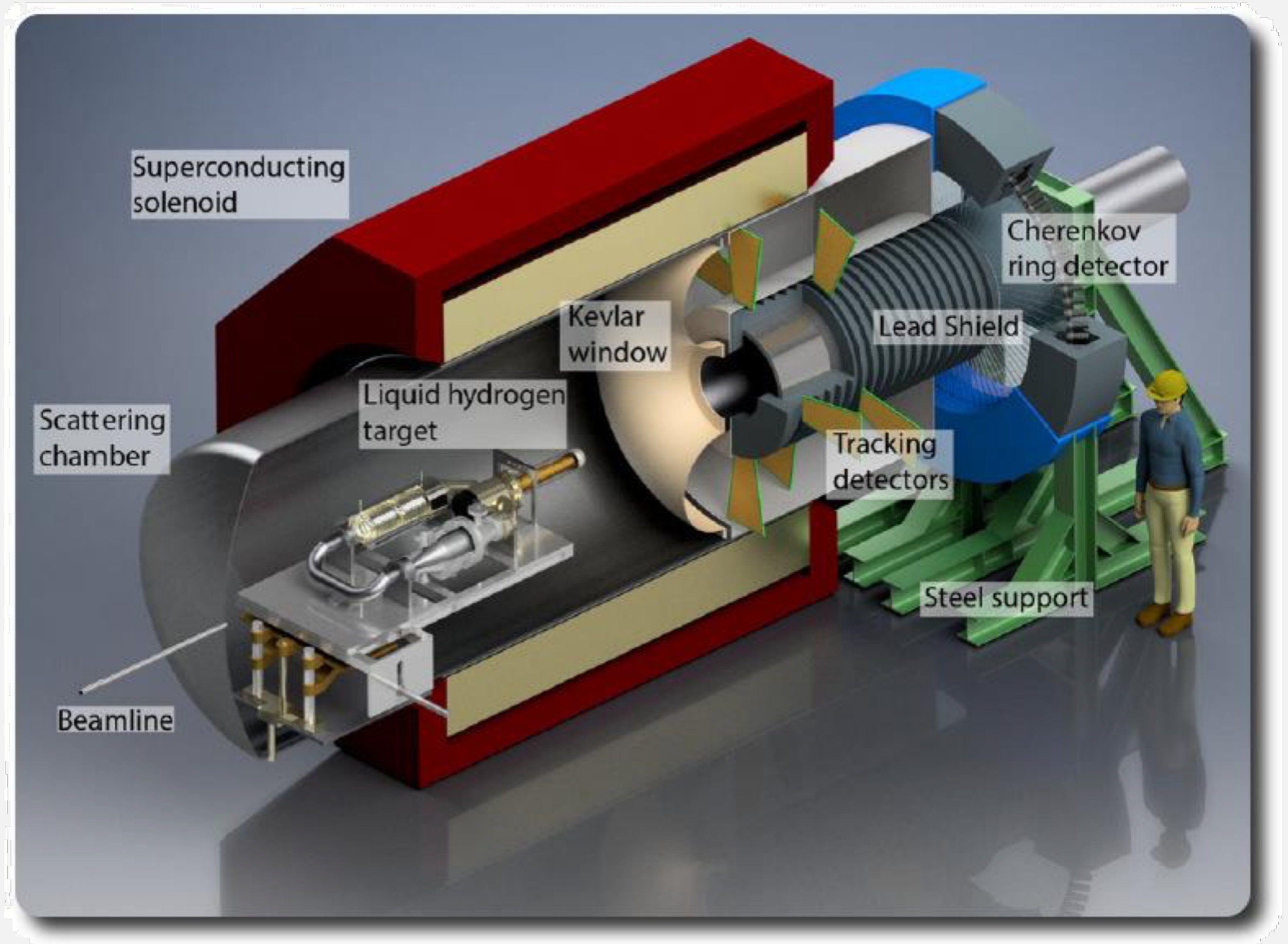

Goal: $\delta R_{n\text{-}p} \sim 0.03$ fm

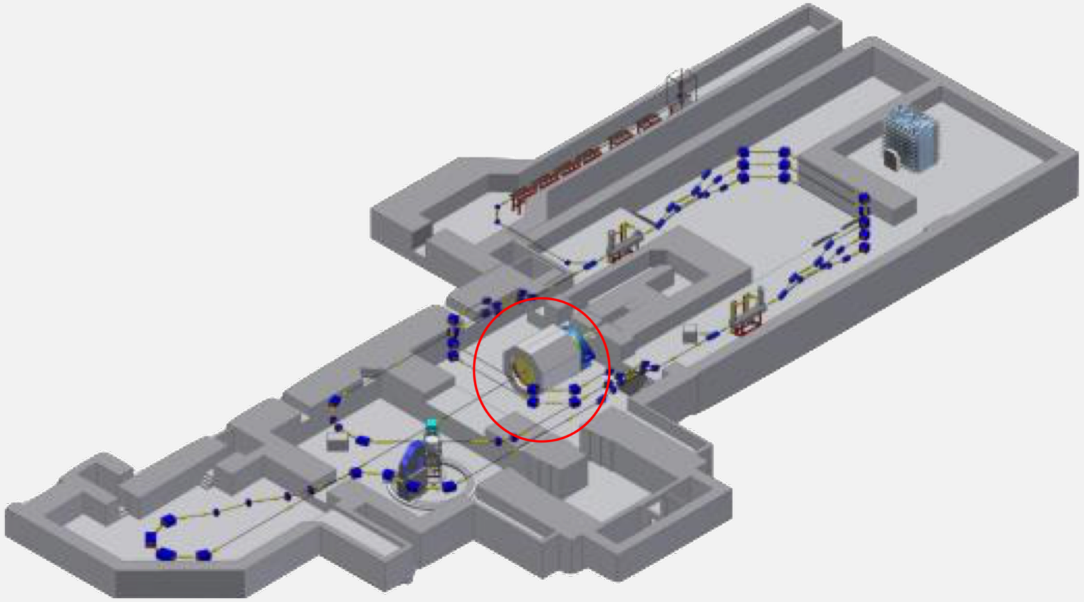

$\Delta\theta=4°$: expected rate = 8.25 GHz, A_{PV} = 0.66 ppm, P = 85%, Q ≈ 86 MeV

1440h → $\delta R_n/R_n$ = 0.52% (^{208}Pb @ 155 MeV)

➢ $\delta R_n/R_n = 0.5\%$
→ L ± 20 MeV

Concettina Sfienti, Michaela Thiel

Congratulations to our crew

Students: Devi Adhikari, Devaki Bhatta Pathak, Quinn Campagna, Yufan Chen, **Cameron Clarke**, Catherine Feldman, **Iris Halilovic**, **Siyu Jian**, **Eric King**, Carrington Metts, Marisa Petrusky, **Amali Premathilake**, **Victoria Owen**, **Robert Radloff**, **Sakib Rahman**, **Ryan Richards**, Ezekiel Wertz, **Tao Ye**, **Adam Zec**, **Weibin Zhang**

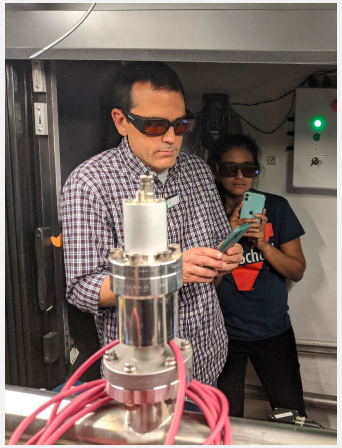



Post-docs and Run Coordinators: Rakitha Beminiwattha, Juan Carlos Cornejo, Mark-Macrae Dalton, Ciprian Gal, Chandan Ghosh, Donald Jones, Tyler Kutz, Hanjie Liu, Juliette Mammei, Dustin McNulty, Caryn Palatchi, Sanghwa Park, Ye Tian, Jinlong Zhang

Spokespeople: Kent Paschke (contact), Krishna Kumar, Robert Michaels, Paul A. Souder, Guido M. Urciuoli

Thanks to the Hall A techs, Machine Control, Yves Roblin, Jay Benesch and other Jefferson Lab staff

Special thanks to: Charles Horowitz and Jorge Piekarewicz for support and insightful conversations
Especially Chuck and grad student Brendan Reed who have worked to help us interpret our results

Backup

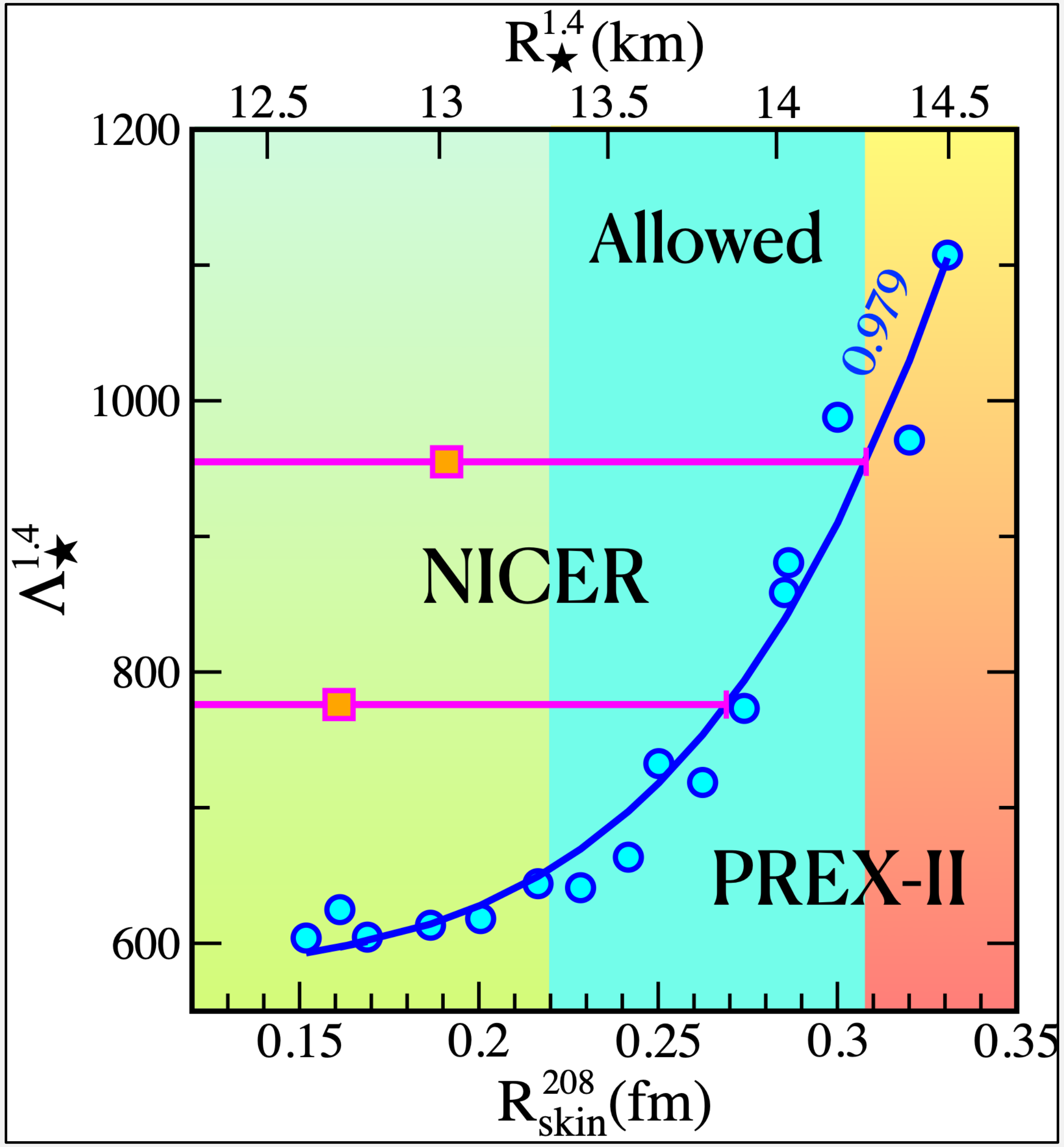

$R_\star^{1.4}$ (km)
12.5
13
13.5
14
14.5
1200
1000
800
600
Allowed
0.979
NICER
PREX-II
$\Lambda_\star^{1.4}$
0.15
0.2
0.25
0.3
0.35
R_{skin}^{208} (fm)

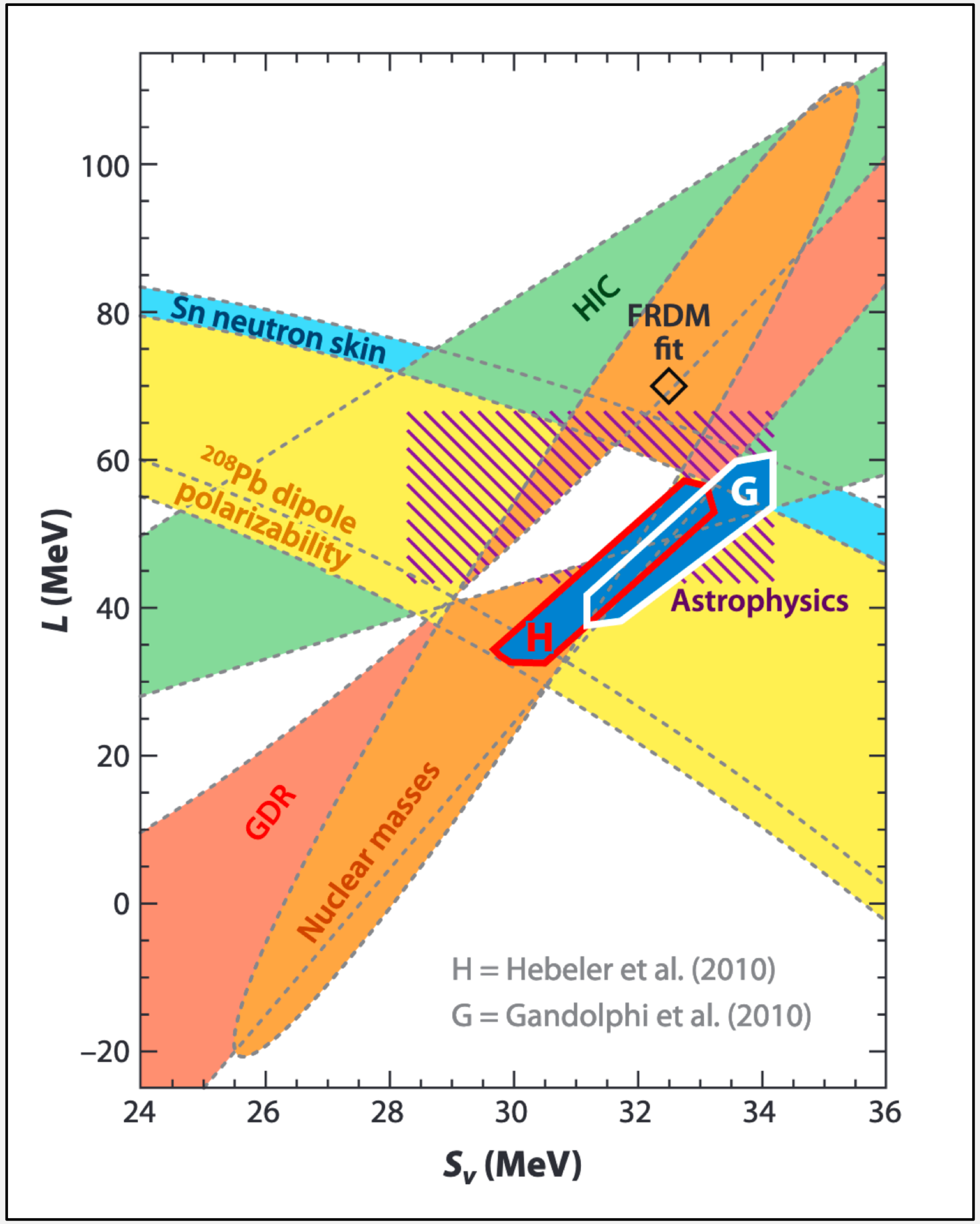

100
80
60
40
20
0
−20
Sn neutron skin
HIC
FRDM fit
^{208}Pb dipole polarizability
G
H
Astrophysics
GDR
Nuclear masses
H = Hebeler et al. (2010)
G = Gandolphi et al. (2010)
L (MeV)
24
26
28
30
32
34
36
S_v (MeV)

Preparing the beam

Injector laser setup crucial towards minimizing beam asymmetries

Double Wien allowed us to further electromagnetically flip the electron beam helicity every few weeks

Beam monitors allowed for injector setup with small beam asymmetries

Mott polarimeter confirm high beam polarization

Pockels cell allowed us to flip the electron helicity at 120 or 240 Hz

Half Wave Plate allowed us to independently flip the laser polarization every few hours

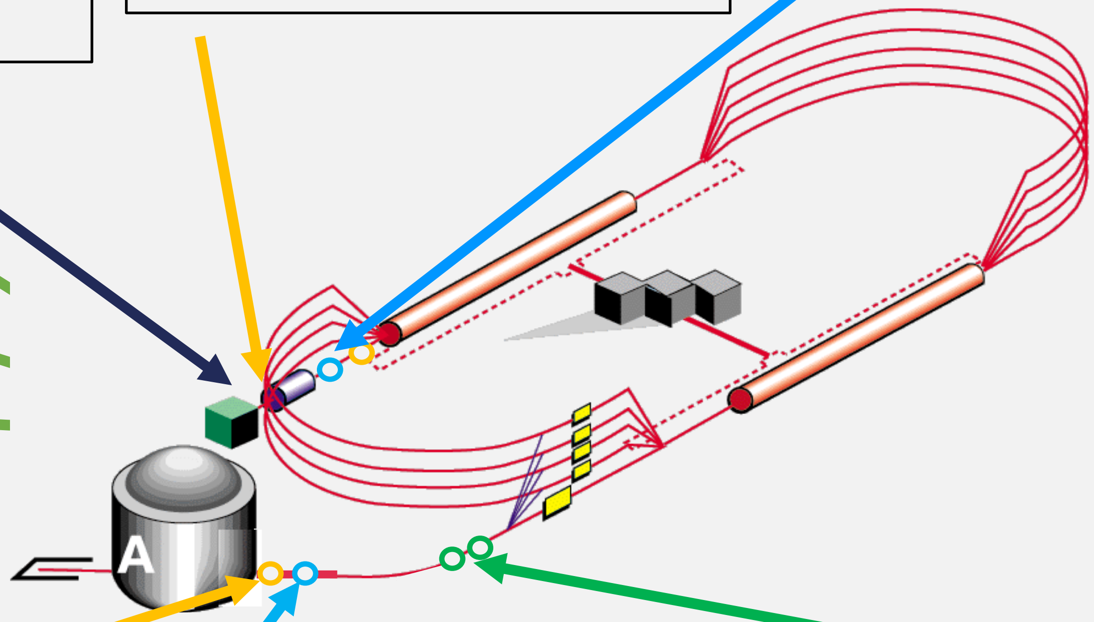

Beam monitors allow us to determine beam properties in front of the target

Polarimeters allow us to monitor polarization and check machine setup

Beam modulation system allows us to span the phase space of beam motion

Polarized Source

- The GaAs strained cathode photoemits selected helicity electrons for a circularly polarized laser tuned to a particular bandgap
- It also acts as an "analyzer" with a preferred axis for linear polarization
- The system relies on a Pockels Cell to produce quick changes between opposite circular polarization states
- Imperfections between the two polarization states will lead to beam asymmetries
  - Careful setup and constant monitoring is needed to mitigate any changes in the accelerator setup that introduce such asymmetries

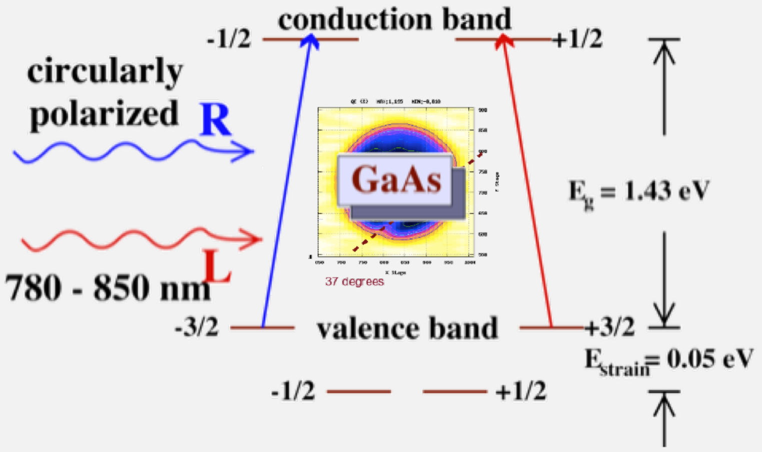

new UVa RTP cell (MOLLER R&D)

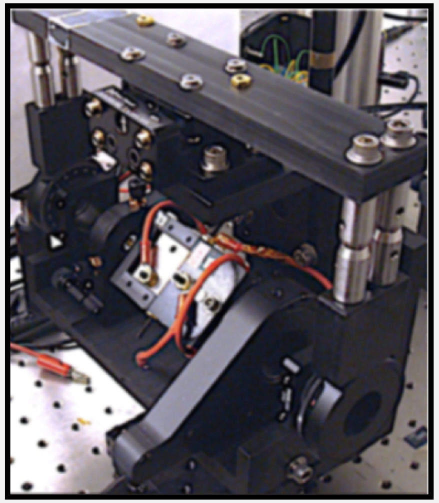

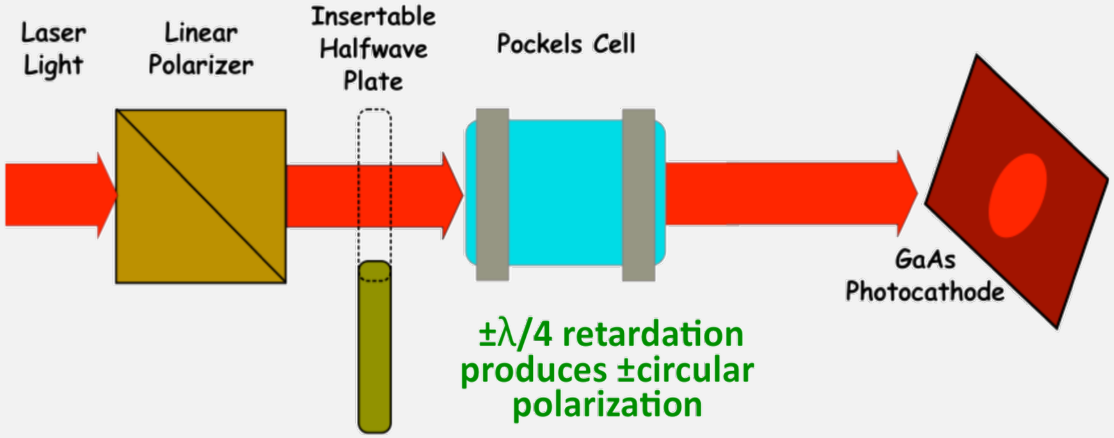

Slow Reversals

- The system relies on a Pockels Cell to produce quick changes between opposite circular polarization states
- Insertable Halfwave Plate: reverses polarization of the laser light, relative to the voltages on the Pockels cell
- The "double Wien" manipulates spin - allows us to reverse the polarization of the electron beam relative to the polarization of the laser light
- These each act to both identify, and cancel, potential beam related asymmetries

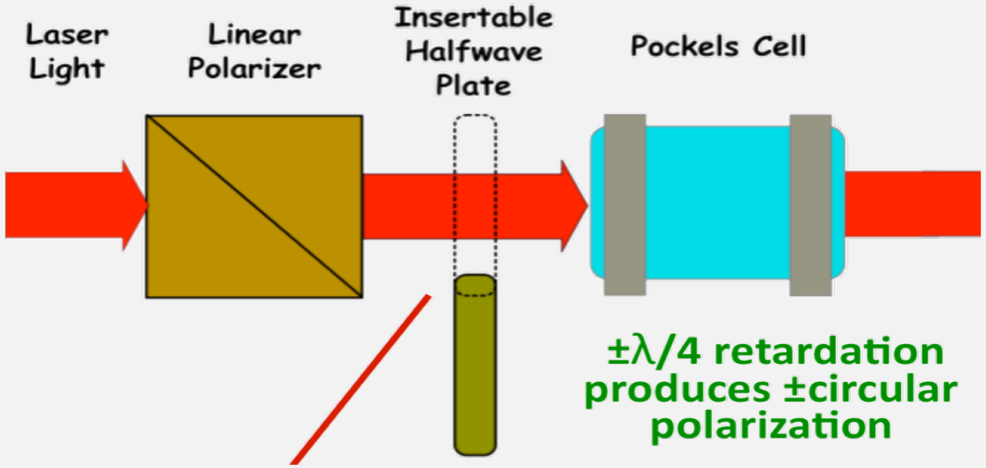

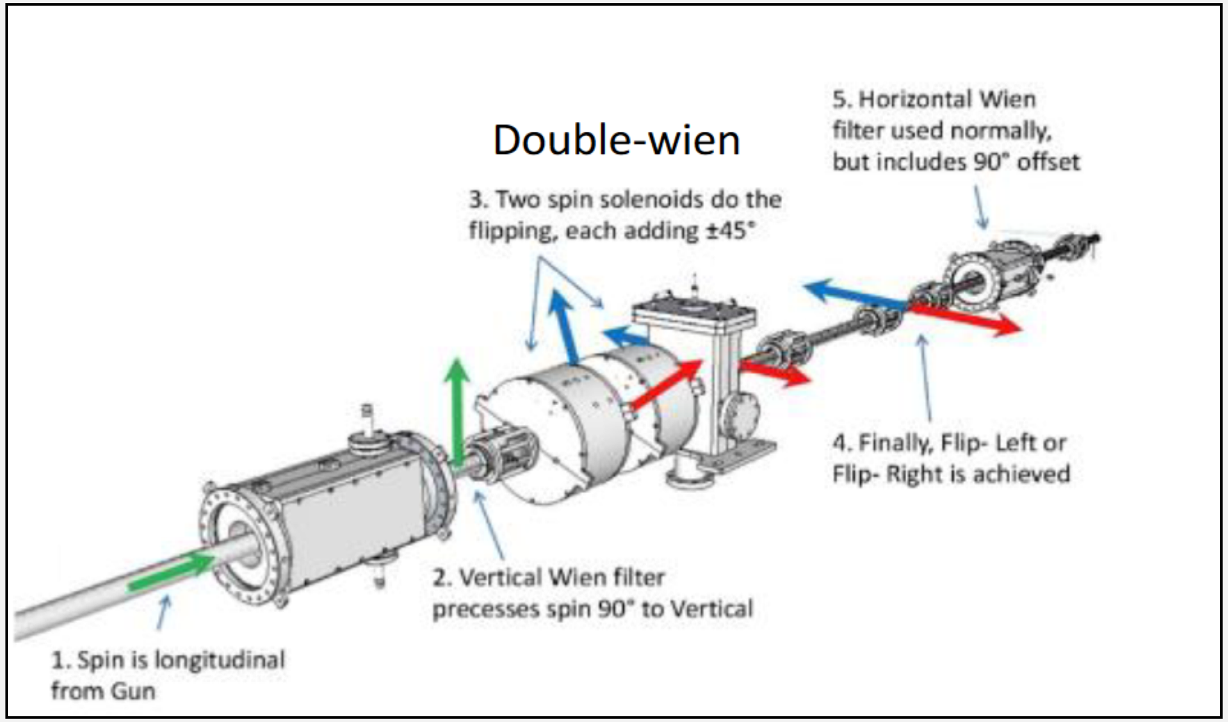

Polarized Source and Injector group!

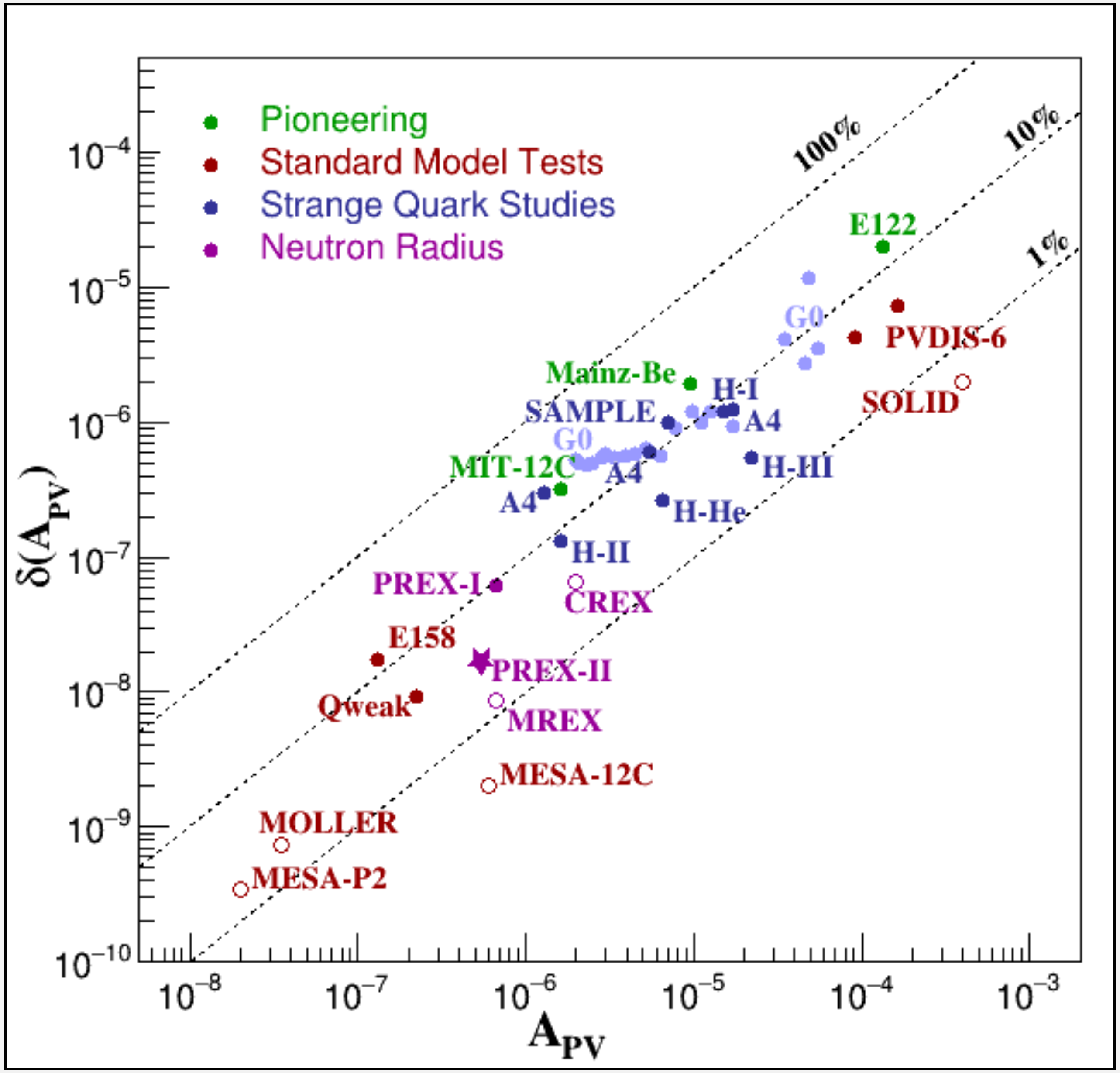

Pioneering
Standard Model Tests
Strange Quark Studies
Neutron Radius
100%
10%
1%
E122
G0
PVDIS-6
Mainz-Be
H-I
SOLID
SAMPLE
A4
G0
MIT-12C
A4
H-III
A4
H-He
H-II
PREX-I
CREX
E158
PREX-II
Qweak
MREX
MESA-12C
MOLLER
MESA-P2
$\delta(A_{PV})$
A_{PV}

Model Dependence

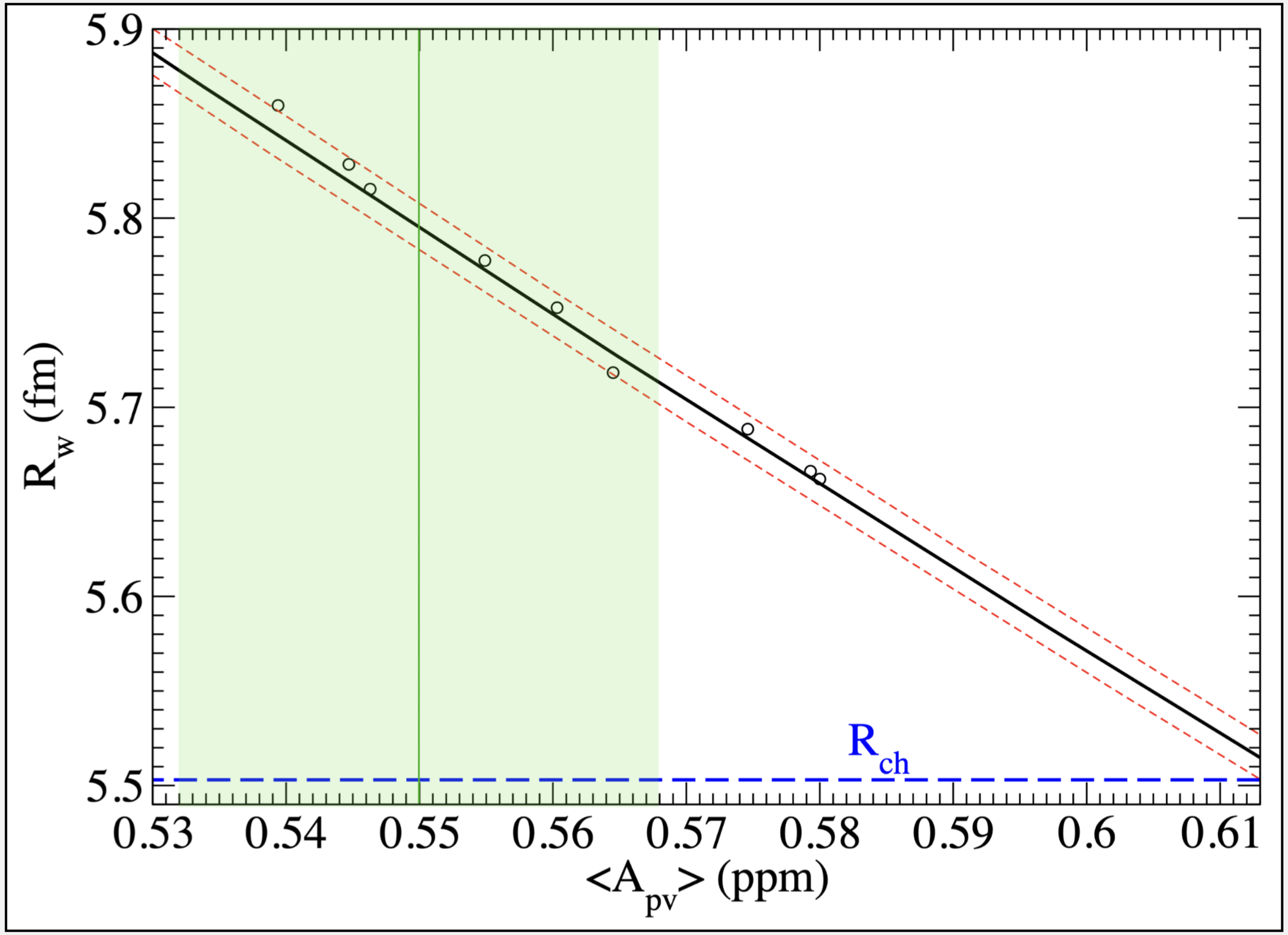

- The points are full nuclear EOS models
- We can make the assumption of a 2-parameter Fermi function for the weak density and take the average surface thickness from these models to obtain the line and uncertainty band (0.013 fm)

Carbon Contamination

$$A_{PV} = \frac{A_{corr}/P_e - \sum_i A_i f_i}{1 - \sum_i f_i}$$

- A_{corr}: Corrected asymmetry
- P_e: Polarization
- A_i: Background asymmetry
- f_f: Background fraction

- We used the same simulation that reproduced our optics data to look at accepted events from Carbon
- We used a theoretical calculation for the C asymmetry for each interaction and evaluated the correction based on the rate weighted average
- Uncertainty on fraction is negligible

A_{corr}/P_e (ppb)	A_C (ppb)	$\delta A_C/A_C$ (%)	δA_C (ppb)	f_C	δf_C	Rel. error (%) due to f_C	Rel. error (%) due to A_C
549.34	539.36	4	21.574	6.29E-02	4.63E-03	0.01	0.26

Transverse asymmetries

Transverse:

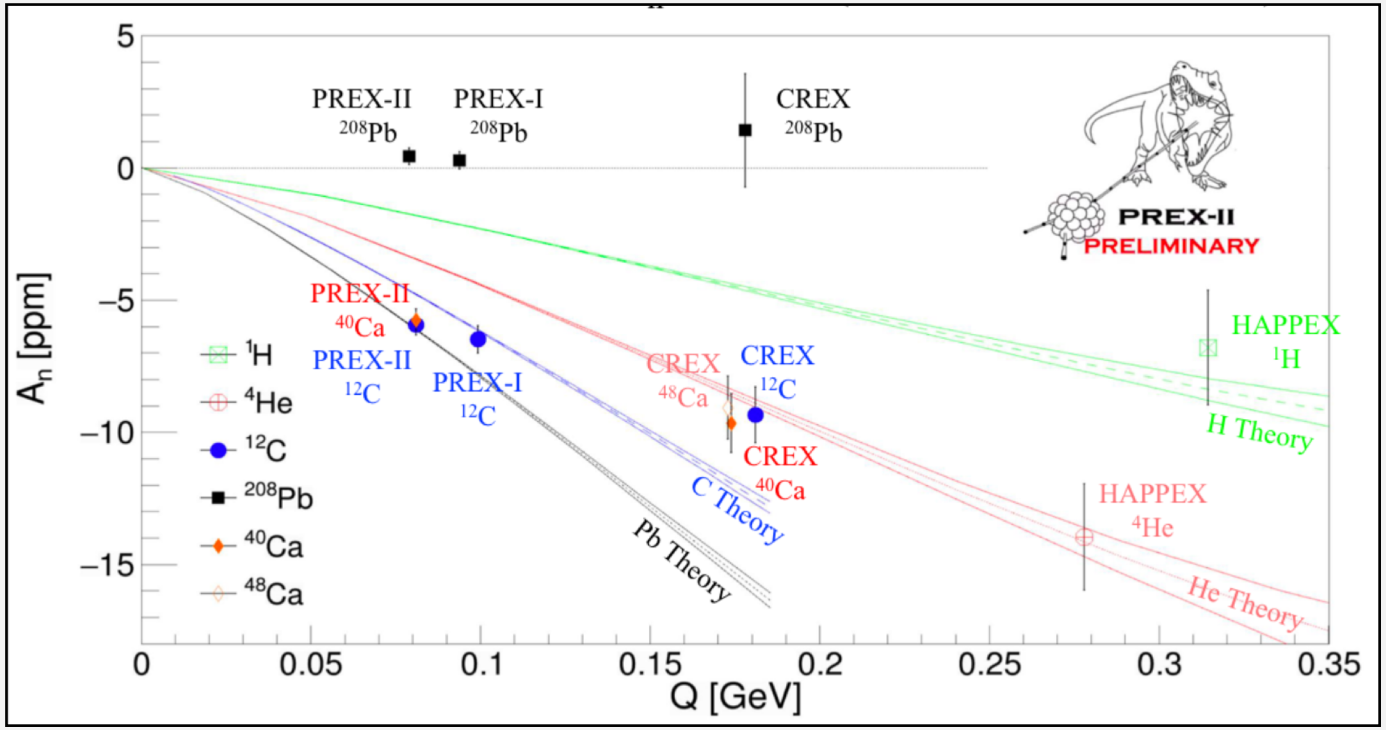

$$A_{trans} = 0 \pm 0.1 \quad \text{ppb}$$

- Transverse asymmetry did not contribute a correction to the main parity violating asymmetry
  - However the uncertainty was taken into account

Beam Corrections vs E-vector Differences

type	Mean(ppb)
X1	-22.33
Y1	22.5
E	-70.44
Y2	-2.84
X2	9.7
	1.27
	-0.01
	1.06
	0.26
	0.24
	0.18
	0.06
Total	-60.38

	Mean(nm)	σ (nm)	RMS(um)
X1	-3.96	2.12	14.9
Y1	2.31	1.38	9.6
E	-1.83	1.01	7.0
Y2	-1.61	0.46	3.3
X2	-1.01	0.38	2.6
	0.16	0.2	1.3
	0.15	0.12	0.9
Mostly BPM Electronic Noise	0.02	0.11	0.7
	-0.08	0.07	0.4
	-0.02	0.06	0.3
	-0.04	0.05	0.3
	-0.01	0.04	0.3

Table: grand averaged eigenvector HC differences

MITP NSkins workshop, May 2016

Workshop examined sources of error in measurements of neutron skin (experimental, reaction dynamics, model interpretation as L or ΔR)

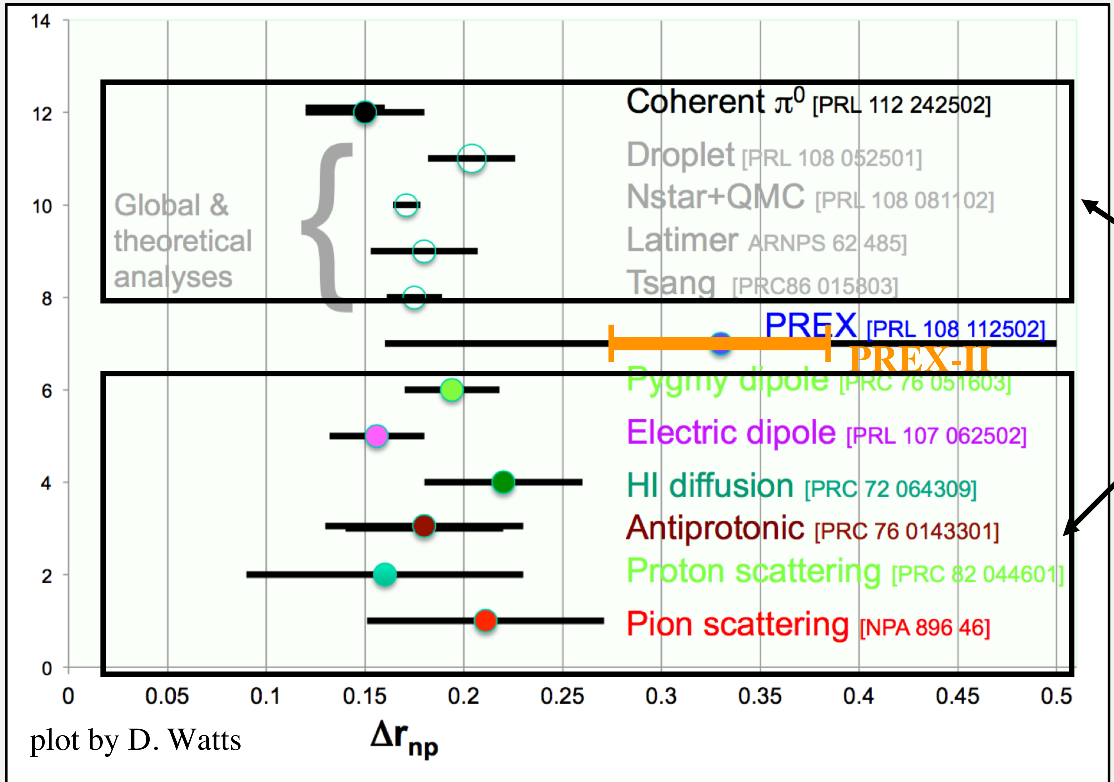

Significant issues were seen in all these

This is why the PV measurements are essential